AD-A136 679 FLOW-INDUCED VIBRATIONS OF TAUT MARINE CABLES WITH   1/2
              ATTACHED MASSES(U) NAVAL RESEARCH LAB WASHINGTON DC
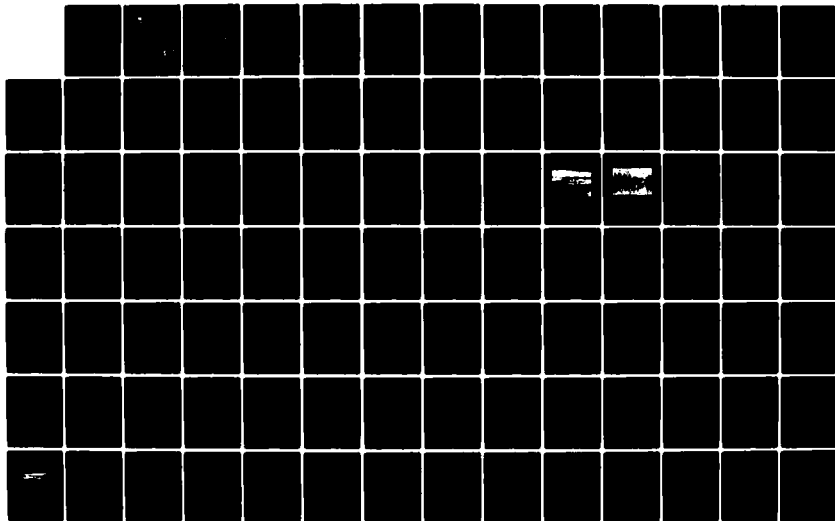   O M GRIFFIN ET AL. NOV 83 NCEL-CR-84.004
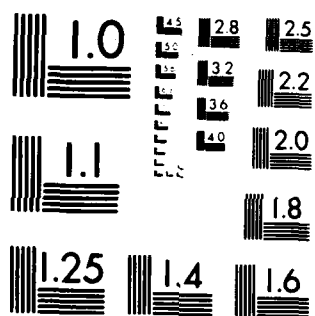UNCLASSIFIED N68305-82-WR-20092   F/G 20/4   NL

MICROCOPY RESOLUTION TEST CHART

NATIONAL BUREAU OF STANDARDS 1963 A

AD-A136679

CR 84.004

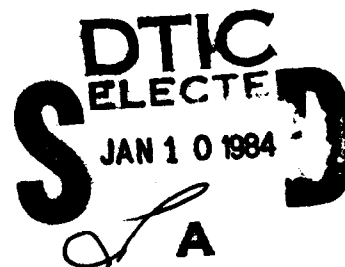NAVAL CIVIL ENGINEERING LABORATORY
Port Hueneme, California

Sponsored by
NAVAL FACILITIES ENGINEERING COMMAND

FLOW-INDUCED VIBRATIONS OF TAUT MARINE CABLES WITH ATTACHED MASSES

November 1983

An Investigation Conducted by
NAVAL RESEARCH LABORATORY
Marine Technology Division
Washington, D.C. 20375

N68305-82-WR-20092
N68305-83-WR-30097

DTIC
SELECTE
JAN 1 0 1984
S   A

84 01 10 046

METRIC CONVERSION FACTORS

Approximate Conversions to Metric Measures

Symbol	When You Know	Multiply by	To Find	Symbol
		LENGTH		
in	inches	*2.5	centimeters	cm
ft	feet	30	centimeters	cm
yd	yards	0.9	meters	m
mi	miles	1.6	kilometers	km
		AREA		
in²	square inches	6.5	square centimeters	cm²
ft²	square feet	0.09	square meters	m²
yd²	square yards	0.8	square meters	m²
mi²	square miles	2.6	square kilometers	km²
	acres	0.4	hectares	ha
		MASS (weight)		
oz	ounces	28	grams	g
lb	pounds	0.45	kilograms	kg
	short tons (2,000 lb)	0.9	tonnes	t
		VOLUME		
tsp	teaspoons	5	milliliters	ml
Tbsp	tablespoons	15	milliliters	ml
fl oz	fluid ounces	30	milliliters	ml
c	cups	0.24	liters	l
pt	pints	0.47	liters	l
qt	quarts	0.95	liters	l
gal	gallons	3.8	liters	l
ft³	cubic feet	0.03	cubic meters	m³
yd³	cubic yards	0.76	cubic meters	m³
		TEMPERATURE (exact)		
°F	Fahrenheit temperature	5/9 (after subtracting 32)	Celsius temperature	°C

*1 in = 2.54 (exactly). For other exact conversions and more detailed tables, see NBS Misc. Publ. 286, Units of Weights and Measures, Price \$2.25, SD Catalog No. C13.10:286.

Approximate Conversions from Metric Measures

Symbol	When You Know	Multiply by	To Find	Symbol
		LENGTH		
mm	millimeters	0.04	inches	in
cm	centimeters	0.4	inches	in
m	meters	3.3	feet	ft
m	meters	1.1	yards	yd
km	kilometers	0.6	miles	mi
		AREA		
cm²	square centimeters	0.16	square inches	in²
m²	square meters	1.2	square yards	yd²
km²	square kilometers	0.4	square miles	mi²
ha	hectares (10,000 m²)	2.5	acres	
		MASS (weight)		
g	grams	0.035	ounces	oz
kg	kilograms	2.2	pounds	lb
t	tonnes (1,000 kg)	1.1	short tons	
		VOLUME		
ml	milliliters	0.03	fluid ounces	fl oz
l	liters	2.1	pints	pt
l	liters	1.06	quarts	qt
l	liters	0.26	gallons	gal
m³	cubic meters	35	cubic feet	ft³
m³	cubic meters	1.3	cubic yards	yd³
		TEMPERATURE (exact)		
°C	Celsius temperature	9/5 (then add 32)	Fahrenheit temperature	°F
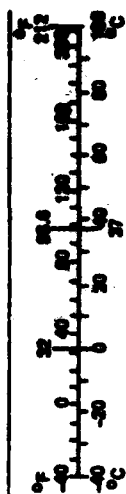
REPORT DOCUMENTATION PAGE		READ INSTRUCTIONS BEFORE COMPLETING FORM
1. REPORT NUMBER CR 84.004	2. GOVT ACCESSION NO. AD-A136 679	3. RECIPIENT'S CATALOG NUMBER
4. TITLE (and Subtitle) FLOW-INDUCED VIBRATIONS OF TAUT MARINE CABLES WITH ATTACHED MASSES		5. TYPE OF REPORT & PERIOD COVERED Final Oct 1981 - Sep 1983
		6. PERFORMING ORG. REPORT NUMBER
7. AUTHOR(s) O.M. Griffin, Naval Research Laboratory J.K. Vandiver, Massachusetts Institute of Technology		8. CONTRACT OR GRANT NUMBER(s) N68305-82-WR-20092 N68305-83-WR-30097
9. PERFORMING ORGANIZATION NAME AND ADDRESS NAVAL RESEARCH LABORATORY Marine Technology Division Washington, D.C. 20375		10. PROGRAM ELEMENT. PROJECT, TASK AREA & WORK UNIT NUMBERS YF.60.534.091.01.A354 PE62760N
11. CONTROLLING OFFICE NAME AND ADDRESS Naval Civil Engineering Laboratory Port Hueneme, CA 93043		12. REPORT DATE November 1983
		13. NUMBER OF PAGES 132
14. MONITORING AGENCY NAME & ADDRESS(if different from Controlling Office) Naval Facilities Engineering Command 200 Stovall Street Alexandria, VA 22332		15. SECURITY CLASS. (of this report) Unclassified
		15a. DECLASSIFICATION/DOWNGRADING SCHEDULE

16. DISTRIBUTION STATEMENT (of this Report)

Approved for public release; distribution unlimited.

17. DISTRIBUTION STATEMENT (of the abstract entered in Block 20, if different from Report)

18. SUPPLEMENTARY NOTES

19. KEY WORDS (Continue on reverse side if necessary and identify by block number)

Taut cables, cable strumming, vortex shedding, natural fre-
quencies, mode shapes, cable dynamics, drag coefficients,
computer model, mooring systems, underwater-cable arrays

20. ABSTRACT (Continue on reverse side if necessary and identify by block number)

A series of cable strumming field experiments have been con-
ducted at Castine Bay, Maine. The test site, instrumentation,
cable, and experimental procedures are described in detail.
The purpose of this test series was to provide an accurate data
base for the validation of the computer code NATFREQ. This
code was developed at the California Institute of Technology

DD FORM 1473 EDITION OF 1 NOV 65 IS OBSOLETE
1 JAN 73

for the Naval Civil Engineering Laboratory to predict the natural frequencies and mode shapes for taut cable systems subjected to flow-induced vibration. In addition, the drag amplification model developed at the Naval Research Laboratory has been included in the NATFREQ code for the prediction of amplified drag coefficients for strumming cables. The predicted natural frequencies and drag coefficients obtained from a NATFREQ analysis of the Castine Bay experimental series have been compared to the measured values. Good correlation between the predicted and measured values has been obtained. A detailed description of these comparisons and the NATFREQ code is provided.

Distribution/
Availability Codes

Dist	Avail and/or Special
A-I	

CONTENTS

FOREWORD AND ACKNOWLEDGMENTS

NOMENCLATURE AND LIST OF SYMBOLS

A	Cross section area (ft^2)
A_i	Cable parameter, see equation (3).
B_i	Cable parameter, see equation (3).
C_D, C_{DO}	Steady drag coefficient on a vibrating (stationary) cylinder or cable.
D	Cable or cylinder diameter (ft).
E_c	Cable elastic modulus (lb_f/ft^2).
f_n	Natural frequency (Hz).
f_s	Strouhal frequency (Hz).
g	Gravitational acceleration (32.2 ft/sec^2).
H	Critical tension, see equation (16).
I_i	Modal scaling factor; see equation (C4).
k_s	Reduced damping; see equation (C3).
l	Cable segment length.
L	Cable length (ft).
m	Cable physical mass per unit length (kg/m or lb_m/ft).
m_e	Effective mass per unit length (kg/m or lb_m/ft). (physical plus added mass).
m'	Cable virtual mass (physical plus added mass) per unit length (kg/m or lb_m/ft).
M_i	Mass of attachment, see equation (7).
Re	Reynolds number, VD/ν.
SG	Specific gravity.
St	Strouhal number, $f_s D/V$.
T	Cable static tension (N or lb_f).
V	Incident flow velocity (m/s or ft/sec or knots).
V_r	Reduced velocity, $V/f_n D$.
$V_{r,crit}$	Critical reduced velocity.

W	Total cable weight, see equation (17).
w_r	Response parameter, $(1 + 2\,\bar{Y}/D)\,(V_R \mathrm{St})^{-1}$; see equation (C1).
$\bar{x}$	In line displacement (ft).
$\bar{X}$	In line displacement amplitude (ft).
$\bar{y}$	Cross flow displacement (ft).
$\bar{Y}$	Cross flow displacement amplitude (ft).
Y	Normalized displacement amplitude, $\bar{Y}/D$.
$Y_{\mathrm{EFF,MAX}}$	Normalized displacement amplitude; see equation (C4).
α	Cable parameter, see equation (4).
δ	Log decrement of structural damping; see equation (19).
γ_i	Normalizing factor; see equation (C4).
ν	Kinematic fluid viscosity (ft^2/sec).
ρ	Fluid density (lb$_m$/ft^3).
ρ_c	Cable density (lb$_m$/ft^3).
$\psi_i(z)$	Mode shape for ith flexible cable mode; see equation (C4).
ω	Radian frequency (rad/sec).
ζ_s	Structural damping ratio; see equation (20).

LIST OF FIGURES

Fig. C1 — Steady drag force measured on a free-ended circular cylinder towed steadily through still water.

Fig. C2 — The predicted steady tip deflection $\bar{X}_s$ of a cantilever beam, vibrating due to vortex shedding, compared with the measured values for a beam of comparable construction.

LIST OF TABLES

EXECUTIVE SUMMARY

As part of the overall NCEL marine cable dynamics exploratory development program under the sponsorship of NAVFAC, a series of laboratory and field experiments have been conducted to investigate the effects of attached masses and sensor housings (discrete or lumped masses) on the overall cable system response. Towing channel experiments were conducted with a "strumming rig" developed for the NAVFAC/NCEL cable dynamics program and the test findings recently were reported (3).[*] A field test program was conducted during the summer of 1981 to investigate further the strumming vibrations of marine cables in a controlled environment. The experiments were funded by NCEL, the USGS and industry sponsors, planned by NRL and MIT, and conducted at the field site by MIT. The primary objective of the test program was to acquire data to validate and, if necessary, to provide a basis for modifying the NCEL-sponsored computer code NATFREQ (4). This code was developed at the California Institute of Technology to provide a means for calculating the natural frequencies and mode shapes of *taut* marine cables with large numbers of attached masses.

The vortex-excited oscillations of marine cables, commonly termed *strumming*, result in increased fatigue, larger hydrodynamic forces and amplified acoustic flow noise, and sometimes lead to structural damage and eventually to failure. Flow-excited oscillations very often are a critical factor in the design of underwater cable arrays, mooring systems, drilling risers, and offshore platforms. Many components of these complex structures typically have a cylindrical cross-section which is conducive to vortex shedding when they are placed in a flow. An understanding of the nature of the fluid-structure interaction which results in vortex-excited oscillations is an important factor in the reliable design and long-term operation of offshore structures and cable systems.

As the state of the ocean engineering art steadily progresses, more and more stringent demands are being placed upon the performance of cable structures and moorings. In particular, displacement tolerances and constraints in response to currents are becoming more stringent; fatigue is becoming an important design consideration; and the sensitivity of acoustic sensors has increased to the point that

---

[*] Numbers in parentheses denote references listed at the end of this report.

xi

they cannot differentiate between legitimate acoustic targets and slight variations in their vertical position. All of these are problems that are aggravated by cable strumming. In order to design a structure or cable system to meet the constraints imposed by operational and environmental requirements, the engineer must be able to assess the effect of strumming on the structure in question.

One purpose of this report is to describe the field test program and to present the salient results from it. Time histories of the measured hydrodynamic drag coefficients, current speeds, and cable strumming accelerations and displacement amplitudes are presented and discussed to the extent possible. The natural frequencies and mode shapes for the cable with attached masses were measured in air and in water. Data from the twenty test runs which were conducted are presented in this report.

Validation of the NATFREQ code is an objective of this report. Calculations of cable natural frequencies and mode shapes using the NATFREQ code were made at NRL for all of the field test runs. A comparison is made in this report between the calculated natural frequencies and mode shapes and those experimental test runs which it was possible to analyze in sufficient detail. Also, recommendations are made of modifications that will enhance the utility and the ease of access to the code for prospective users.

The test runs which were conducted during the experimental phase of the test program consisted of ten pairs of equivalent tests in air and in water. The measured in-air natural frequencies are in good agreement with the NATFREQ predictions for the second and higher (up to $n = 5$) cable modes. The first mode frequency apparently was influenced by the sag of the cable. The measured mode shapes of the cable vibrations in air are in agreement with the computed mode shapes, but only limited mode shape comparisons are possible due to the existing capabilities of the code.

Good agreement also was obtained between the NATFREQ-predicted natural frequencies and the frequencies measured in water. It is clear from the comparison given in this report that it is possible to predict the natural frequencies of a *taut* cable with attached masses to better than 10 percent. However, at high cable mode numbers the difference in frequency between modes often is considerably less than

this value. Then it is difficult to positively identify which measured cable frequency is associated with which predicted mode.

The results available to-date tend to validate the NATFREQ computer code as a reliable engineering model for predicting the natural frequencies and mode shapes of *taut* marine cables with arrays of discrete masses attached to them.

Measurements of the hydrodynamic drag forces during the Castine Bay field experiments consistently produced drag coefficients in the range $C_D = 2$ to 3.2 for the bare cable and the cable with attached masses. This is a substantial amplification of the drag force from the expected level for a stationary cable ($C_D = 1$ to 1.5).

The drag coefficient on the strumming cable was predicted by Vandiver (23) with a strumming drag model that was developed at NRL as part of the overall NCEL cable dynamics research program. The predicted drag on the cable was comparable to the measured drag. For a complementary experiment at the test site with a flexible circular steel pipe, the predicted drag coefficients were virtually indistinguishable from the measured drag coefficients (23).

Several recommendations have been developed as a result of the comparison between the NATFREQ code predictions and the Castine Bay field tests. The major recommendations are:

- Cable sag or slack effects often play an important role in the dynamics of marine cables. The NATFREQ code is limited to *taut* cable dynamics. Consideration should be given to the development of a comparable code for the calculation of the natural frequencies and mode shapes of a *slack* cable with attached masses. At least one such code, called SLAK, presently exists in rudimentary form (1).

- Many of the data records from the 1981 Castine field experiment contain lengthy time segments where the cable strumming is nonresonant, i.e., the vibrations and the vortex shedding are not locked-on at a single resonant frequency. Consideration should be given

xiii

to developing a *simple* but still effective method for taking nonresonant strumming effects into account in determining the cable response and the strumming-induced hydrodynamic drag force and coefficient C_D.

1. INTRODUCTiON

1.1 Objectives

At the beginning of FY 1975, technical coordination of the NAVFAC marine cable dynamics exploratory development program was undertaken by the Naval Civil Engineering Laboratory (NCEL). The overall objective of this program, as stated in a research plan put forward by NCEL, is:

"... to provide for the development of effective methods for the analysis of the dynamic response of 3-dimensional, moored cable structures which undergo dynamic motions generated by various natural or man-produced causes. Failure to predict this dynamic behavior by suitable analytical techniques will affect the confidence in the adequacy of the system design as well as the estimated reliability of the system's performance."

"Dynamic response of moored cable structures includes two specific problem areas which are addressed separately in this plan. [One aspect of this problem] is the small-displacement, "high frequency" response generated by shedding vortices as water flows past the cable—this response is commonly referred to as cable strumming. The objective of the plan for this specific area is twofold: (1) development of a capability to predict the strumming response (i.e., deflection, frequency, generated acoustic energy, and drag force) of cable networks which have horizontally or vertically oriented cable segments, in taut or catenary configurations subjected to a current which may vary along the cable length, and (2) development of techniques which can be used to suppress cable strumming."

The resonant strumming response of bare cables is discussed in detail in a recent NCEL/NRL report (1). The suppression of strumming vibrations is dealt with in a separate NCEL-sponsored report (2).

As part of the overall NCEL cable dynamics program, both laboratory and field experiments have been conducted to investigate the effects of attached masses and sensor housings (discrete or lumped masses) on the overall cable system response. Towing channel experiments were conducted with a

"strumming rig" developed for the NCEL cable dynamics program and the test findings recently were reported (3). A test program was conducted during the summer of 1981 to investigate further the strumming vibrations of marine cables in a controlled field environment. The experiments were funded by NCEL, the USGS and industry sponsors, planned by NRL and MIT, and conducted at the field site by MIT. A primary objective of the test program was to acquire data to validate and, if necessary, to provide a basis for modifying the NCEL-sponsored computer code NATFREQ (4). This code was developed at the California Institute of Technology to provide a means for calculating the natural frequencies and mode shapes of taut marine cables with large numbers of attached masses.

1.2 Background

It often is found that bluff, or unstreamlined, cylindrical structures undergo damaging oscillatory instabilities when wind or water currents flow over them. A common mechanism for resonant, flow-excited oscillations is the organized and periodic shedding of vortices as the flow separates alternately from opposite sides of a long bluff body. The flow field exhibits a dominant periodicity and the body is acted upon by time-varying pressure loads. These pressures result in steady and unsteady drag or resistance forces in line with the flow and unsteady lift or side forces normal to the flow direction. If the structure is flexible and lightly damped as in the case of a marine cable, then resonant oscillations can be excited normal or parallel to the incident flow direction. For the more common cross flow oscillations, the body and the wake have the same frequency of oscillation which is near one of the natural frequencies of the system. The shedding meanwhile is shifted away from the usual, or Strouhal, frequency at which pairs of vortices would be shed if the structure or cable was restrained from oscillating. This phenomenon is known as "lock-in" or "wake capture."

The oscillations of marine cables caused by vortex shedding, commonly termed *strumming*, result in increased fatigue, larger hydrodynamic forces and amplified acoustic flow noise, and sometimes lead to structural damage and eventually to costly failures. Flow-excited oscillations very often are a critical factor in the reliable and economical design of underwater cable arrays, mooring systems, drilling risers, and offshore platforms. Many components of these complex structures typically have a cylindrical

cross-section which is conducive to vortex shedding as water flows past them.

As the state of the ocean engineering art steadily progresses, more and more stringent demands are being placed upon the performance of cable structures and moorings. In particular, displacement tolerances and constraints in response to currents are becoming more stringent; fatigue is becoming an important design consideration; and the sensitivity of acoustic sensors has increased to the point that these sensors cannot differentiate between legitimate acoustic targets and slight variations in their verti- cal position. All of these are problems that are aggravated by cable strumming. In order to design a structure or cable system to meet the constraints imposed by operational and environmental require- ments, the engineer must be able to assess the effect of strumming on the structure in question.

1.3 Scope of the Report

One purpose of this report is to describe the field test program and to summarize the results from it. Time histories of the measured hydrodynamic drag coefficients, current speeds, and cable strum- ming responses are presented and discussed. Predictions are made of the hydrodynamic drag on a bare cable and these predictions are compared with the field test data for selected conditions when the cable was observed to be resonantly strumming. The natural frequencies for the cable with attached masses were measured in air and in water. Mode shapes were measured in air. Data for the test runs con- ducted at the field site are presented in this report.

Validation of the NATFREQ code is an objective of this report. Calculations of cable natural fre- quencies and mode shapes using the NATFREQ code were made at NRL for all of the field test runs A comparison is made in this report between the calculated natural frequencies and mode shapes and those experimental test runs that have been analyzed in sufficient detail. Also, recommendations are made of modifications that will enhance the utility of and ease of access to the code for prospective users

3

2. THE NATFREQ COMPUTER CODE

2.1 Background of NATFREQ

The NATFREQ code was developed at the California Institute of Technology for the Naval Civil Engineering Laboratory (NCEL) to calculate the natural frequencies and mode shapes of taut cables with large numbers of attached discrete masses (4). An algorithm was developed to solve the transcendental equations of cable motion by an iterative technique which permits the calculation of extremely high mode numbers. The algorithm has been implemented as a FORTRAN computer code that is available from NCEL and NRL. The algorithm that forms the basis of the NATFREQ code is described in this section of the report. A listing of the code is given in Appendix A. The methodology embodied in the NATFREQ code is computationally efficient and shows excellent convergence properties even for high mode numbers. The flexibility of the code provides the capacity for treating a wide range of cable system configurations.

The static and dynamic analyses of a cable system that experiences environmental loading require the calculation of the hydrodynamic drag forces. Strumming of the cables due to vortex shedding increases the overall mean drag force and causes a corresponding increase in the cable drag coefficient. The methods that now have been developed to calculate the drag due to strumming require as inputs the natural frequencies and mode shapes of the cable. The NATFREQ code provides a fast and accurate means for computing these parameters for taut cables with complex distributions of attached masses. It now is possible with NATFREQ to calculate the strumming drag on the cable according to the method developed at NRL (see Ref. 1), including the drag on the attached masses (see Appendix C). These drag amplification factors can be used as inputs to the DESADE and DECEL1 cable structure analysis codes which are described in Ref. 1.

2.2 Strumming of Multi-Segment Cable Systems

The natural frequencies and mode shapes of cable oscillation are obtained by an iterative substitution algorithm which finds the solution satisfying the imposed boundary conditions of the problem. The following development of the solution is essentially the same as the previous work of Sergev and Iwan (4).

4

Cable Dynamics. The system considered is shown in Fig. 1. It consists of n cable segments attached to $n - 1$ masses. The cable segments have an effective mass per unit length m_i and a tension T_i which is assumed to be constant over the length l_i of the segment. The effective attached mass (including added mass) is M_i.

Equations of Motion. The equation of motion for the displacement y_i of the ith cable segment, assuming no bending rigidity, is (see Fig. 2)

$$m_i \frac{\partial^2 y_i}{\partial t^2} = T_i \frac{\partial^2 y_i}{\partial x^2}; \quad i = 1, \ldots n. \tag{1}$$

The harmonic solution of this equation has the form

$$y_i(x,t) = Y_i(x) e^{j\omega t} \tag{2}$$

where $Y_i(x)$ gives the shape of the deformation and ω is the frequency of oscillation. Substituting Eq. (2) into Eq. (1) and solving the resulting equation gives

$$Y_i(x) = A_i \sin \alpha_i \omega x + B_i \cos \alpha_i \omega x; \quad 0 \leq x \leq l_i \tag{3}$$
$$= 1, \ldots, n$$

where

$$\alpha_i = \sqrt{m_i / T_i}. \tag{4}$$

Boundary Conditions. In addition to satisfying the equation of motion, the deflection of each cable segment must satisfy certain boundary conditions. These result from the geometric conditions imposed on the ends of the cable assembly, the continuity of displacement at each attached mass, and the balance of forces at each attached mass.

Continuity of Displacement. The displacement must be continuous at each attached mass. Therefore,

$$Y_{i+1}(0) = Y_i(l_i). \tag{5}$$

Substituting from Eq. (3) yields

$$B_{i+1} = A_i \sin \alpha_i \omega l_i + B_i \cos \alpha_i \omega l_i. \tag{6}$$

If A_i and B_i are known, Eq. (6) may be used to find B_{i+1}.
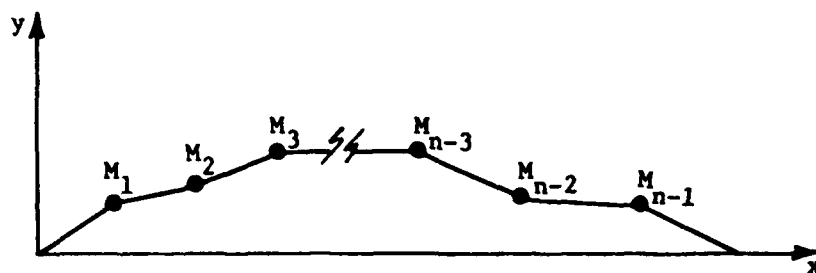
Fig. 1 — System of masses and cable segments; from Sergev and Iwan (4).
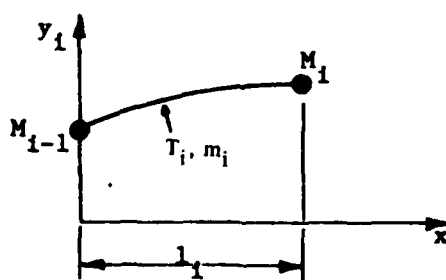
Fig. 2 — Displacement of the *i*th segment; from Sergev and Iwan (4).

6

Force Balance. Figure 3 shows the forces acting at each attached mass. The balance of forces at each of these points gives for small angles

$$T_{i+1} \left.\frac{\partial y_{i+1}}{\partial x}\right|_{x=0} - T_i \left.\frac{\partial y_i}{\partial x}\right|_{x=l_i} = M_i \left.\frac{\partial^2 y_{i+1}}{\partial t^2}\right|_{x=0}. \tag{7}$$

Substituting from Eqs. (2) and (3) yields

$$T_{i+1}\alpha_{i+1}A_{i+1} - (\alpha_i A_i \cos \alpha_i \omega l_i$$
$$- \alpha_i B_i \sin \alpha_i \omega l_i) T_i = -M_i \omega B_{i+1} \tag{8}$$
$$i = 1, \ldots, n.$$

Using Eq. (6) and solving Eq. (8) for A_{i+1} gives

$$A_{i+1} = \frac{1}{\alpha_{i+1}T_{i+1}} [(\alpha_i T_i \cos \alpha_i \omega l_i - M_i \omega \sin \alpha_i \omega l_i) A_i$$
$$- (\alpha_i T_i \sin \alpha_i \omega l_i + M_i \omega \cos \alpha_i \omega l_i) B_i]. \tag{9}$$

If A_i and B_i are known, Eq. (9) may be used to find A_{i+1}.

Geometric Boundary Conditions. At the left hand end of the cable assembly, the displacement is assumed to be zero. Thus,

$$Y_1(0) = 0. \tag{10}$$

Substituting from Eq. (3) thus implies that

$$B_1 = 0. \tag{11}$$

Since the scale of the deflected shape of the cable (mode shape) is, at this point, arbitrary, let

$$A_1 = 1. \tag{12}$$

With conditions (11) and (12) on A_1 and B_1 and Eqs. (6) and (9) for A_{i+1} and B_{i+1}, all subsequent A's and B's can be determined provided ω (the natural frequency) is known.

The system must satisfy one additional boundary condition at the right hand end of the cable assembly, where the displacement is again assumed to be zero. This gives

$$Y_n(l_i) = 0 = Y_{n+1}(0). \tag{13}$$

Equation (13) in turn implies that

$$B_{n+1} = 0. \tag{14}$$

The values of ω which give solutions satisfying condition (14) are the natural frequencies of the system. This is a shooting technique.

2.3 Solution Algorithm for Mode Shapes and Frequencies

If ω is varied from zero to some large value and the corresponding values of B_{n+1} calculated, the result will be as shown in Fig. 4. Each point for which $B_{n+1} = 0$ represents a valid solution of the free oscillation problem. The ω_k so obtained are the natural frequencies of the system. Mathematically there are an infinite number of such frequencies.

The mode shape associated with each natural frequency ω_k will be denoted by $Y_i^{(k)}(x)$. Then,

$$Y_i^{(k)}(x) = A_i^{(k)} \sin \alpha_i \omega_k x + B_i^{(k)} \cos \alpha_i \omega_k x. \tag{15}$$

Let ω_k be the kth natural frequency. Then the deflected shape of the cable system will be such that the number of internal zero crossings (nodes) is equal to $k - 1$. The mode number of a particular mode shape may therefore be determined by counting the number of internal zeros associated with the function $Y_i^{(k)}$; $i = 1, \ldots, n$.

One of the example cases computed with NATFREQ was a 15400 ft long cable with 380 attached bodies. The calculated modal pattern for mode number 162 is shown in Fig. 5. The complexity of the response is evident. Some additional examples and a comparison of NATFREQ results with a small-scale laboratory simulation are given by Sergev and Iwan.

2.4 Summary of the Solution Procedure

The solution process for the mode shapes and frequencies can be summarized as follows (4):

1.   Assume a value for ω_k.

2.   Let $B_1 = 0$, $A_1 = 1$

8
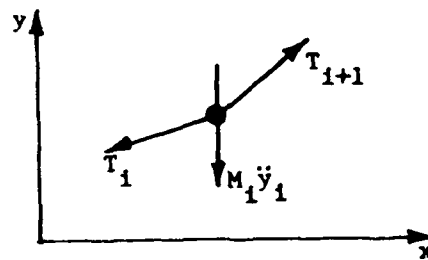
Fig. 3 — Force balance; from Sergev and Iwan (4)
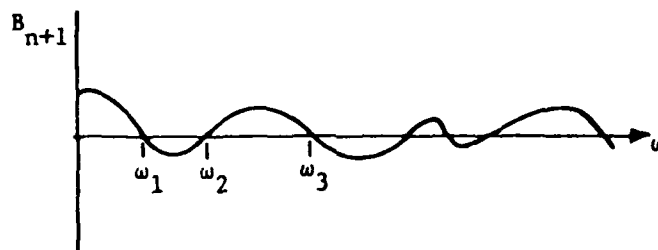
Fig. 4 — Schematic of system natural frequencies; from Sergev and Iwan (4)

9

3. Solve for B_2, A_2; B_3, A_3; ...; B_n, A_n; B_{n+1} from Eqs. (6) and (9).

4. Check for $B_{n+1} = 0$. If $B_{n+1} \neq 0$, compare with previous value and estimate a new trial value for ω.

5. Go to step 2 and repeat until B_{n+1} is less than some prescribed value or the change in ω_k is less than some prescribed limit.

6. Determine the mode number by calculating the number of internal zeros of the mode shape $Y_i^{(k)}(x)$; $i = 1, ... n$.

A listing of the NATFREQ computer code presently in use at NRL is given in Appendix A.

3. THE TEST SITE AND INSTRUMENTATION

3.1 The Test Site

The site chosen for the experiment was a sandbar located at the mouth of Holbrook Cove near Castine, Maine. This was the same site used for previous experiments during the 1970's by Vandiver and Mazel (5,6). At low tide the sandbar was exposed allowing easy access to the test equipment, while at high tide it was covered by about ten feet of water. The test section was oriented normal to the direction of the current which varied from 0 to 2.4 ft/s over the tidal cycle with only small spatial variation over the test section length at any given moment.

The data acquisition station for the experiment was the *R/V Edgerton* which was chartered from the MIT Sea Grant Program. The *Edgerton* was moored for the duration of the experiment approximately 300 feet from the sandbar and connected to the instruments on the sandbar by umbilicals.

Prior to the data acquisition phase of the experiment, several days were needed to prepare the site. A foundation for the experiment was needed to anchor the supports which were to hold the ends of the test cylinders. To accomplish this, six 4.5-inch diameter steel pipes were water jetted into the sandbar utilizing the fire pump aboard the *Edgerton*. These six pipes were made of two five foot sections joined by couplings so that the overall length of each was ten feet. In addition, one two-inch diameter by six-foot long steel pipe was jetted into the sandbar to be used as a current meter mount. Finally, a section of angle iron was clamped to the pipe used to support the drag measuring mechanism and attached to another support pipe to prevent any rotation of the drag mechanism mount. Figure 6 shows a schematic diagram of the set-up of the experiment.

3.2 Test Instrumentation

Drag measurement system. The drag measurement system was located at the west end of the cable system as shown in Fig. 6. The device was welded onto a support pipe 2.5 feet above the mud line. The mean drag force at the termination of the cable was used to generate a moment about a freely

11

MODE NO. = 162

X = 15400.0 FT

X = 0

+4

-4

DISPLACEMENT/in.

Fig. 5 — The NATFREQ-computed mode shape (mode-number n = 162) for a 15400 ft long marine cable with 380 attached masses; from Sergev and Iwan (4). 1 in = 25.4 mm.

12

SCHEMATIC DIAGRAM OF THE EXPERIMENT TEST SECTION

Fig. 6 — Schematic diagram of the Castine Bay field test set-up; from Vandiver and Griffin (7)   1 in = 25.4 mm.

13

rotating vertical shaft located a few inches beyond the termination point. The bearings supporting the shaft carried the entire tension load without preventing rotation. The moment was balanced by a load cell which restrained a lever arm connected to the shaft (see Fig. 7). From the known lever-arm lengths and the load cell measurements the mean drag force on one half of the cable could be determined. The load cell signal was carried by wires in the cable and umbilical to the *Edgerton* where it was conditioned and recorded.

Current measurement system. The current was measured by a Neil Brown Instrument Systems DRCM-2 Acoustic Current Meter located 12.5 ft from the west end of the test cable and 2 ft upstream. It was set so that it determined both normal and tangential components of the current at the level of the test cable. Signals from the current meter traveled through umbilicals to the *Edgerton* where they were monitored and recorded. In addition, a current meter traverse was made using an Endeco current meter to determine any spatial variations in current along the test section. The current was found to be spatially uniform to within ±3.0 percent from end to end for all but the lowest current speeds (V < 0.5 ft/s).

Tension measurement system. The tension measuring and adjusting system was located at the east end of the experimental test set up (see Fig. 6). Extensions were made to the two inner water-jetted posts at this end. As shown in the diagram, a five-foot extension was made to the center post and a three foot extension was made to the innermost post. This three-foot extension was different from the rest in that its attachment to the jetted pipe at the mudline was a pin connection as compared to the standard pipe couplings used on the other extensions. A hydraulic cylinder was mounted 2.5 ft above the mudline onto this pivoting post. The test cable in the experiments was connected at one end to this hydraulic cylinder and at the other end to the drag measuring device. To the back of the hydraulic cylinder one end of a Sensotec Model RM In-Line load cell was connected. The other end of the cell was attached via a cable to the center post. The output from the tension load cell was transmitted through the umbilicals to the *Edgerton* where it was monitored. Hydraulic hose ran from a pump on the *Edgerton* to the hydraulic cylinder so that the tension could be changed as desired. Additional details

14
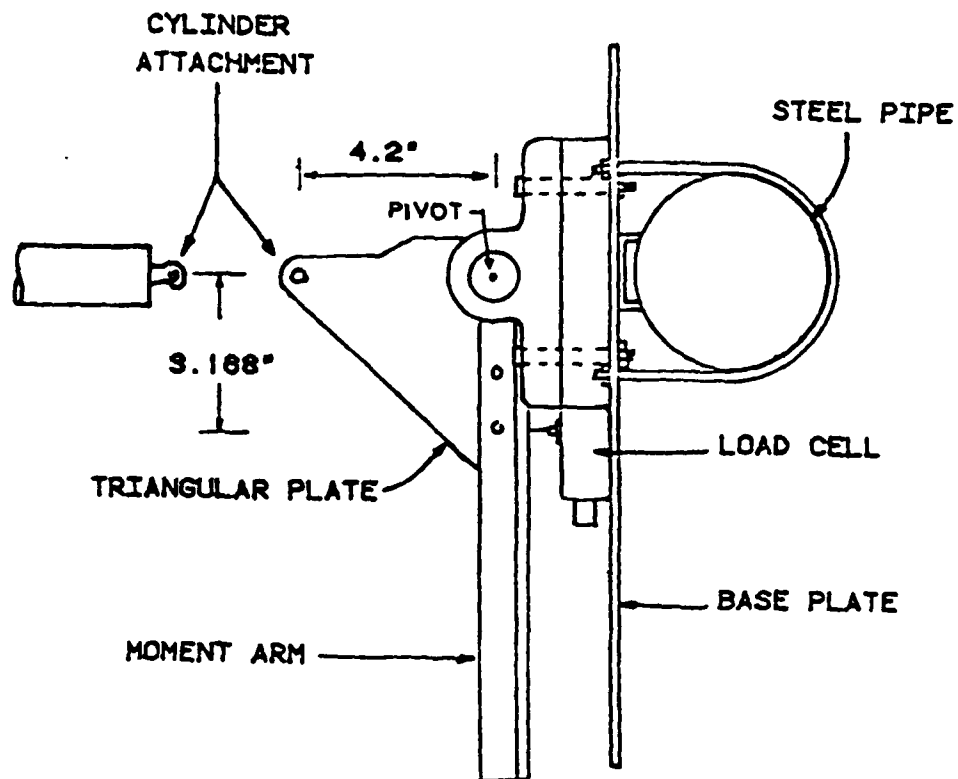
Fig. 7 — Line diagram of the drag measuring device—top view; from Vandiver and Griffin (7). 1 in = 25.4 mm.
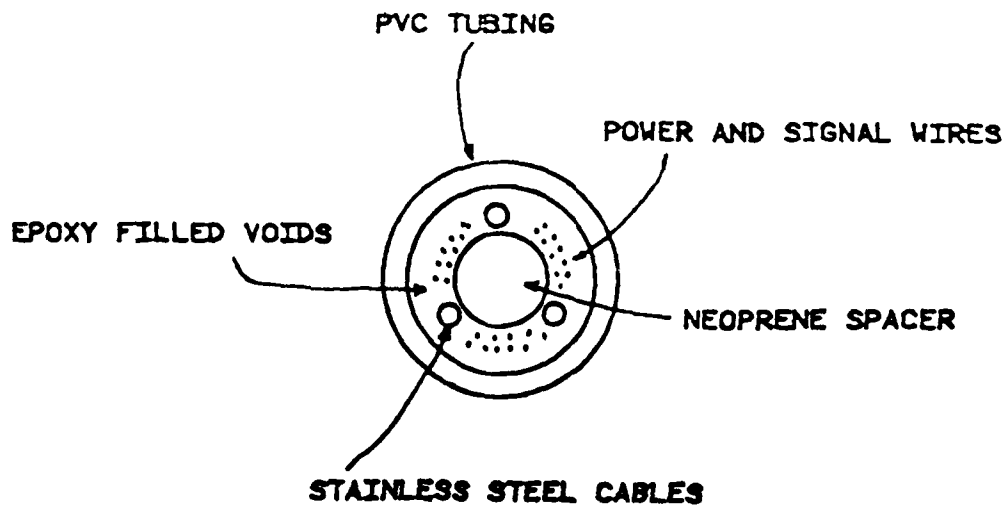
Fig. 8 — A cross-section of the test cable; from Vandiver and Griffin (7).

concerning the test instrumentation are given by McGlothlin (8).

3.3 Data Acquisition Systems

During the experiment, data taken from the instruments on the sandbar were recorded in two ways. First, analog signals from the fourteen accelerometers in the cable as well as current and drag were digitized, at 30.0 Hz per channel, onto floppy disks using a Digital Equipment MINC-23 Computer. Second, analog signals from the drag cell, current meter, and six accelerometers were recorded by a Hewlett-Packard Model 3968A Recorder onto eight-track tape. The disks were limited to record lengths of eight and one half minutes and were used to take data several times during each two and one half hour data acquisition period. A Hewlett-Packard 3582A Spectrum Analyzer was set up to monitor the real time outputs of the accelerometers. The eight-track tape was used to provide a continuous record of the complete two and one half hour test run.

4. THE TEST CABLE SYSTEM

4.1 The Cable

A 75-foot long composite cable was developed at MIT specifically for the experiments that were conducted in the summer of 1981. Figure 8 shows a cross-section of the test cable. The outer sheath for this cable was a 75-foot long piece of clear flexible PVC tubing, which was 1.25-in. O.D. by 1.0-in I.D. Three 0.125-in. stainless steel cables ran through the tubing and served as the tension carrying members. A cylindrical piece of 0.5-in. O.D. neoprene rubber was used to keep the stainless steel cables spaced 120 degrees apart. The neoprene rubber spacer was continuous along the length except at seven positions where biaxial pairs of accelerometers were placed. Starting at the east end, these positions were at L/8, L/6, L/4, 2L/5, L/2, 5L/8, and 3L/4 These accelerometers were used to measure the response of the cable as it was excited by the vortex shedding. The accelerometers were Sundstrand Mini-Pal Model 2180 Servo Accelerometers which were sensitive to the direction of gravity The biaxial pairing of these accelerometers made it possible to determine their orientation and to extract real vertical and horizontal accelerations of the cable at the seven locations.

Three bundles of ten wires each ran along the sides of the neoprene spacer to provide power and signal connections to the accelerometers and also to provide power and signal connections to the drag measuring system. Finally, an Emerson and Cuming flexible epoxy was used to fill the voids in the cable and make it watertight. The weight per unit length of this composite cable was 0.77-lb/ft in air. A photograph of the test cable being installed for one of the test runs is shown in Fig. 9.

4.2 The Attached Masses

In some experiments, lumped masses were fastened to the bare cable to simulate the effects of sensor housings and other attached bodies. The lumped masses were made of cylindrical PVC stock and each was 12.0-in. long and of 3.5-in. diameter. A 1.25-in. hole was drilled through the center of each lumped mass so that the cable could pass through. In addition, four 0.625-in. holes were drilled symmetrically around this 1.25-in. center hole so that copper tubes filled with lead could be inserted to change the mass of lumps. In the field, it was difficult to force the cable through the holes drilled in the PVC so the masses were split in half along the length of their axes. The masses were then placed on the cable in halves and held together by hose clamps. Different tests were run by varying the number and location of lumped masses and by changing the mass of the attachments. A photograph of one of the masses attached to the test cable is shown in Fig. 10.

5. THE TEST MATRIX AND SPECIFICATIONS

5.1 Test Matrix and Specifications

The test cases conducted for the combination of the cable and the various attached masses is given in Table 1. The input data for the NATFREQ calculations of the twenty test runs are listed in Appendix B. The specifications for the cable and the various attached mass configurations are given in Table 2. The notation for the location of and type of attached mass in Table 1 is, as one example,

$$\frac{5L}{8} \ (H).$$

This notation means that the mass was heavy (H), i.e., that lead weights were inserted into the PVC cylinder, and that the attachment point was located 5/8 of the cable length from the reference

17

Fig. 9 -- Setting up for a test run at the Castine Bay field site.
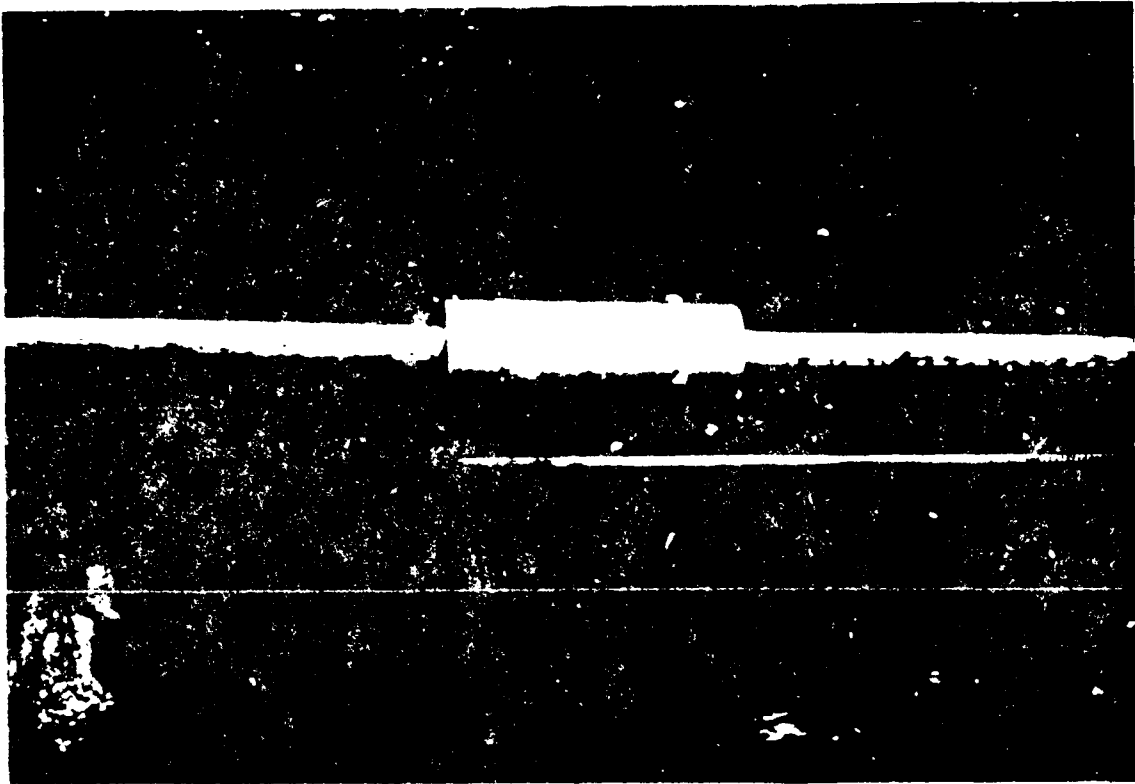
Fig. 10 — A photograph of a cylindrical mass attached to the test cable

Table 1 — Test Run Sequence
1981 Castine Bay Field Experiments,
Marine Cables with Attached Masses

Run	Location, Type of Attached Mass	Tension (pounds)	Medium
1	$\frac{L}{3}$ (L), $\frac{2L}{3}$ (L)[‡]	512**	Air[†]
2	same as above	450	Water
3	$\frac{L}{6}$ (L), $\frac{L}{3}$ (L), $\frac{L}{2}$ (L), $\frac{2L}{3}$ (L), $\frac{5L}{6}$ (L)	500	Air
4	same as above	520	Water
5	$\frac{L}{8}$ (L), $\frac{3L}{8}$ (L), $\frac{5L}{8}$ (L), $\frac{7L}{8}$ (L)	532	Air
6	same as above	475	Water
7	$\frac{L}{8}$ (L), $\frac{L}{4}$ (L), $\frac{3L}{8}$ (L), $\frac{L}{2}$ (L), $\frac{5L}{8}$ (L), $\frac{3L}{4}$ (L), $\frac{7L}{8}$ (L)	504	Air
8	same as above	475	Water
9	$\frac{L}{3}$ (H) $\frac{2L}{3}$ (H)	540	Air
10	same as above	500	Water
11	$\frac{L}{6}$ (H), $\frac{L}{3}$ (H), $\frac{L}{2}$ (H), $\frac{2L}{3}$ (H), $\frac{5L}{6}$ (H)	728	Air
12	same as above	580	Water
13	$\frac{L}{8}$ (H), $\frac{3L}{8}$ (H), $\frac{5L}{8}$ (H), $\frac{7L}{8}$ (H)	650	Air
14	same as above	650	Water
15	$\frac{L}{6}$ (H), $\frac{L}{3}$ (H), $\frac{L}{2}$ (H), $\frac{5L}{8}$ (H), $\frac{3L}{4}$ (H), $\frac{7L}{8}$ (H)	732	Air
16	same as above	556	Water
17	$\frac{L}{6}$ (H), $\frac{L}{2}$ (H), $\frac{5L}{6}$ (H), $\frac{L}{3}$ (L) $\frac{2L}{3}$ (L)	800	Air
18	same as above	765	Water
19	$\frac{L}{6}$ (L), $\frac{L}{2}$ (L), $\frac{L}{3}$ (H), $\frac{5L}{8}$ (H), $\frac{3L}{4}$ (H), $\frac{7L}{8}$ (H)	800	Air
20	same as above	800	Water

* All tensions were taken from data records from which natural frequencies were obtained.
[†] (L) = light mass. (H) = Heavy mass.
**One pound = 4.4 Newtons (SI units)

Table 2 — Cable and Attached Mass Parameters
1981 Castine Bay Field Experiments,
Marine Cables with Attached Masses

Cable Specifications:

L = 75.0 feet
D = 1.25 inches in diameter
w = 0.7704 pounds/foot in air
μ = 0.0239 slugs/foot in air
SG_c = 1.408 specific gravity

PVC Attached Mass Specifications:

Length = 12.0 inches
Outside diameter = 3.5 inches
Inside diameter = 1.25 inches
Ballast hole diameter = 0.625 inches

Weight in air =

No lead ballast, 4.4 pounds (2 kg)
Weight of water trapped in the 5/8 inch ballast
    holes when submerged in water, 0.55 pounds (0.25 kg)
Weight with lead, 9.97 pounds (4.52 kg)

termination point. The notation L in parentheses (L) means that the light mass (no lead weights) was attached at that location. The two specific gravities were chosen to match the cable's specific gravity SG = 1.3 to 1.4 (nominal) and the specific gravity SG = 2 (nominal) of typical Navy hydrophones and other cable-mounted sensor housings.

5.2 Slack Cable Limitations

Extensible slack cables are characterized by complex dynamic response behavior that is dependent upon the sag-to-span ratio and the elastic properties of the cable. One especially complicated feature of this response is a frequency "crossover" phenomenon. This modal crossover is a complex phenomenon associated with the dynamics of slack cables with small sag-to-span ratios. At the crossover *three* modes of the cable have the same natural frequency and include a symmetric in-plane mode, an anti-symmetric in-plane mode and an out-of-plane or sway mode. The symmetric modes contain an even number of nodal points along the cable while the anti-symmetric modes contain an odd number of nodes. The dynamics of slack marine cables are discussed further in Appendix B of Ref. 1, and in several other references cited there.

The onset of slack cable effects occurs near the limit of cable sag-to-span $s/l \rightarrow 0$, and the critical tension H_{crit} can be estimated with the equation (see Ref. 1)

$$H_{crit} = 0.93 \ (W^2 E_c A_c)^{1/3}, \tag{16}$$

where

W = *total* cable weight;

E_c = cable elastic modulus;

A_c = cable cross-section area.

The weight of the cable in water is

$$W = (\rho_w g) L_c A_c (SG_c - 1) \tag{17}$$

where

22

$$SG_c = \text{cable specific gravity;}$$

$$L_c = \text{cable length;}$$

$$\rho_w, \, g = \text{water density, gravitational}$$

$$\text{acceleration}$$

The Castine Bay test cable $(L_c = 75\text{-ft}, \, A_c = 1.23\text{-in.}^2)$ in sea water has the following total net weight (in water),

$$W = 41.0 \, (SG_c - 1) \, \text{lb}.$$

For a cable with a nominal value of specific gravity $SG_c = 1.41$, $W = 16.8$ lb. The product $E_c A_c$ was measured at MIT for the Castine test cable. The result was $E_c A_c = 2(10^5)$ lb. Based upon this value the critical tension in water is

$$H_{crit} = 0.93 \, (E_c A_c \, W^2)^{1/3} \, \text{lb} = 360 \, \text{lb}.$$

From this estimate a minimum tension $H = 400$ lb was recommended for the Castine Bay field experiments in order to minimize slack cable effects. The NATFREQ code algorithm is valid only for *taut* cables with arrays of attached masses.

6. NATFREQ PREDICTIONS

The NATFREQ code was used to simulate all of the test runs listed in Table 1. All of the computations were done on the Hewlett-Packard Model 1000 computer in the Fluid Dynamics Branch at NRL. A listing of the code is given in Appendix A. The listed version of the code is identical to that discussed by Sergev and Iwan (4) except for some minor input/output modifications. Input to the code typically consists of cable properties (density, tension, drag coefficient, etc.), attached mass properties (density, cross-section area, drag coefficient, etc.), and cable segment length (point masses are assumed) as shown in Appendix B. The added mass of both the cable and the attached masses was accounted for in all of the in-water test simulations. Some elaborations on the algorithm employed in NATFREQ, but not included in the code, are given by Iwan (9).

A summary of the computer simulation is given here. Typically only the first six or seven cable

23

modes were excited by the tidal current regime at the Castine field site. However, in some cases cable modes up to $n = 11$ have been identified. The computed natural frequencies and mode shapes for five pairs of typical test runs are plotted in Figs. 11 to 18. The configurations chosen for the plots are representative of the field test measurements that are discussed in the next section. Three cases with light masses attached (PVC only) and two cases with heavy masses (PVC plus lead weight inserts) are plotted in the figures.

Several points concerning the natural frequencies are of note. First, the added mass effect of the water is clearly evident in all of the computed frequencies. As expected, the added mass due to the cable vibration reduces the frequency of any given in-water mode below the corresponding in-air modal frequency. An added mass coefficient of $C_{am} = 1$ was assumed; i.e., the added masses of the cable and cylindrical attachments are equal to the respective displaced masses of water. This point is discussed further in a following section of this report.

Second, the distribution of computed modal frequencies is dependent upon the number and spacing of attached masses. For evenly spaced masses there are discontinuous jumps in the natural frequencies at multiples of the number of cable segments. This is clearly evident in Fig. 11 (two and five attached masses) and the same effect can be observed in Figs. 14, 16 and 18 (five, six and seven attached masses). The discontinuity emerges when the mode number n is equal to the number of cable segments or a multiple thereof. The difference in the cable vibration pattern due to different numbers of attached masses is evident from the $N = 2$ and $N = 5$ results in Fig. 11. The discontinuities occur at $n = 3$, 6 and 9 for the cable with two masses, whereas the first discontinuity occurs at $n = 6$ for the cable with five masses. Note that the $n = 6$ natural frequencies (and mode shapes) are equal for the two cases. This behavior also was computed by Sergev and Iwan and verified by their small scale experiment with a thin wire and four or six attached masses in air (4).

There is a relatively simple physical explanation for the discontinuous behavior of the natural frequencies. Consider as an example the computed frequencies in Fig. 14, for test runs seven and eight with seven light masses. For the first seven mode shapes plotted in Figs. 15(a) and 15(b) some or all

of the masses are in motion at their various locations in the vibration pattern. Thus the natural frequencies of the cable are reduced from the bare cable values due to the inertia of the masses. When the vibration frequency reaches the $n = 8$ mode all of the seven evenly-spaced attached masses are located at nodes of the modal vibration pattern. Then the mode shape and frequency are identical to those of the bare cable. The natural frequencies for the $n = 9$ and 10 modes fall below the bare cable frequencies when the masses attached to the cable again are in motion. Similar behavior can be observed in all of the natural frequencies plotted in Figs. 11, 14, 16 and 18.

The distribution of six masses for the test runs plotted in Fig. 16 is unevenly spaced. The discontinuity between the $n = 6$ and $n = 7$ modes still is clear, but the $n = 7$ mode in air frequency is not equal to the bare cable value as in the runs discussed previously. The mode shapes plotted in Fig. 17 show that several of the masses are in motion for $n = 7$, so that both the in-air and in-water natural frequencies are less than the bare cable value. There is a difference in tension between the two tests but that has a minimal effect on the major features of the overall cable system response.

Two otherwise identical runs with five light and five heavy masses are plotted in Fig. 18. Test runs 11 and 12 were recomputed with the cable tension $T = 500$ pounds to match the tensions of runs 3 and 4. The inertial effect of the heavier of the two attached masses is evident from the reduced natural frequencies in air and in water below the corresponding values for the lighter masses. The masses are evenly spaced and the discontinuity between the $n = 5$ and $n = 6$ modes appears as expected. For the $n = 6$ mode both sets of masses are at the same nodal points of the vibration pattern and they have no effect. The two respective pairs of natural frequencies in air and in water are equal.

Fig. 11 — In-air and in-water natural frequencies for a cable with attached masses, computed with NATFREQ. —, Test Run 1, Table 1; ——, Test Run 2; —·—, Test Run 3; ······, Test Run 4; ⊙, bare cable.

Fig. 12(a) — Test Run 1, Table 1

Fig. 12 — Mode shapes for a cable with two light attached masses, computed with NATFREQ.

27

1981 CASTINE BAY TESTS * MARINE CABLES
WITH ATTACHED SENSOR HOUSINGS * RUN 1

MODE NO. - 6

MODE NO. - 7

MODE NO. - 8

MODE NO. - 9

MODE NO. - 10

Fig. 12(a) — Continued

28
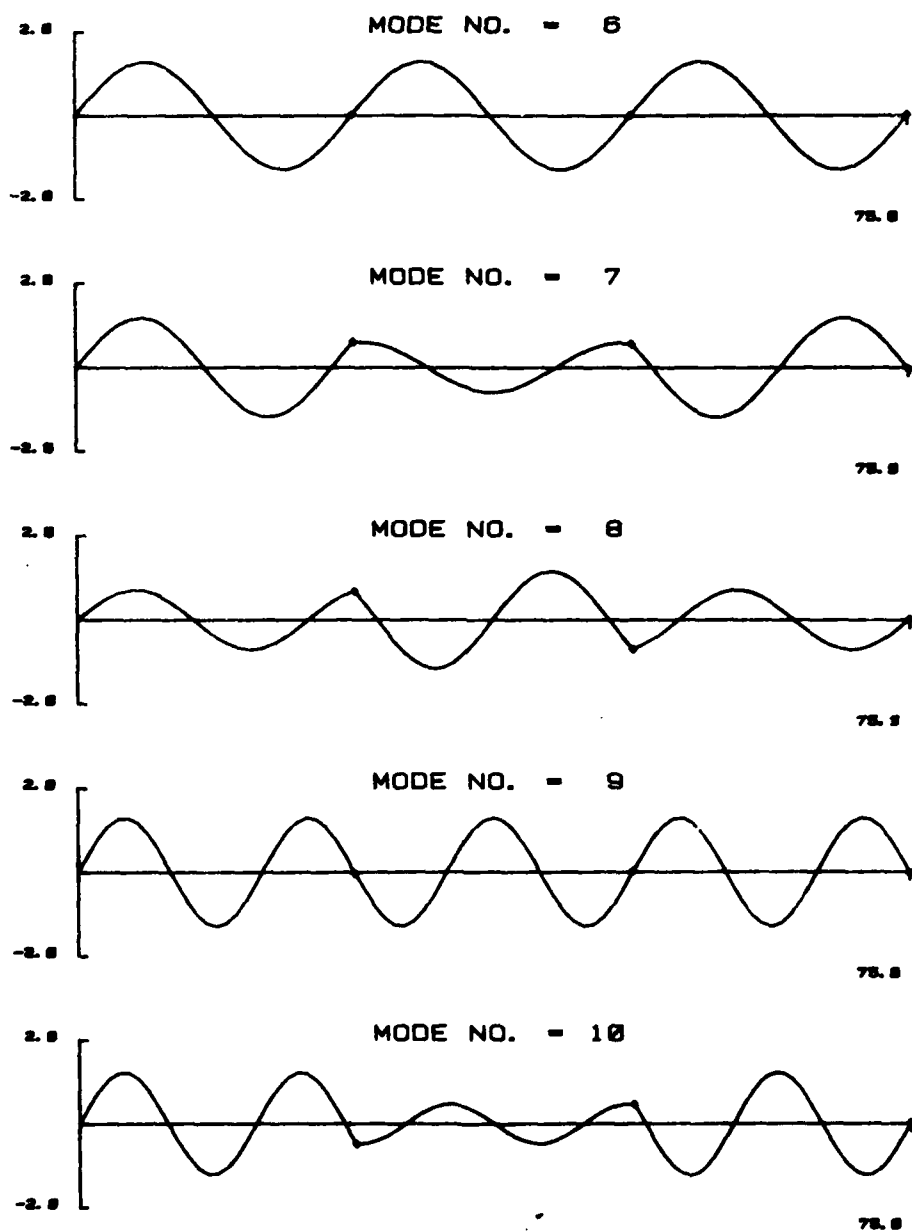
1981 CASTINE BAY TESTS * MARINE CABLES
*ITH ATTACHED SENSOR HOUSINGS * RUN 2
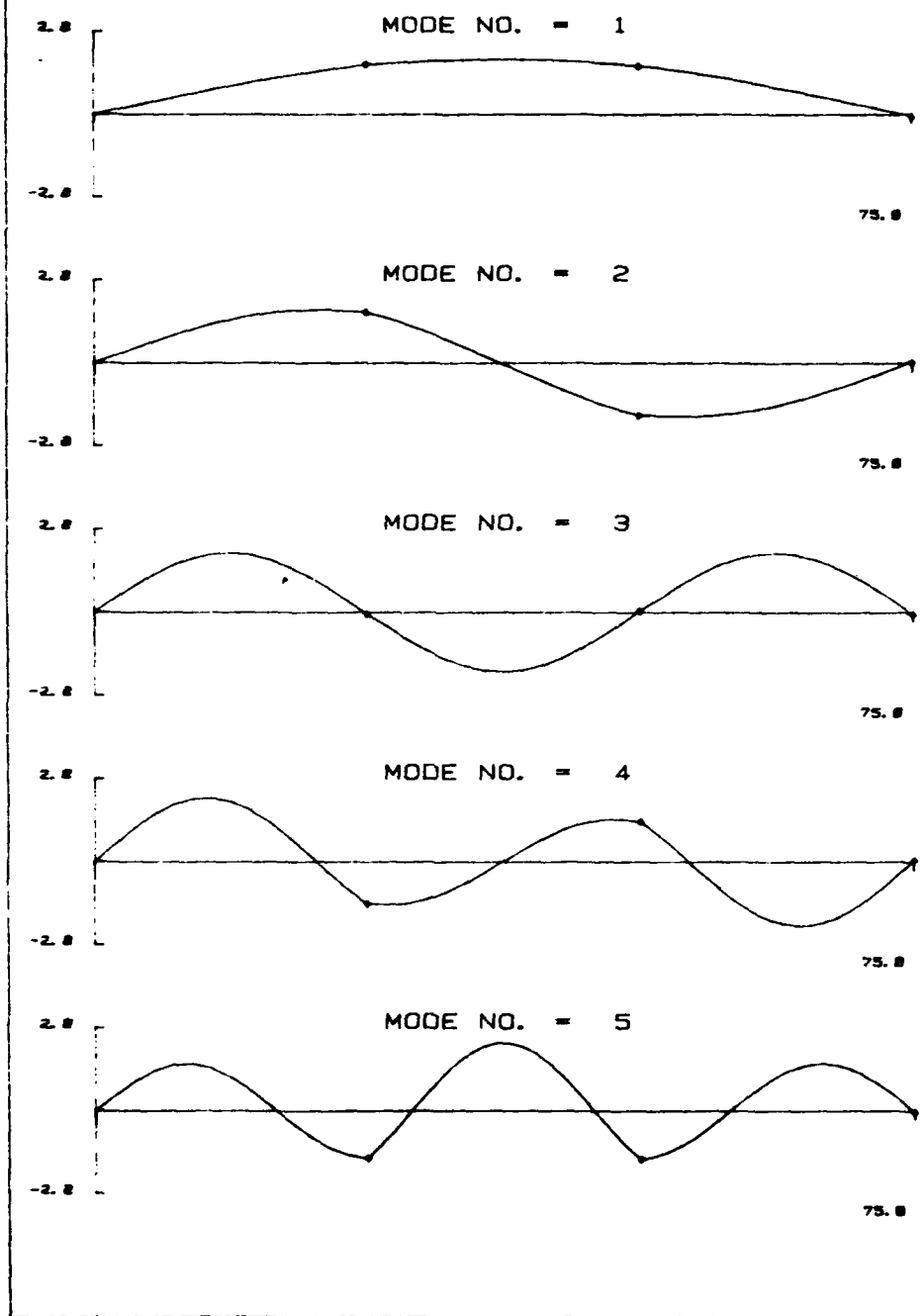
Fig. 12(b) — Test Run 2, Table 1.

29

1981 CASTINE BAY TESTS * MARINE CABLES
WITH ATTACHED SENSOR HOUSINGS * RUN 2

Fig. 12(b) — Continued

30
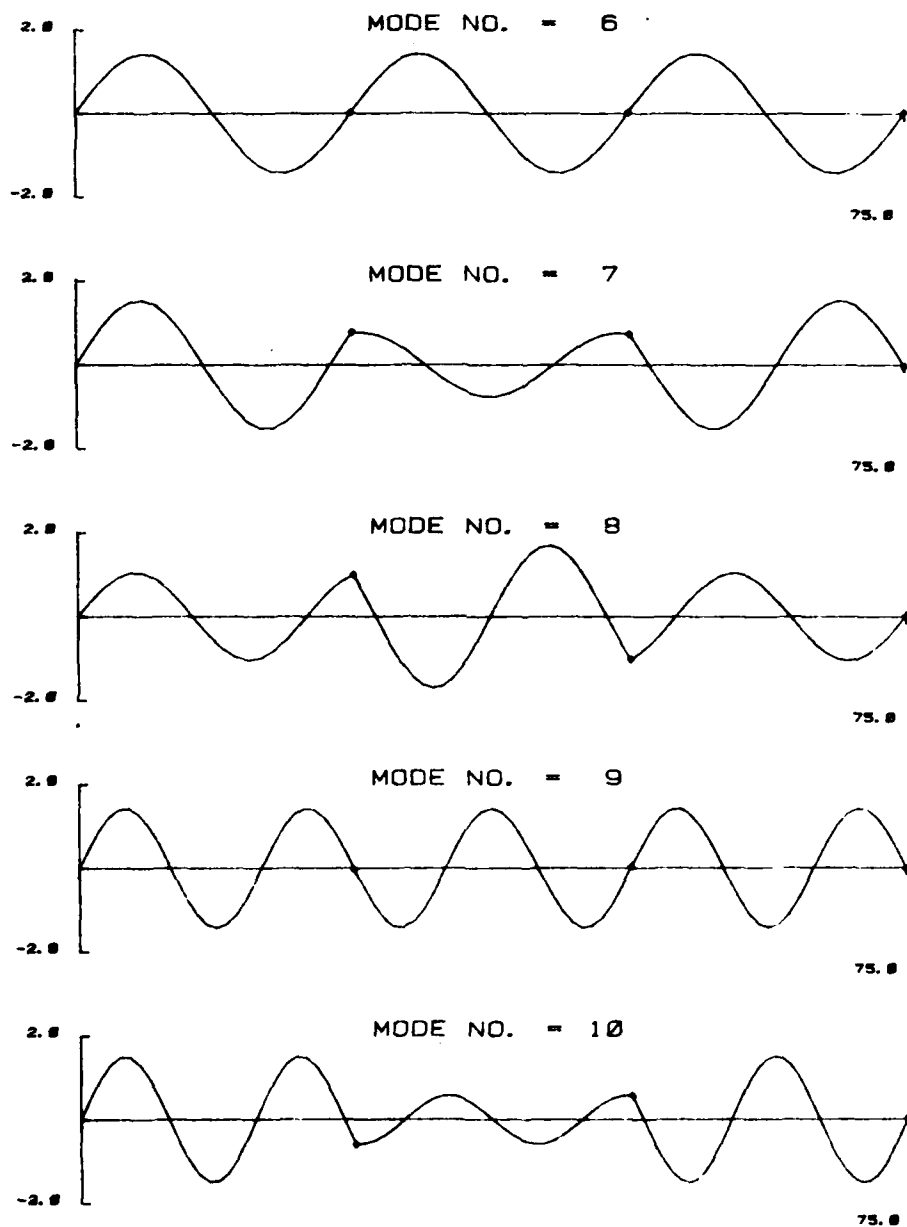
1981 CASTINE BAY TESTS * MARINE CABLES
WITH ATTACHED SENSOR HOUSINGS * RUN 3
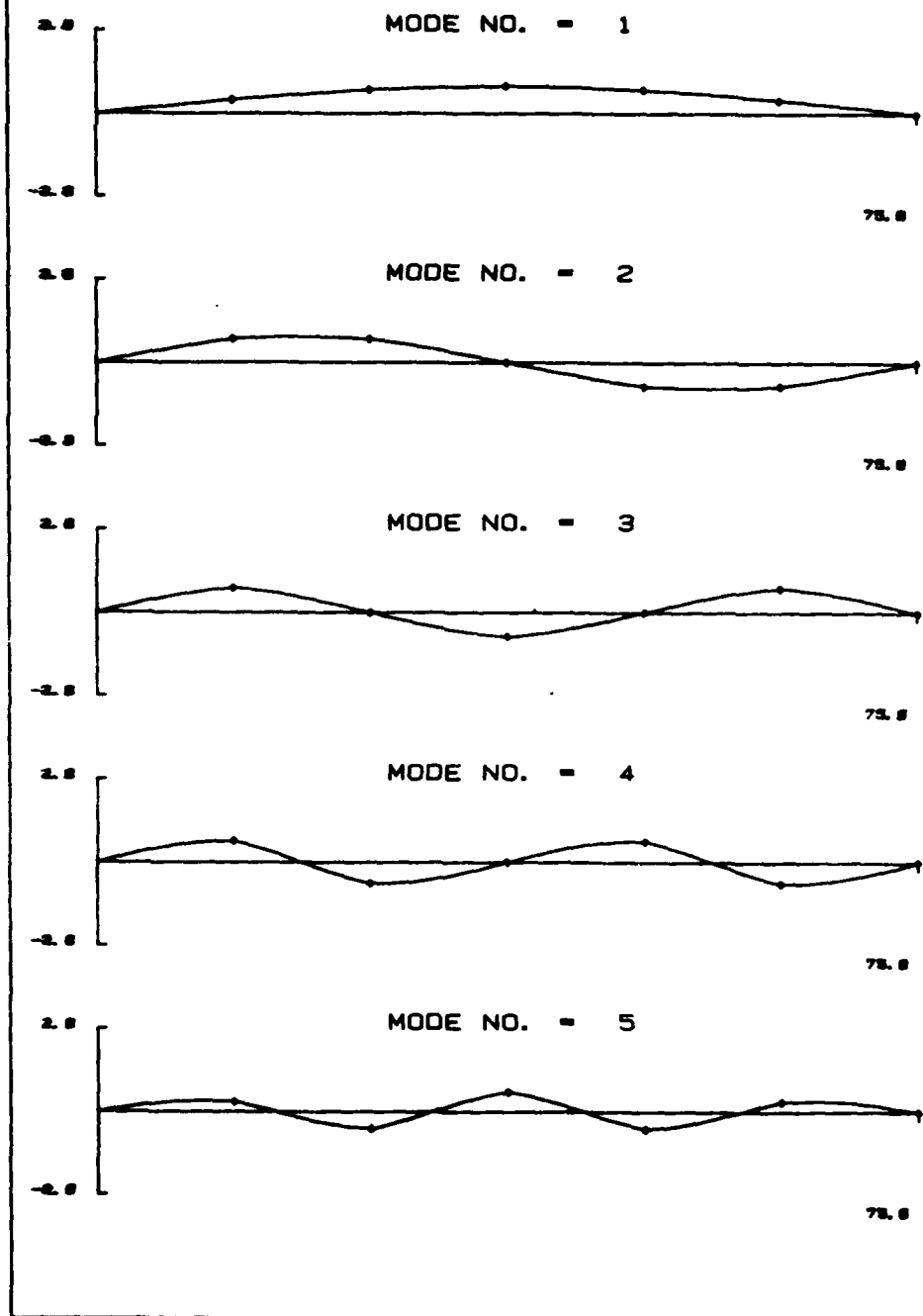
Fig. 13(a) — Test Run 3, Table 1

Fig 13 — Mode shapes for a cable with five light attached masses, computed with NATFREQ.

31

1981 CASTINE BAY TESTS * MARINE CABLES
WITH ATTACHED SENSOR HOUSINGS * RUN 3
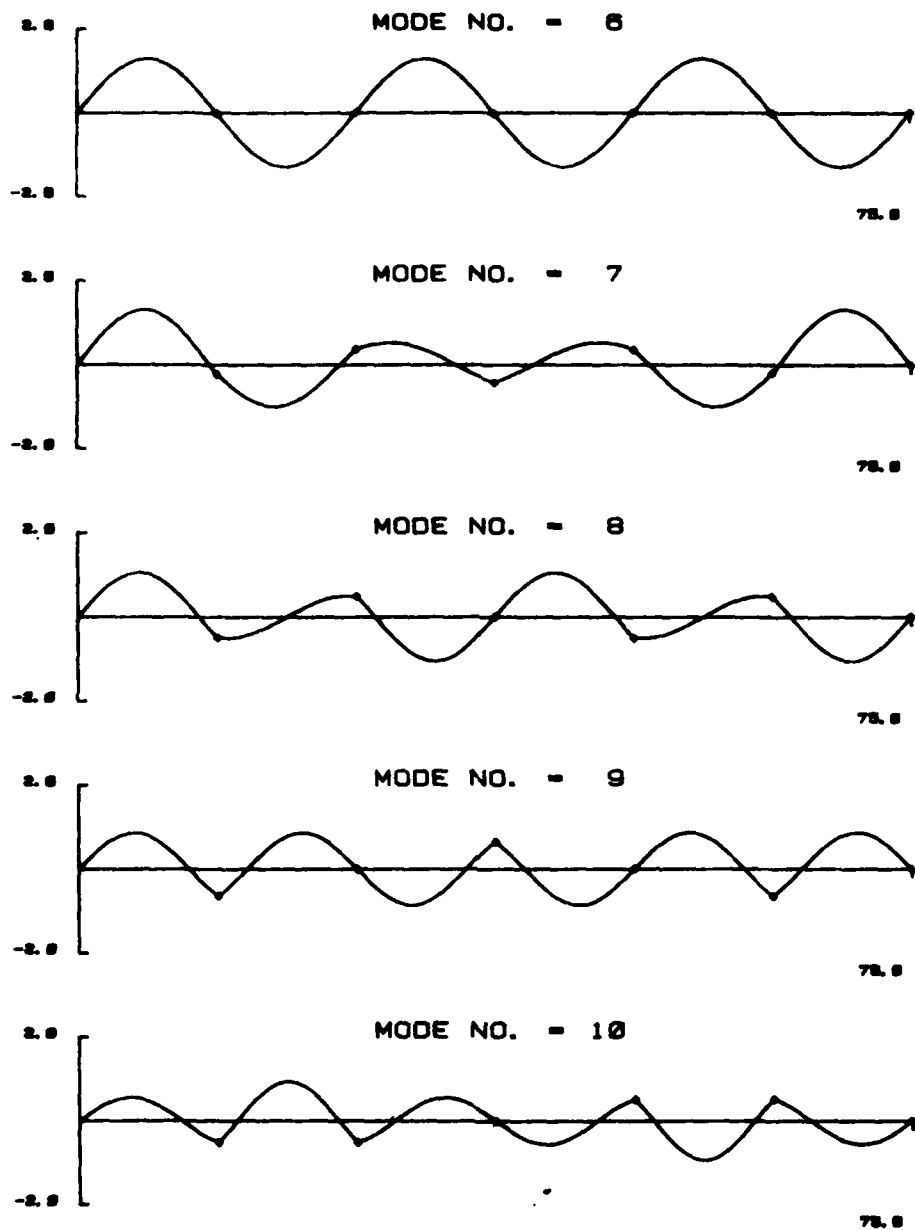
Fig. 13(a) — Continued

1981 CASTINE BAY TESTS * MARINE CABLES
WITH ATTACHED SENSOR HOUSINGS * RUN 4
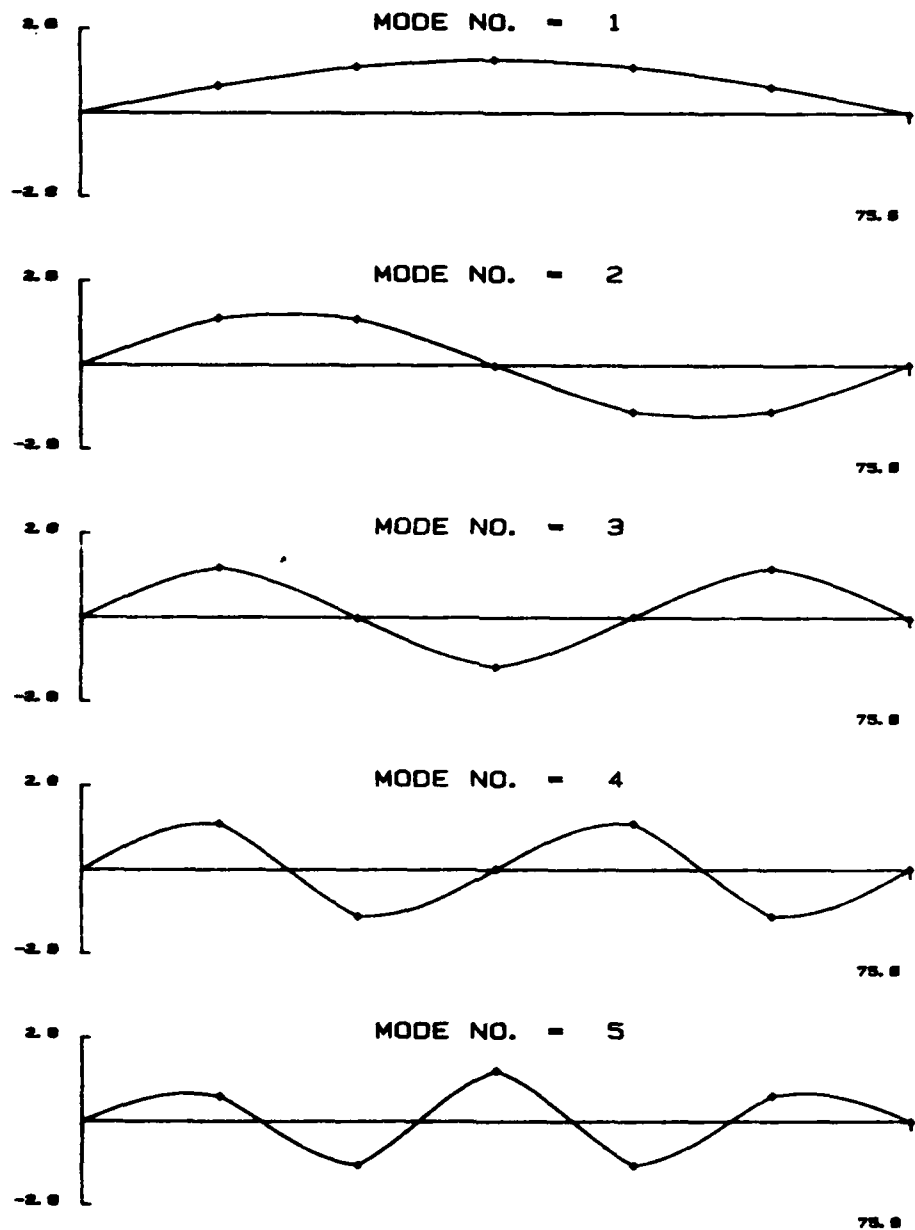
Fig. 13(b) — Test Run 4, Table 1

33

1981 CASTINE BAY TESTS * MARINE CABLES WITH ATTACHED SENSOR HOUSINGS * RUN 4
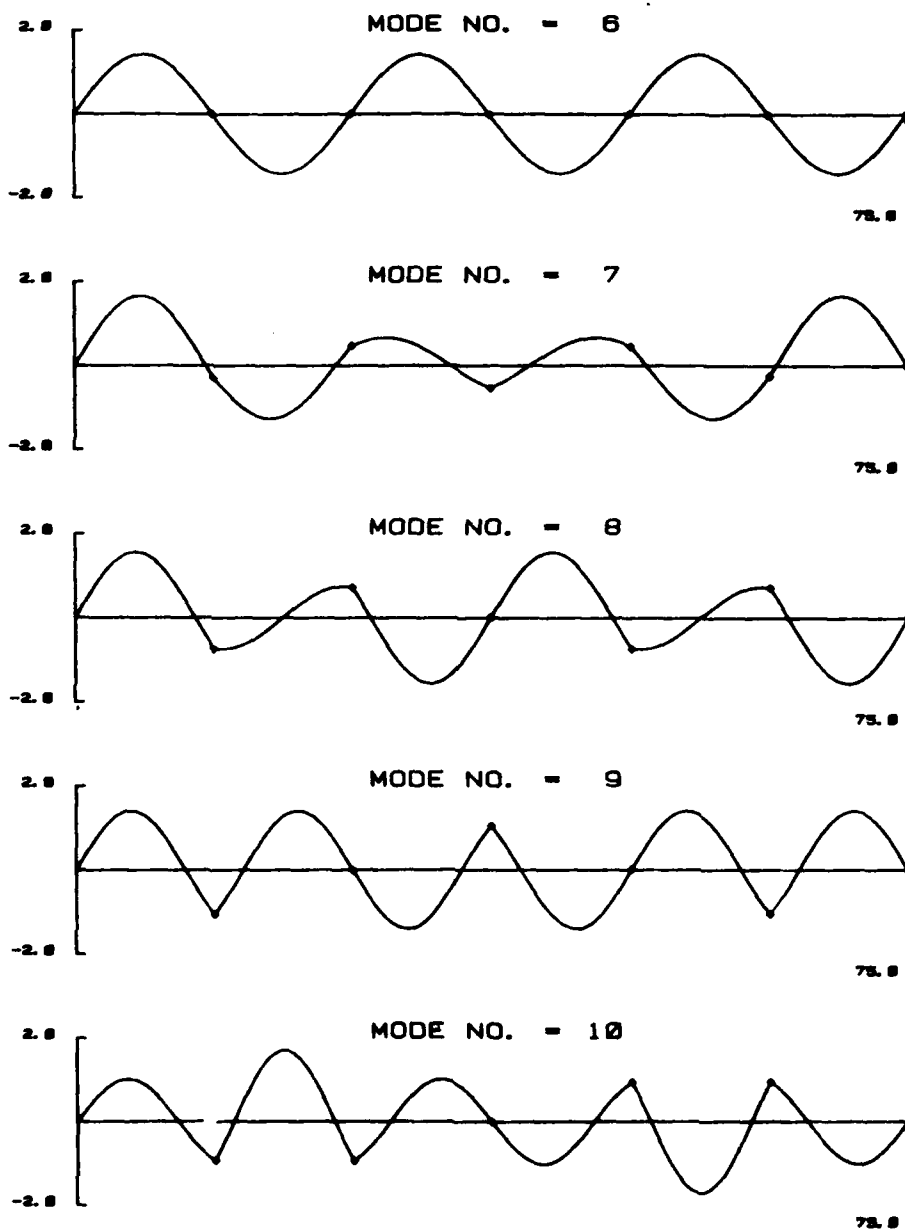
Fig. 13(b) — Continued
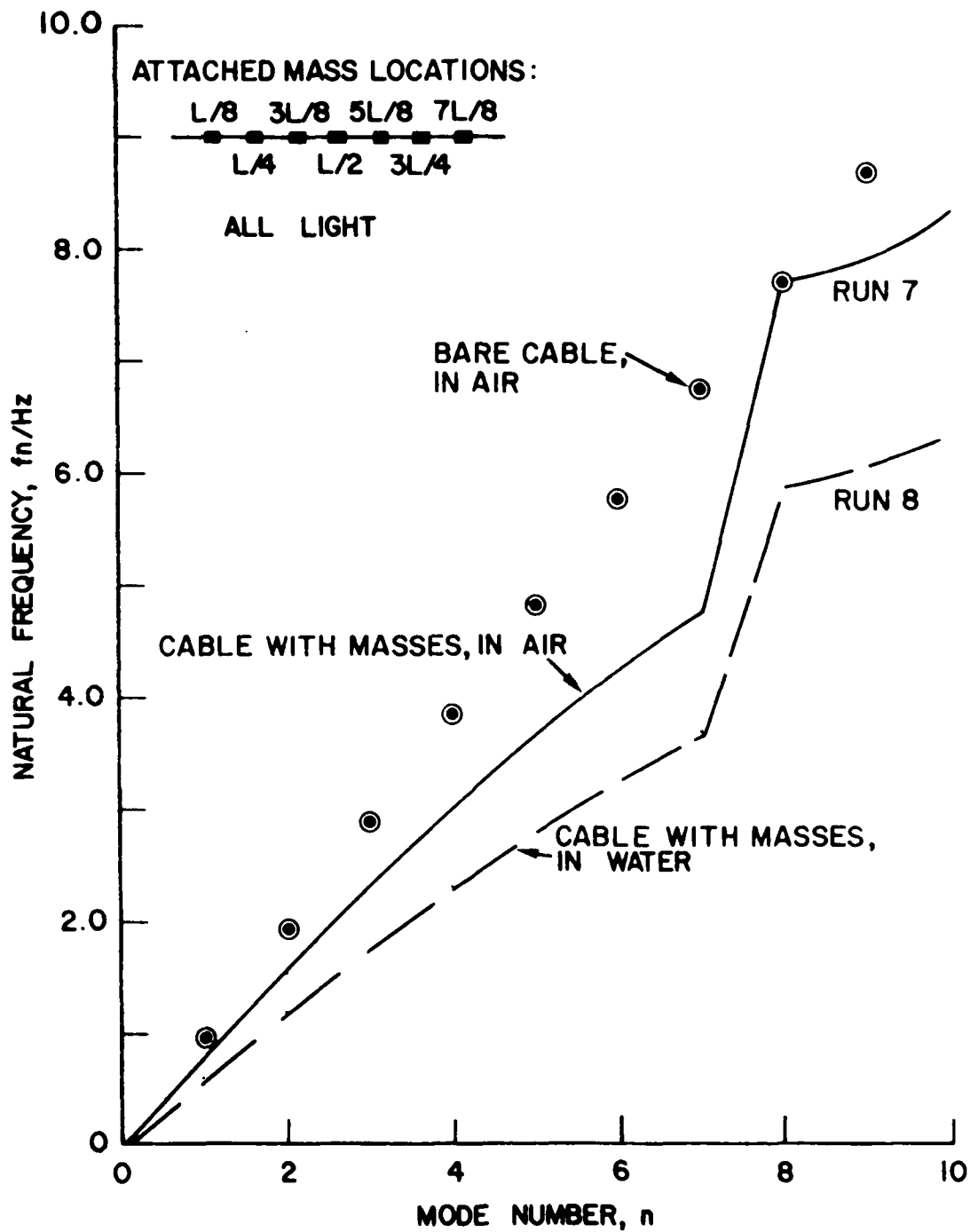
Fig. 14 — In-air and in-water natural frequencies for a cable with seven light attached masses, computed with NATFREQ —. Run 7, Table 1. ———, Run 8. ○, bare cable.

35

1981 CASTINE BAY TESTS * MARINE CABLES
WITH ATTACHED SENSOR HOUSINGS * RUN 7

MODE NO. - 1

MODE NO. - 2

MODE NO. - 3

MODE NO. - 4

MODE NO. - 5

Fig. 15(a) — Test Run 7, Table 1.

Fig. 15 — Mode shapes for a cable with seven light attached masses, computed with NATFREQ.

36

Fig. 15(a) — Continued

37
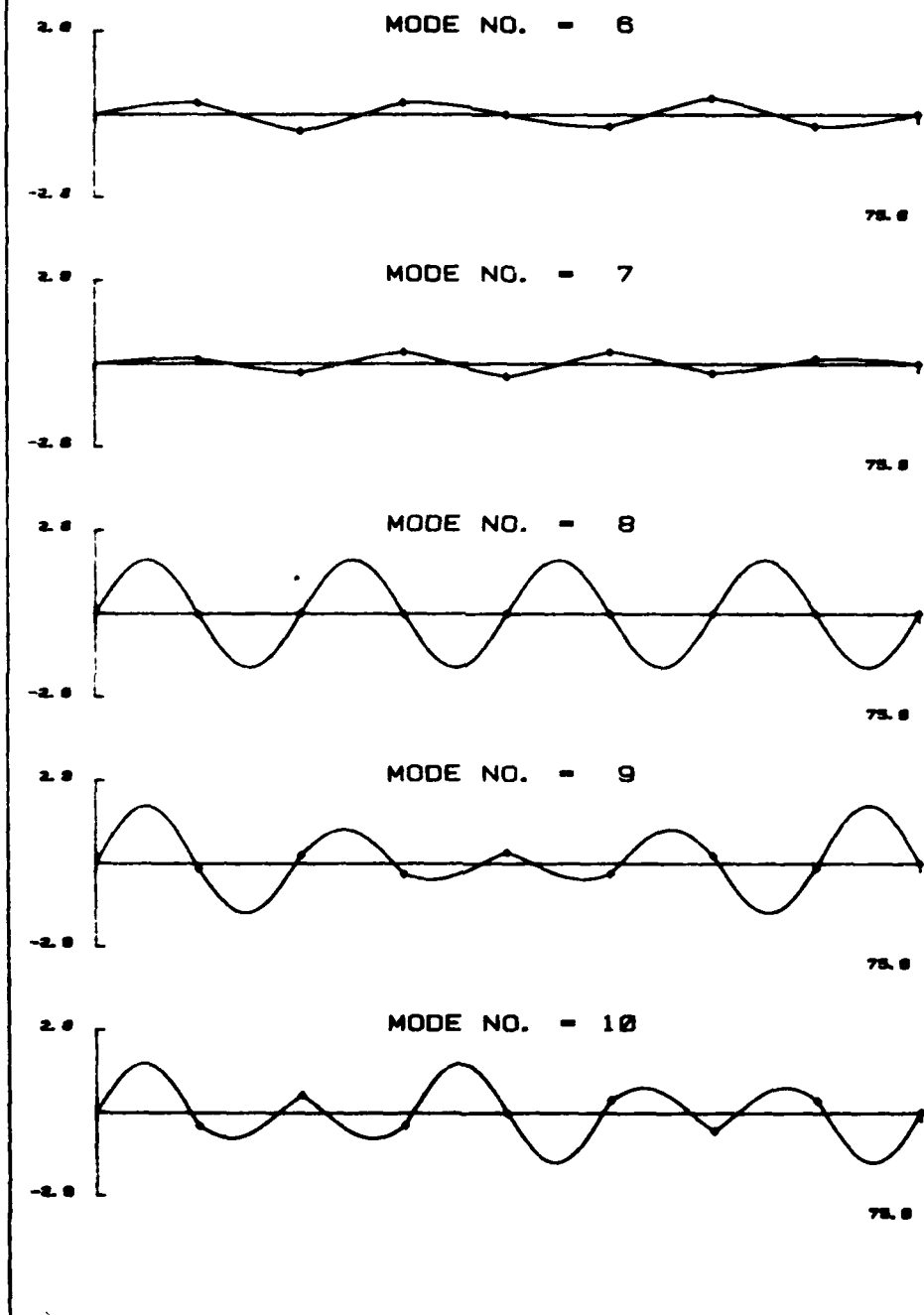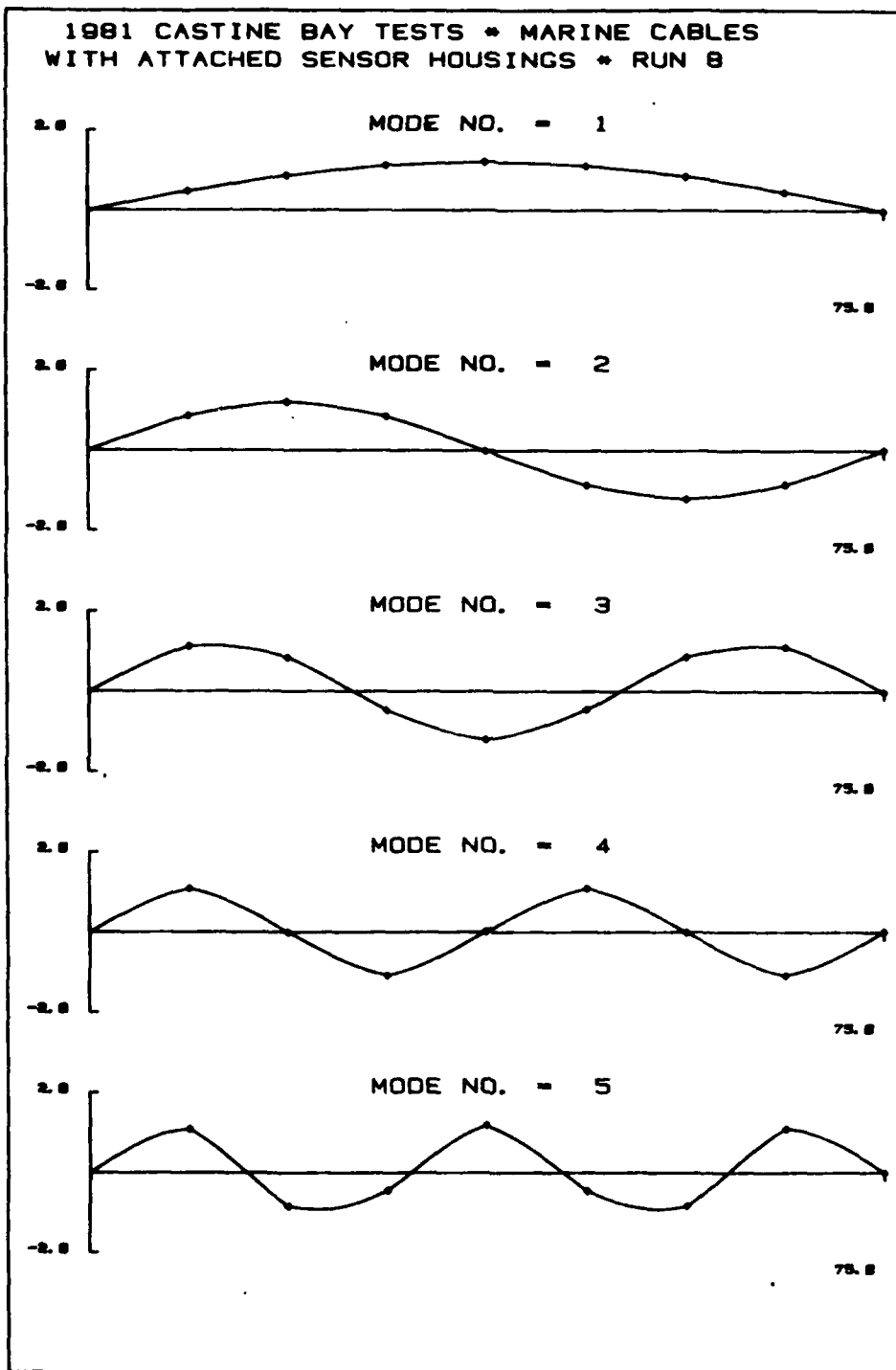
1981 CASTINE BAY TESTS * MARINE CABLES
WITH ATTACHED SENSOR HOUSINGS * RUN 8

Fig. 15(b) — Test Run 8, Table 1.

1981 CASTINE BAY TESTS * MARINE CABLES
*ITH ATTACHED SENSOR HOUSINGS * RUN 8

MODE NO. = 6

MODE NO. = 7

MODE NO. = 8

MODE NO. = 9

MODE NO. = 10

Fig. 15(b) — Continued

39
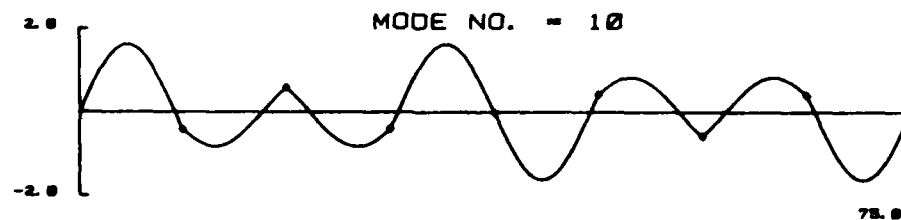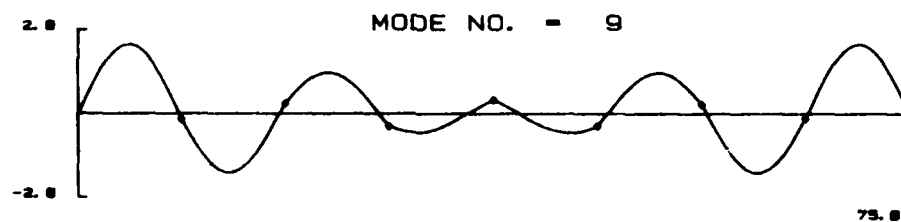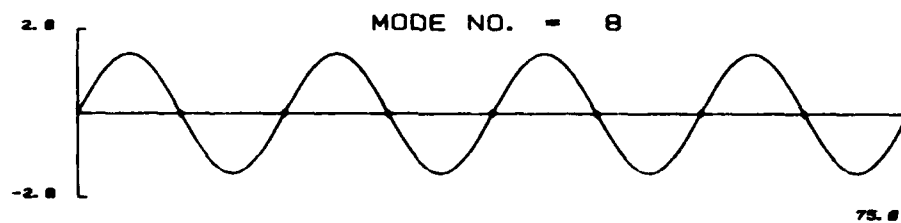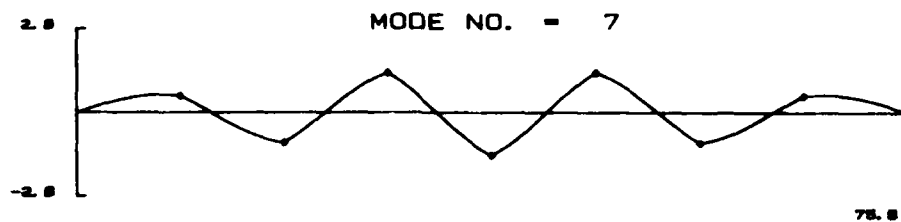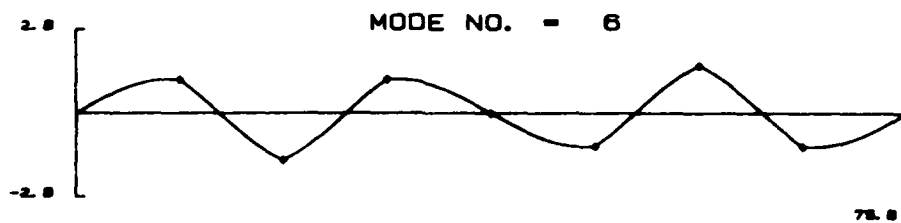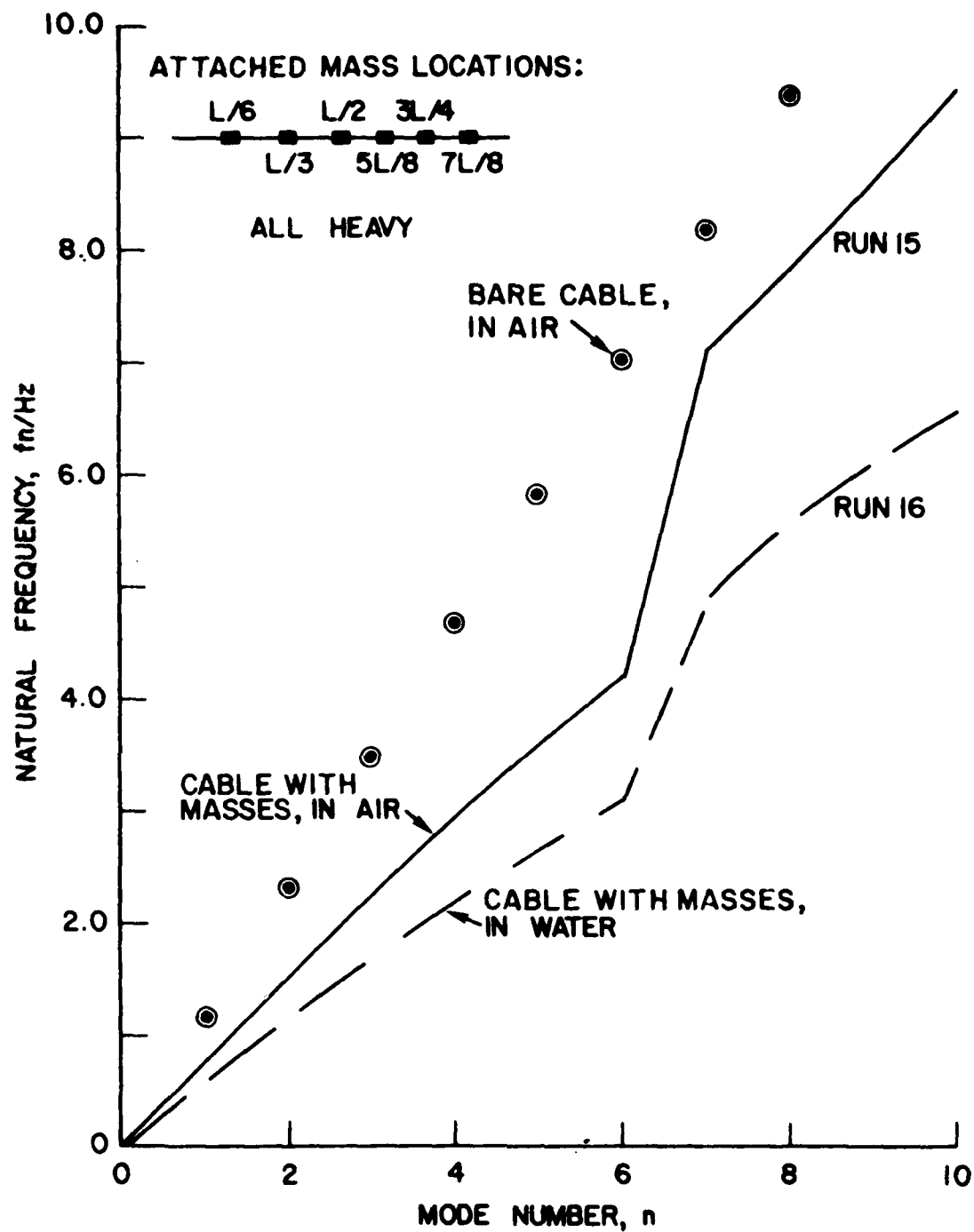
Fig. 16 — In-air and in-water natural frequencies for a cable with six heavy attached masses, computed with NATFREQ. —. Run 15, Table 1; — —. Run 16; ○, bare cable.

1981 CASTINE BAY TESTS * MARINE CABLES
WITH ATTACHED SENSOR HOUSINGS * RUN 15

MODE NO. = 1

MODE NO. = 2

MODE NO. = 3

MODE NO. = 4

MODE NO. = 5
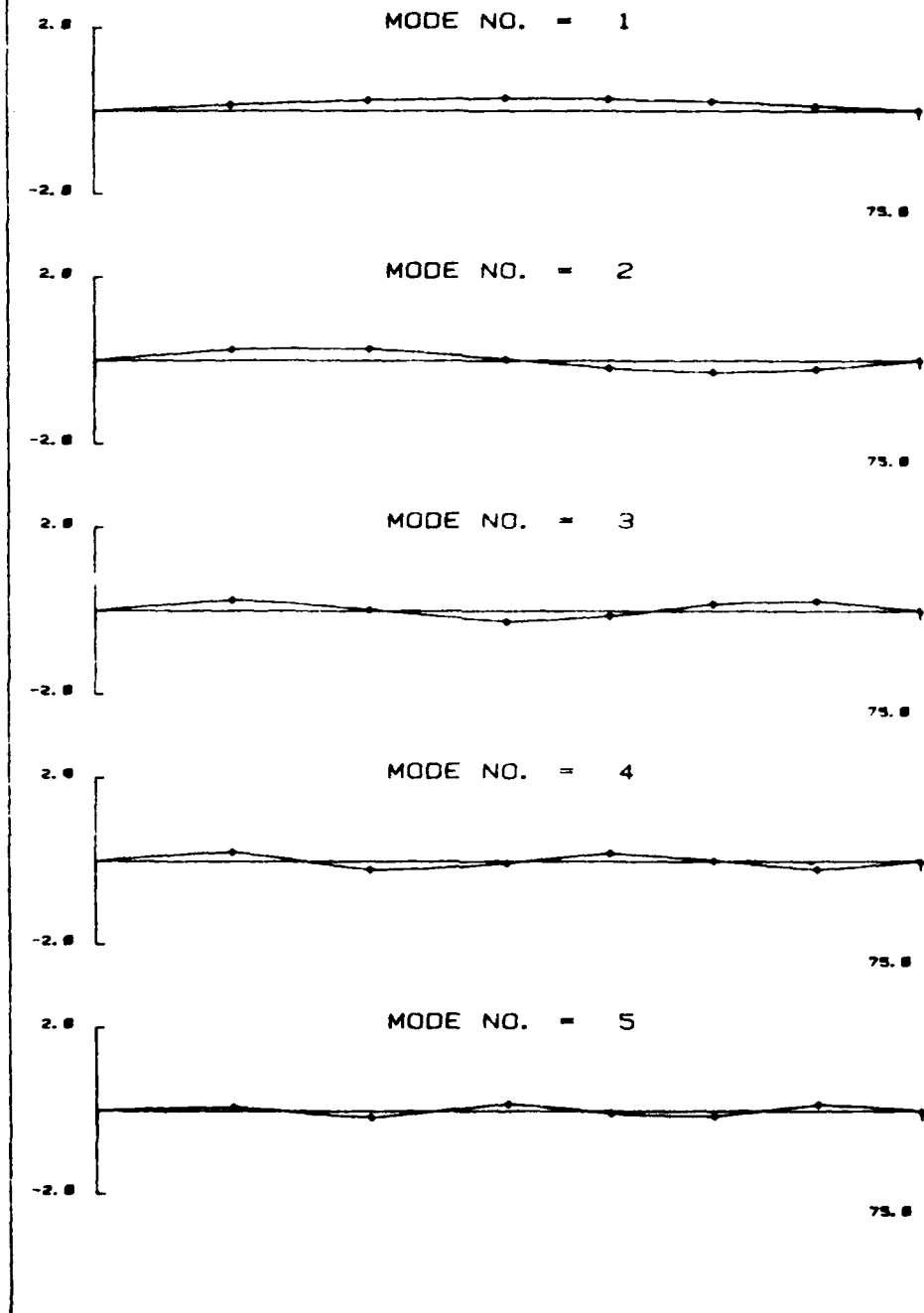
Fig. 17(a) — Test Run 15, Table I

Fig. 17 — Mode shapes for a cable with six heavy attached masses, computed with NATFREQ.

41

1981 CASTINE BAY TESTS * MARINE CABLES
WITH ATTACHED SENSOR HOUSINGS * RUN 15
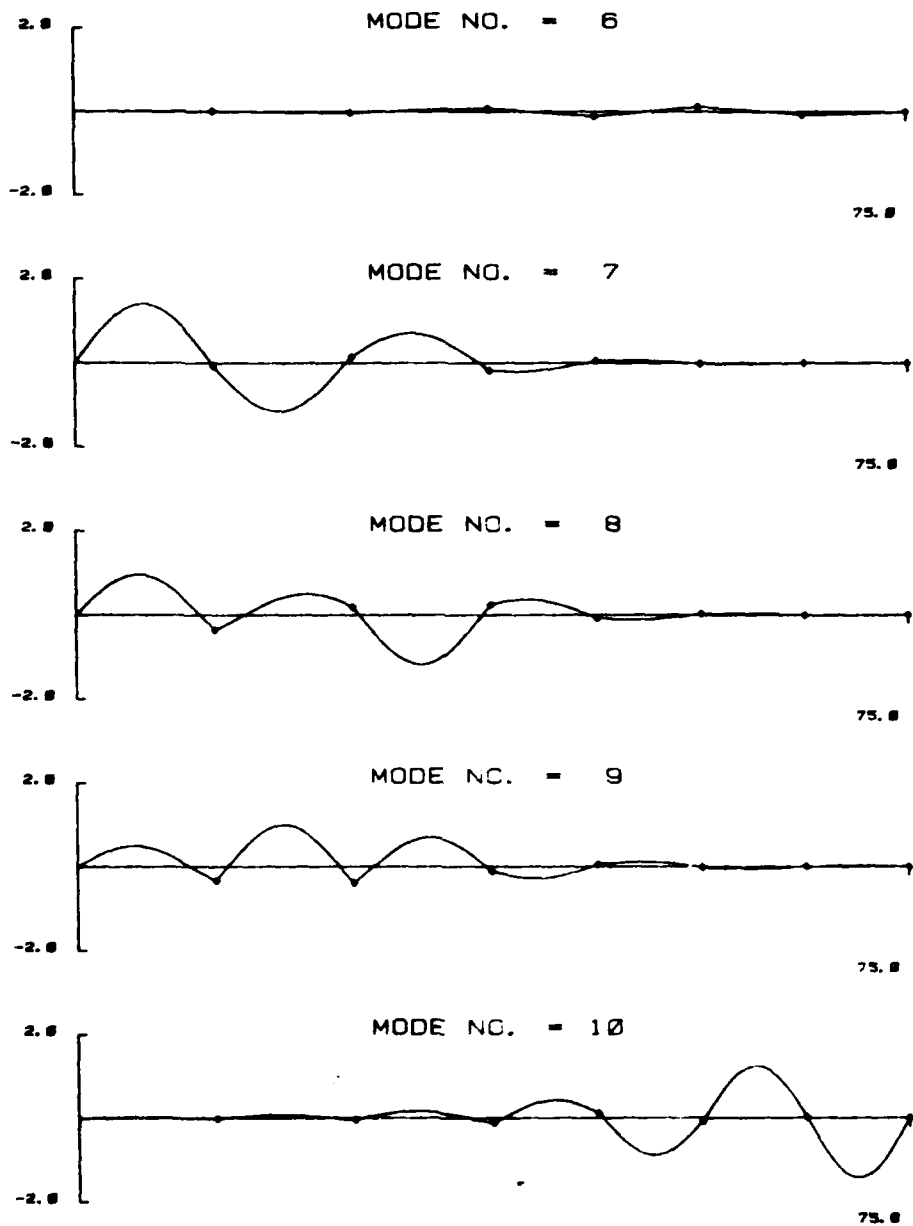
Fig 17(a) — Continued

1981 CASTINE BAY TESTS * MARINE CABLES
WITH ATTACHED SENSOR HOUSINGS * RUN 16
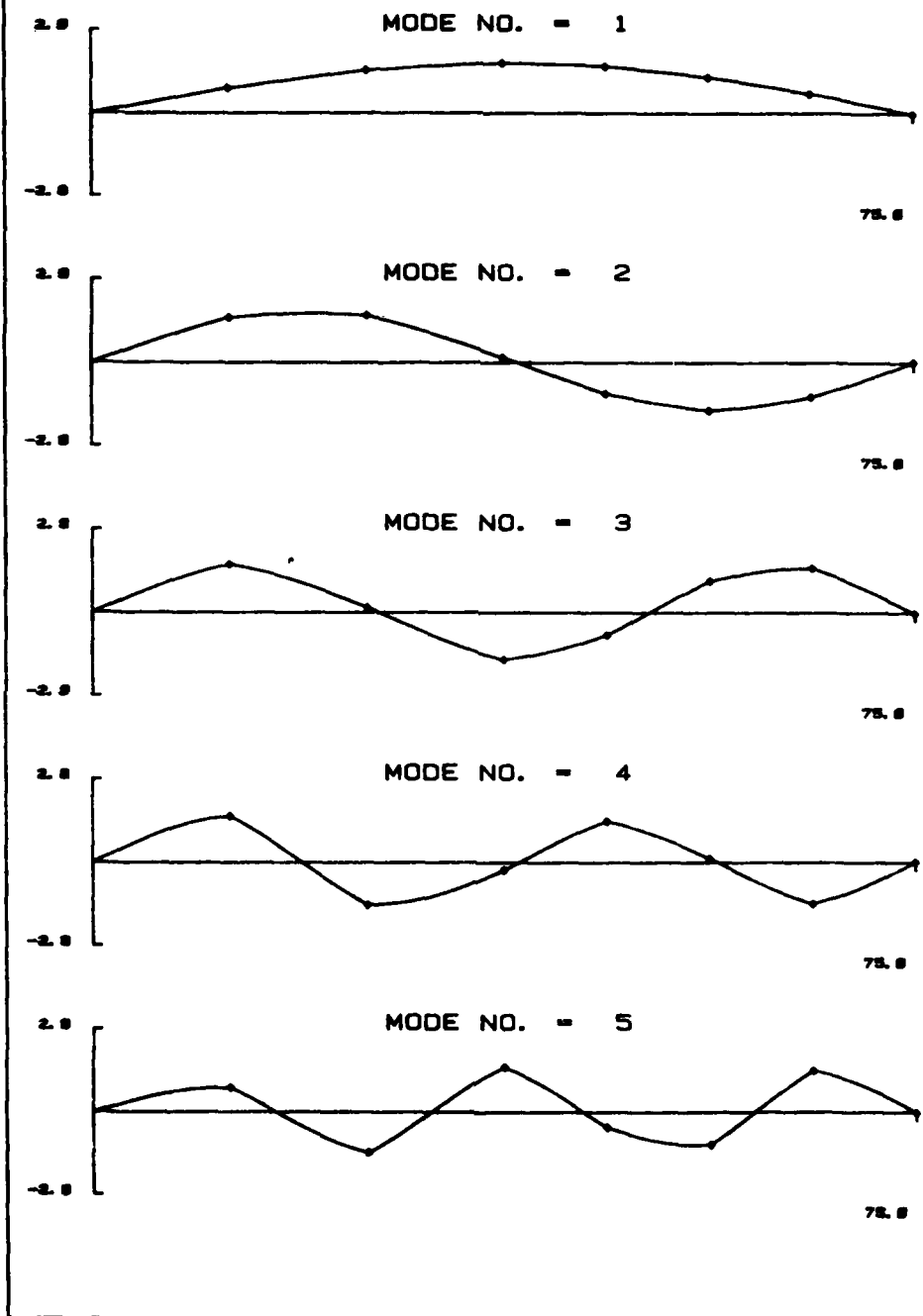
Fig. 17(b) — Test Run 16, Table 1.

43

1981 CASTINE BAY TESTS * MARINE CABLES
WITH ATTACHED SENSOR HOUSINGS * RUN 16

Fig. 17(b) — Continued

44
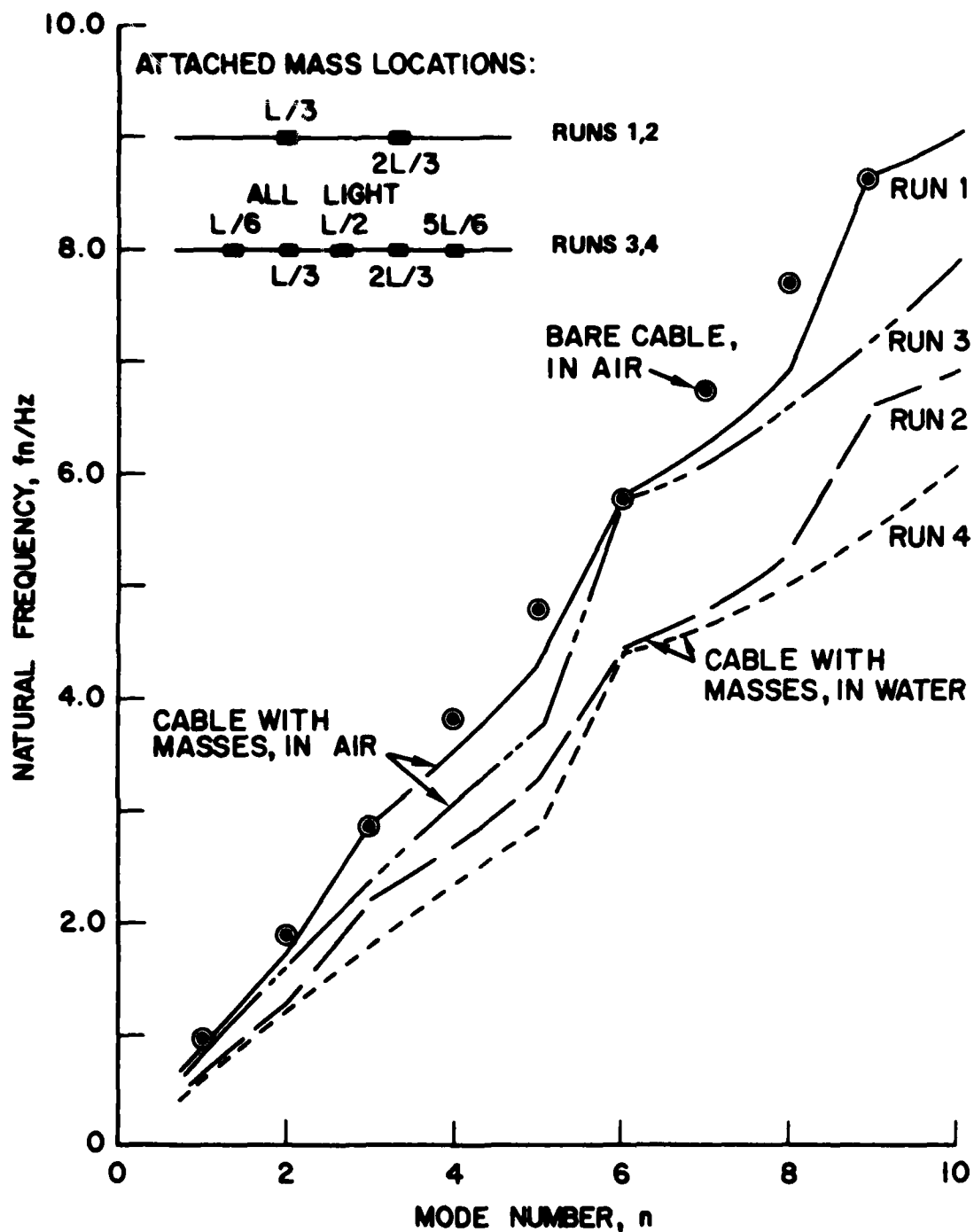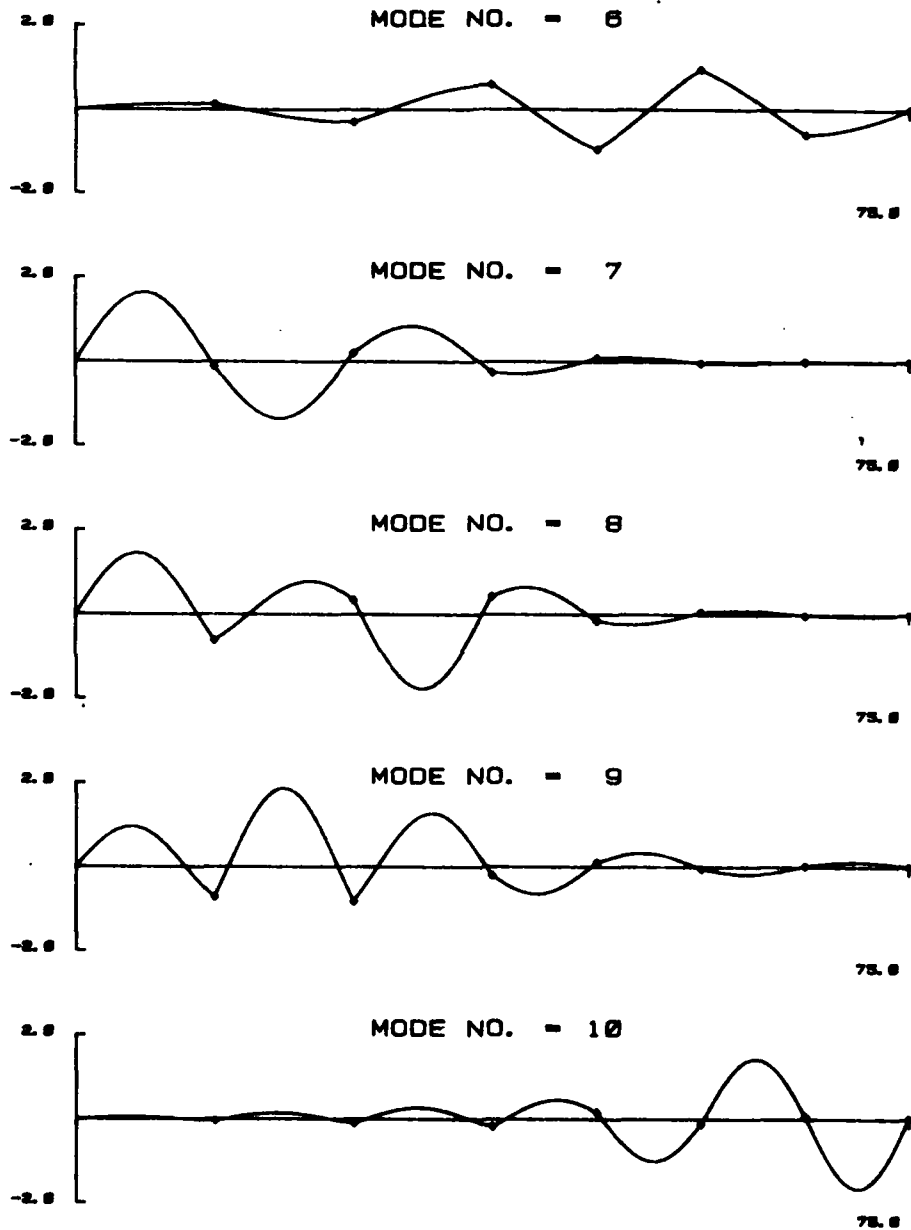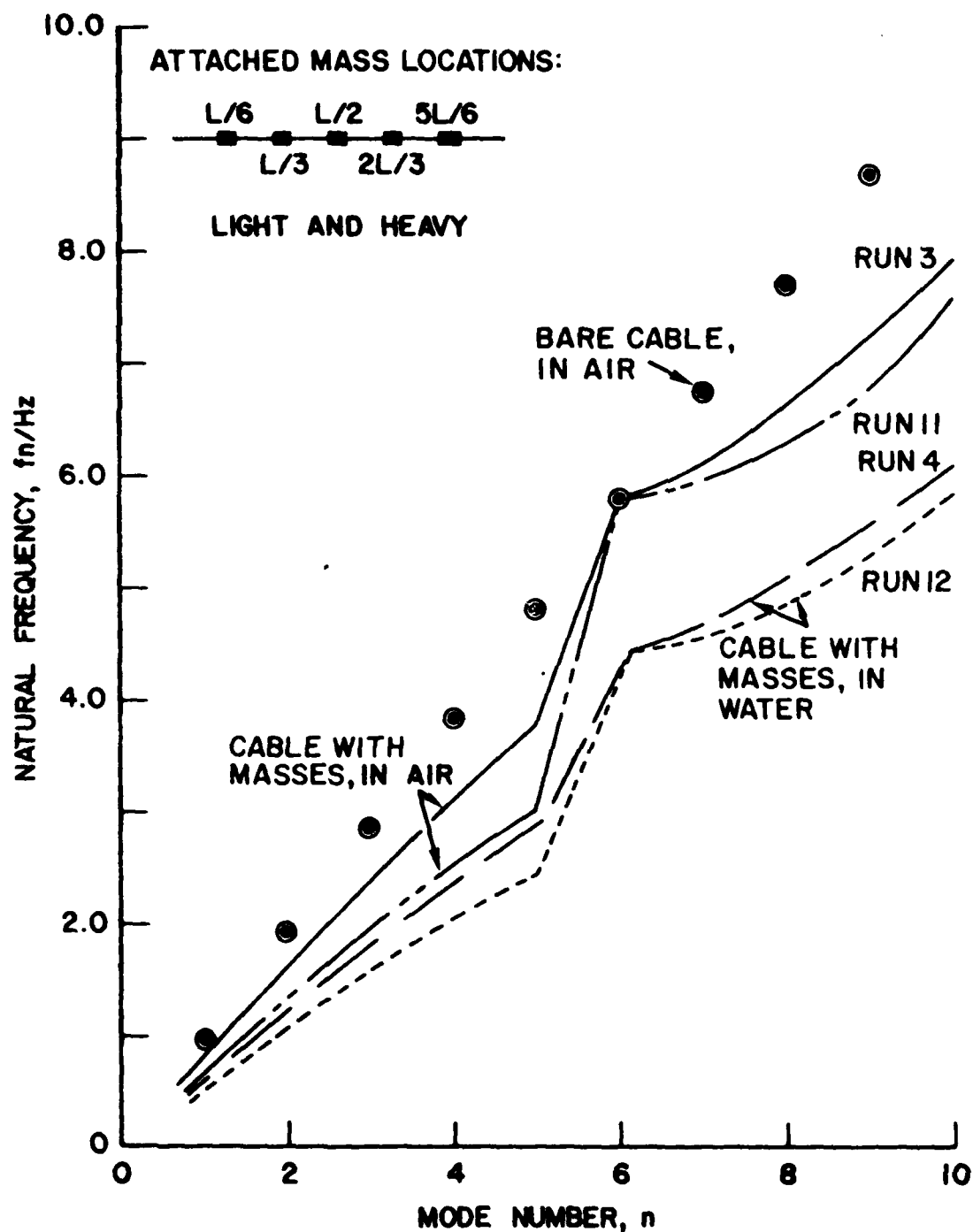
Fig. 18 — In-air and in-water natural frequencies for a cable with five attached masses, computed with NATFREQ. —, Run 3,
Table 1; — —, Run 4, — — —, same as Run 11, except $T = 500$ lb; -----, same as Run 12, except $T = 500$ lb; $\odot$, bare cable.

The modal distributions of vibration amplitude along the cable, respectively corresponding to the plotted frequencies, are shown in Figs. 12, 13, 15, and 17. The vertical scales are uniform but arbitrary, having been chosen only for clarity. The maximum strumming vibration amplitude for a given cable mode is dependent upon the effective reduced damping parameter k_s; see Eq. (C3) of Appendix C. For vibrations of a cable in water the typical level of strumming amplitudes is on the order of ($\pm$) one cable diameter. Vortex-induced vibrations of cables and structures in air are an order of magnitude lower in amplitude. Thus even though the relative mode shapes in air and in water may appear to be very similar on a nondimensional basis, the actual distributions of strumming amplitude levels spanwise along a cable are very different in the two medias.

It is evident from the plotted mode shapes that the attached masses do not act in general as nodes of the overall modal cable pattern. This is true for all of the cases shown with up to seven attached masses. The complexity of the modal vibration patterns along the cable increases in the higher modes. Thus the higher mode shapes for a cable with large numbers of attached masses cannot be guessed intuitively from previous experience. However, the mode shape and peak strumming amplitude must be accurately known in order to correctly estimate the drag effects due to strumming of a complex cable segment.

7. MEASUREMENTS OF CABLE STRUMMING

7.1 Natural Frequencies, Mode Shapes and Damping

Measurements in Air. The natural frequencies and damping ratios were measured in air for each cable test run with attached masses and for several tests with the bare cable (10, 11). A method for extracting the natural frequencies, mode shapes, cable material damping, and strumming displacement from the outputs of the accelerometer pairs was developed and calibrated as part of the data reduction phase of the test program (12). A summary of the experimental data for in-air natural frequencies, mode shapes, and damping ratios is given by Vandiver (13). An example of the good agreement that was achieved between the measured and calculated natural frequencies is given in Table 3. The natural

46

Table 3 — Natural Frequencies and Damping of a Bare Cable (In Air)
1981 Castine Bay Field Experiments,
Marine Cables with Attached Masses;
From Refs. 11 and 13
(Cable Tension = 792 pounds)

Mode	Natural Frequency (predicted, Hz)	Natural Frequency (observed, Hz) Vertical	Material Damping Ratio, ζ	
			based on energy contained in principal direction (ζ)	based on total energy
1	1.21			
2	2.42	2.40	$0.0065 \leqslant \zeta_2 \leqslant 0.0084$	$0.0024 \leqslant \zeta \leqslant 0.0065$
3	3.63	3.60	$0.0045 \leqslant \zeta_3 \leqslant 0.0049$	$0.0017 \leqslant \zeta \leqslant 0.0056$
4	4.84	4.67	$\zeta_4 = 0.005$	$0.0021 \leqslant \zeta \leqslant 0.0046$
5	6.05	5.86		
6	7.26	7.23		
7	8.47			
8	9.68			
9	10.89	10.92		
10	12.10			

frequencies were calculated with the standard equation

$$\omega_n = 2\pi f_n = \frac{n\pi}{L} \sqrt{\frac{T}{m'}} \tag{18}$$

for the undamped frequencies of a taut cable per unit length. Here $\dot{m}'$ is the virtual (physical + added) mass of the cable per unit length. Excellent agreement was obtained for the measured and calculated natural frequencies of the bare cable, and considerable confidence was gained in the data reduction technique in the process. The very small material damping of the cable is characteristic of marine cables (1).

The accelerometer pairs embedded in the cable were of the force-balanced type and sensitive to the direction of gravity. Thus the true horizontal and vertical accelerations of the cable could be obtained. Once the true vertical and horizontal accelerations were found, it was necessary to undertake a complex process to determine the displacements. To do this, a step-by-step process was developed.

A summary of the procedure for double integrating a digital acceleration signal follows. The procedure consists of the following eleven steps as outlined by Jong (12):

Step 1   Find the rotated angle of the accelerometers and perform vector rotation to recover real vertical and horizontal accelerations.

Step 2   Fit a linear least-squares zero baseline to the acceleration signal to remove the DC offset and any linear trend.

Step 3   Obtain the acceleration spectrum and from it compute the theoretical displacement spectrum, as an aid in the determination of the cutoff frequency in the high-pass filter The theoretical fast Fourier transform (FFT) of the displacement is obtained by dividing the magnitude of the acceleration FFT by ω^2.

Step 4   High-pass filter the acceleration signal using an infinite impulse response (IIR) elliptic filter to remove low frequency noise components.

48

Step 5 Integrate the acceleration signal using the Schuessler-Ibler integrator to obtain the velocity.

Step 6 Fit a linear least-squares zero baseline to the velocity signal to remove any DC offset and linear trend.

Step 7 High-pass filter the velocity signal using an IIR elliptic filter to remove any low frequency noise components that were expanded in step 5.

Step 8 Integrate the velocity signal using the Schuessler-Ibler integrator to obtain the displacement.

Step 9 Fit a linear least-squares zero baseline to the displacement signal.

Step 10 High-pass filter the displacement signal using an IIR elliptic filter to remove any low frequency noise components that were expanded in step 8.

Step 11 Plot summary data, e.g. root-mean-squares, spectra, time series of displacement, velocity, acceleration and two dimensional cylinder or cable motion time series.

From the horizontal and vertical acceleration spectra it was possible to determine the natural frequencies of vibration for each responding mode. These natural frequencies then can be compared with those predicted by the NATFREQ computations of the cable with attached masses. The frequencies found in this manner actually are not the undamped natural frequencies but the damped natural frequencies. However, because the damping is so low in air the two are essentially the same.

From free vibration decay tests logarithmic decrements were estimated from the acceleration-time histories by measuring two acceleration amplitudes separated by an integer number, M, of complete cycles. The logarithmic decrement is found from the equation

$$\delta = \frac{1}{M} \ln \frac{A_1}{A_{M+1}} \tag{19}$$

where A_1 is the acceleration amplitude at some time t_1 and A_{M+1} is the amplitude at t_{M+1}. The damping ratio ζ then is given by

<center>49</center>

$$\zeta = \frac{\delta}{\sqrt{\delta^2 + (2\pi)^2}}. \tag{20}$$

When δ is very small ($\delta \ll 1$) it is clear that $\zeta \cong \delta/2\pi$. Details of the analysis procedure are given by Moas (11).

The natural frequencies of several modes and the material damping were measured for the cable with attached masses. The damping measurements are summarized in Table 4. The numbers designating the test runs in the table correspond to the numbers in Table 1 where the various attached mass configurations are given. The damping often was found to be nonlinear over the range of in-air displacement amplitudes (10). Therefore, when two damping ratios are quoted in Table 4 for a particular test run the first value corresponds to low amplitudes and the second to high amplitudes of vibration. In both cases, however, the material damping is very small for the cable with up to seven cylindrical attached masses.

The measured natural frequencies for the cable with attached masses are listed in Table 5 for the same test runs listed in Table 4. The natural frequencies of the system were measured by exciting the various modes in both the vertical (in-plane) and horizontal (out-of-plane) directions. Generally the results are comparable in both cases. A discussion of the data reduction sequence employed in obtaining the natural frequencies is given in Refs. 10 and 11. It was found in general that the vertical accelerometer had a negligible response when the cable was excited in the horizontal plane, and vice versa. The natural frequencies were determined from the peaks in the spectral density plots of the vibration. Typically there were no mixed mode vibrations and only one peak was evident in the spectrum. The lowest ($n = 1$) mode of the cable apparently was influenced by the sag of the cable (13). This is typical of the vibrations of slack cables, where the influence of the cable sag diminishes as the cable vibrations progress to higher modes (1,14). Some of the higher mode frequencies were probably influenced to some extent by the bending stiffness of the cable. A more extensive appraisal of cable sag and bending stiffness effects should be undertaken as a follow-up to the present study.

A typical spectral plot is given in Fig. 19. This measurement was by the accelerometer pair

Table 4 — Measurements of Cable Material Damping (in Air)
1981 Castine Bay Field Experiments,
Marine Cables with Attached Masses:
From Refs. 10 and 13

Test Number*	Mode	Direction of Excitation	Damping Ratio, ζ
1	2	Horizontal	0.005
	3	Horizontal	0.001, 0.007
3	2	Horizontal	0.005
	3	Horizontal	0.007
	3	Vertical	0.002, 0.003
5	2	Horizontal	0.004, 0.007
	2	Vertical	0.001, 0.003
	3	Vertical	0.001, 0.002
7	2	Horizontal	0.005, 0.006
	3	Vertical	0.002, 0.005
	4	Vertical	0.002, 0.004
9	2	Vertical	0.004
	2	Horizontal	0.007
	3	Vertical	0.002, 0.006
	3	Horizontal	0.004, 0.005
11	2	Vertical	0.008
	2	Vertical	0.005
	2	Horizontal	0.008
	3	Horizontal	0.008
	3	Vertical	0.004
	5	Unknown	0.004
	5	Vertical	0.003, 0.005
19	2	Horizontal	0.002, 0.003
	3	Vertical	0.001
	3	Horizontal	0.003, 0.004
	4	Horizontal	0.002

*From Table 1.

Table 5 — Measurements of Natural Frequency (In-Air)
1981 Castine Bay Field Experiments,
Marine Cables with Attached Masses;
From Refs. 10 and 13

Test Number[*]	Mode	Direction of Excitation	NATFREQ-Predicted Frequency, Hz	Measured Frequency, Hz
1	2	Horizontal	1.72	1.74
	3	Horizontal	2.89	3.036
3	2	Horizontal	1.59	1.60
	3	Horizontal	2.36	2.37
	3	Vertical	2.36	2.40
5	2	Horizontal	1.73	1.74
	2	Vertical		1.74
	3	Vertical	2.550	2.63
7	2	Horizontal	1.51	1.53
	3	Vertical	2.26	2.34
	4	Vertical	2.98	3.07
9	2	Vertical	1.57	1.58
	2	Horizontal		1.61
	3	Vertical	3.00	3.10
	3	Horizontal		3.09
	5	Vertical	4.04	4.25
11	2	Vertical	1.60	1.62
	2	Horizontal		1.62
	3	Horizontal	2.36	2.41
	3	Vertical		2.46
	4	Horizontal	3.03	3.18
	5	Vertical	3.55	3.80
19	2	Vertical	1.69	1.75
	3	Vertical	2.62	2.80
	3	Horizontal		2.80
	5	Horizontal	3.98	4.30

[*]From Table 1.

located at the position $L/4$ along the cable. The light (L) attached masses were located at $NL/6$, $N =$ 1 to 5. For this example, the second mode ($n = 2$) with five light masses attached to the cable, the measured natural frequency was 1.60 Hz. The natural frequency computed with NATFREQ was 1.59 Hz, which resulted in an error of 0.9 percent (10). The error between the measured and predicted natural frequencies ranged from this value to about 11 percent. However in most of the cases listed in Table 5 the error between the measured and predicted frequencies was less than 5 percent.

The measured in-air mode shapes for the cable with seven light attached masses (Test Run 7) are shown in Fig. 20. The normalized measured mode shapes are denoted by the distribution of individual displacement spikes at the seven locations of the accelerometer pairs. All of the data were corrected for rotation of the accelerometers. Superimposed on the measured displacements is an equivalent sine wave. The measured displacement amplitudes are a good approximation to the sine wave in all three modes ($n = 2$, 3 and 4). Reference to Fig. 15(a) readily shows that the NATFREQ-generated mode shapes also closely resemble sine waves in the second and fourth modes where the masses are evenly distributed over a half-wavelength of the cable vibration pattern. Even for the third mode, where the masses are not evenly distributed over the half-wavelength, there appears to be little variation from the sinusoidal distribution. The mode shape of the cable does not resemble a nonsinusoidal wave form until the higher modes ($n = 5$ and greater) are excited.

53
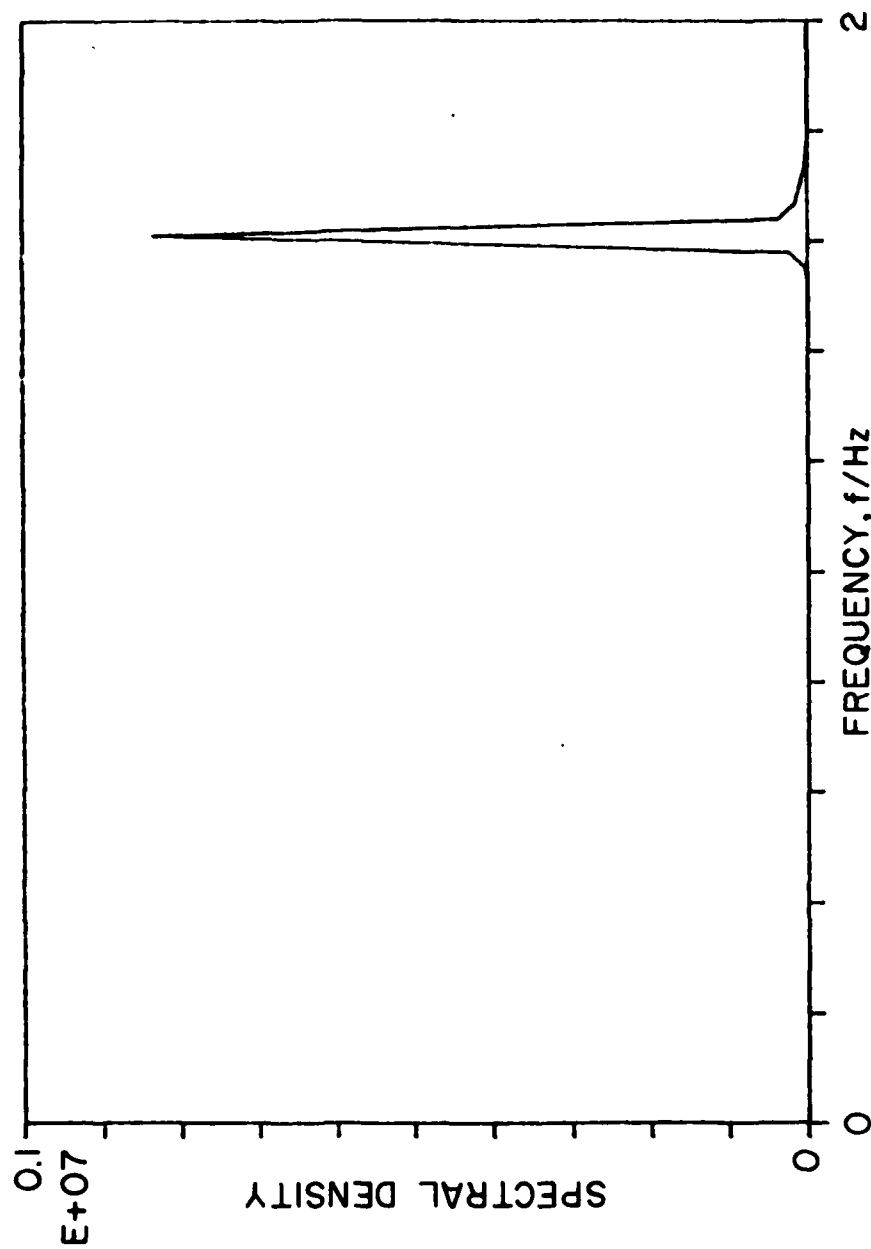
Fig. 19 — A plot of the in-air response frequency spectrum for the cable with six light attached masses (Test Run 3 of Table 1); from Ref. 10.

54

Fig. 20(a) — Second mode.

Fig. 20(b) — Third mode.
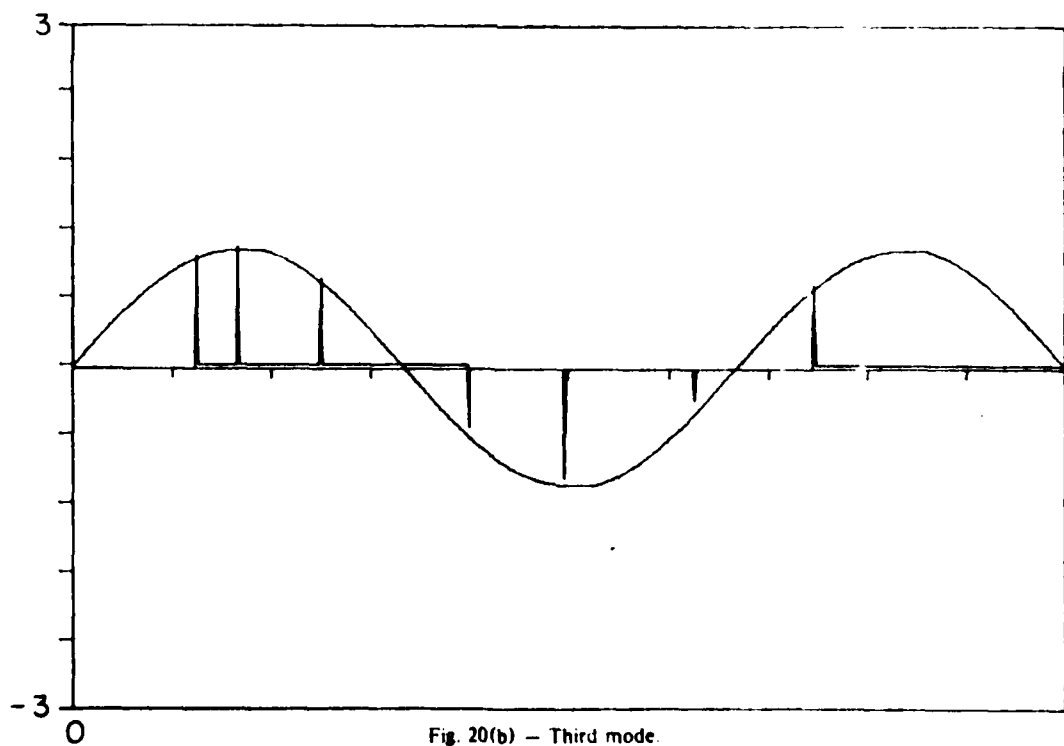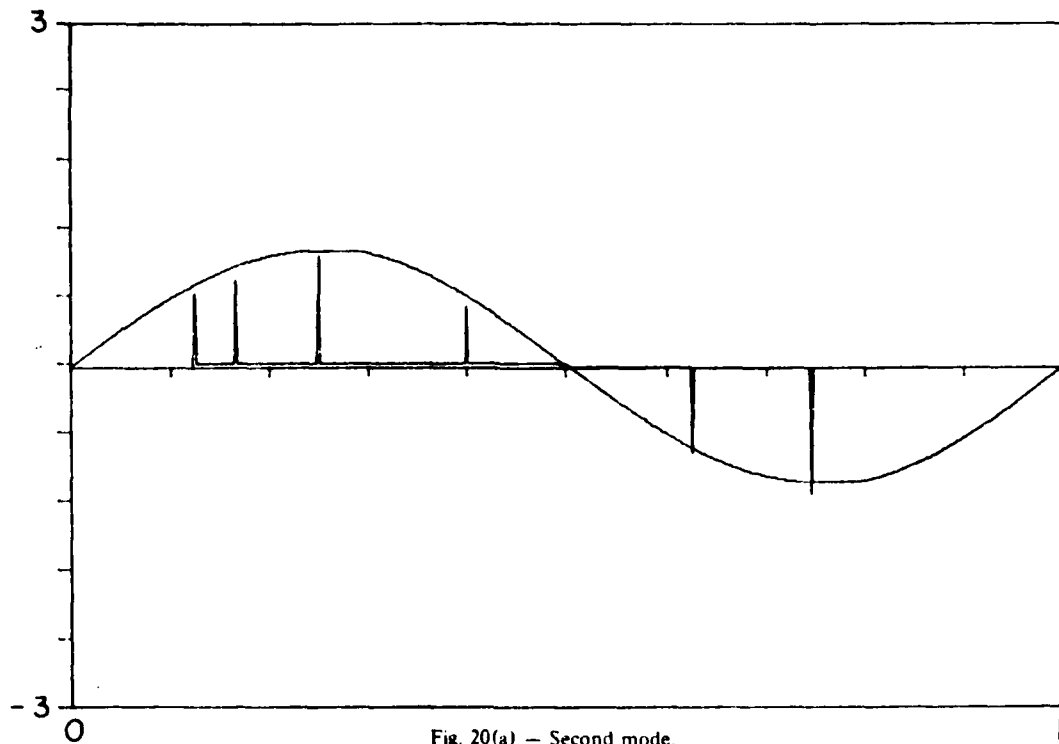
Fig 20 — Mode shape estimation for three in-air modes of a cable with seven light attached masses (Test Run 7 of Table 1); from Ref. 13.
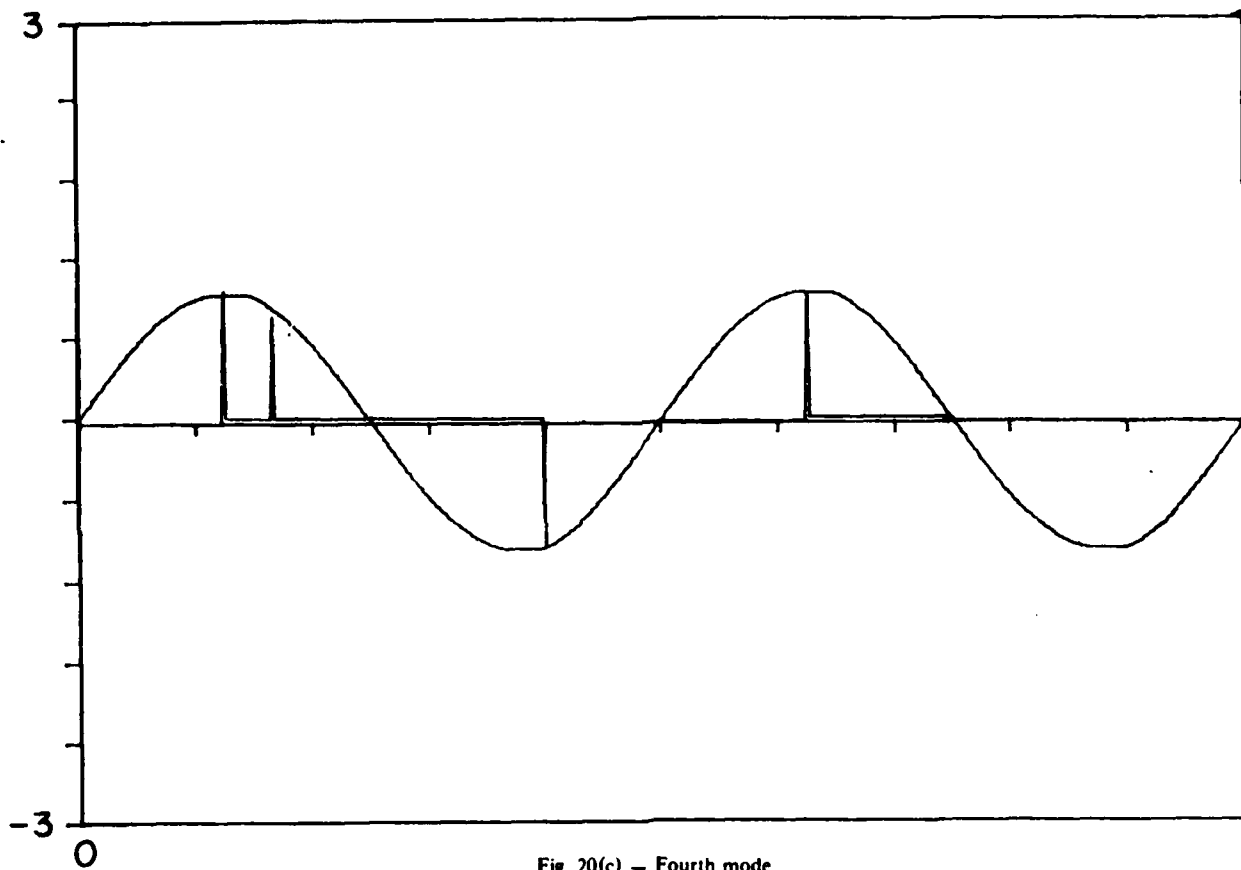
Fig. 20(c) — Fourth mode.

7.2 Strumming of Cables

Laboratory-Scale Experiments. Experiments were conducted by Peltzer (16) to study the effects of shear on vortex shedding from stationary and vibrating marine cables. In some of the experiments, a distribution of spheres was attached to the cable to simulate the effect of attached bodies such as sensor housings and buoyancy elements. The cable of 11.4 mm (.045 in) diameter had a length to diameter ratio of $L/D = 107$, which resulted in a shear flow steepness parameter $\bar{\beta} = 0.0053$ over the Reynolds number range $Re = 1.8 \times 10^3$ to 4×10^4. Some of the results obtained with and without the attached masses are summarized here for comparison.

The spanwise Strouhal number variation along the stationary cable in the shear flow is shown in Fig. 21. There are ten cells of constant Strouhal number along the cable span. The average length of the cells is eleven cable diameters and the change in the Strouhal number from cell to cell is $\Delta St_M = 0.0086$. There is a total change in the Strouhal number of $\Delta St_M = 0.067$ across the span from $-48 \leqslant \bar{z}/D \leqslant 48$. The clarity of the cellular structure is due to a careful optimization of the location of the hot-wire probe that was used to sense the frequency of vortex shedding from the cable (15).

The cable was oscillated in its first mode with an antinodal displacement amplitude of $2\bar{Y} = 0.29D$ and at a reduced velocity of $V_r = 5.6$. The vortex shedding pattern in Fig. 21 was changed by the oscillations as shown in Fig. 22. The vortex shedding was locked-on to the cable vibration over the central portion of the cable span from $-14 \leqslant \bar{z}/D \leqslant 30$, so that the locked-on cell was 44 diameters long. The remainder of the vortex shedding pattern not influenced by end effects was stabilized as well. Two cells were increased in length to fourteen diameters each and no fluctuations in the cell boundaries were observed. The change in the Strouhal number across the span was increased to $\Delta St_m = 0.078$.

One of the objectives of these experiments was to investigate the effects of attached bluff bodies on the vortex shedding. The vortex shedding pattern along the cable with five spheres (ping pong balls) attached is shown in Fig. 23. The flow conditions were the same as in Figs. 21 and 22, except
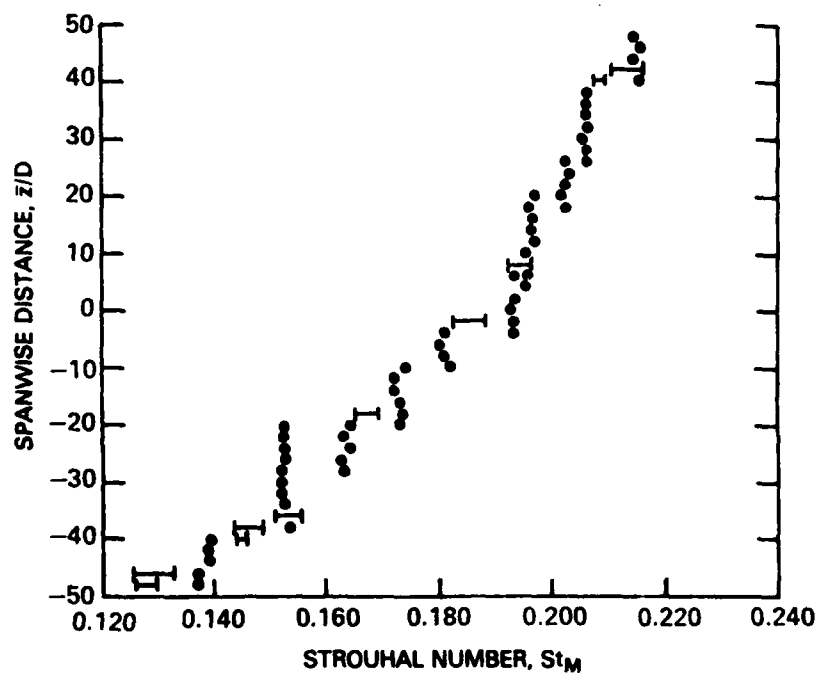
Fig. 21 — Strouhal number St_M plotted against spanwise distance along a stationary flexible cable in a linear shear flow; from Peltzer (16). Reynolds number $Re_M = 2.96 \times 10^3$, shear flow steepness parameter $\bar{\beta} = 0.0053$.

58
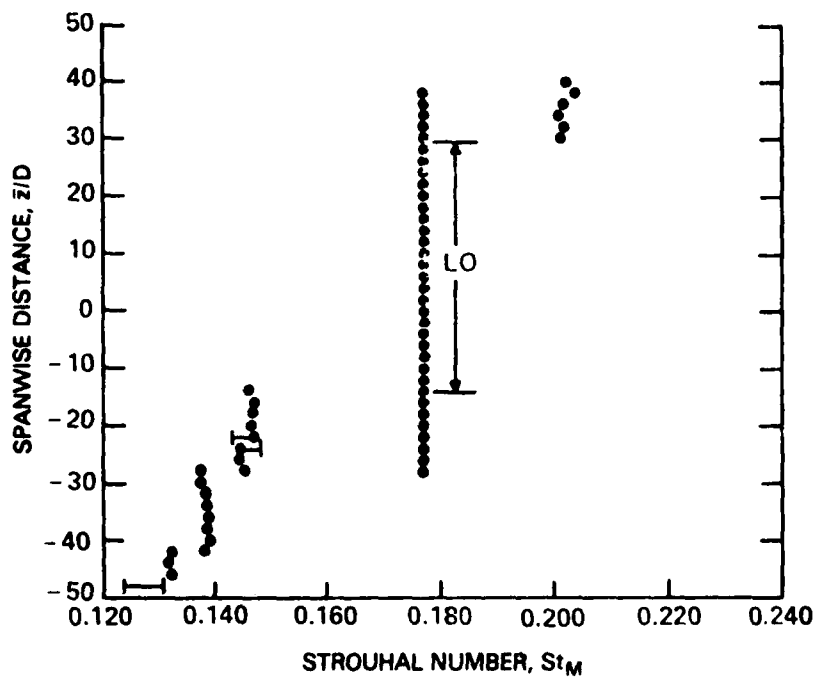
Fig. 22 — Strouhal number St_M plotted against spanwise distance along a vibrating flexible cable in a linear shear flow; from Peltzer (16). Reynolds number $Re_M = 2.96 \times 10^3$, shear flow steepness parameter $\bar{\beta} = 0.0053$, reduced velocity $V_r = 5.6$, displacement amplitude (first mode) $2\bar{Y} = 0.29D$.
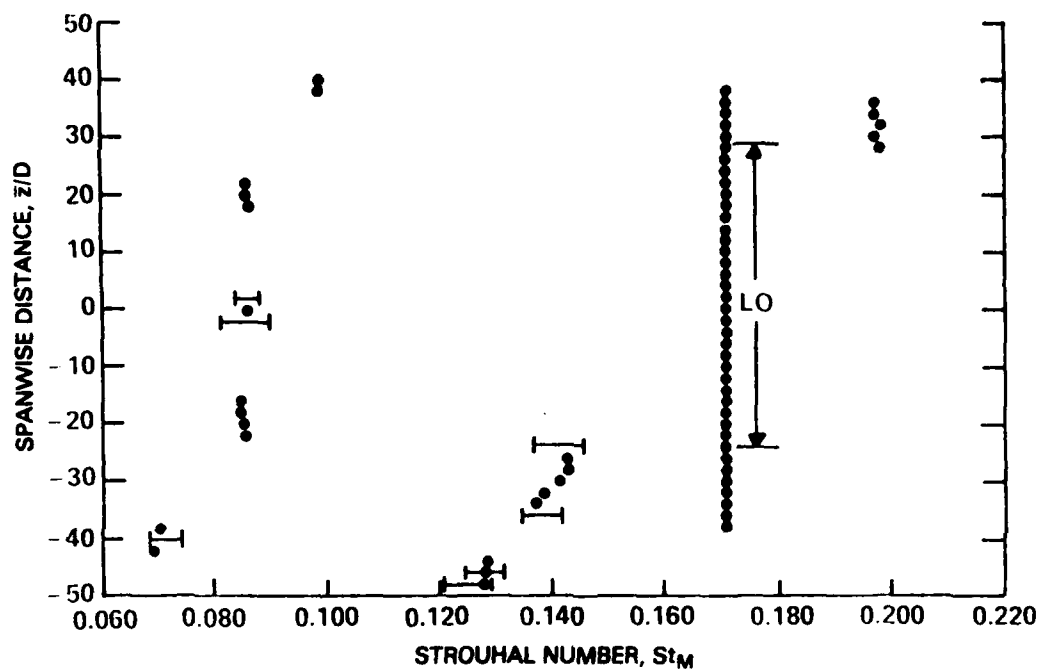
Fig. 23 — Strouhal number St_M plotted against spanwise distance along a vibrating flexible cable with five attached spheres in a linear shear flow; from Peltzer (16). Conditions as in Fig. 22 except that $2\bar{Y} = 0.23D$.

that the antinodal displacement amplitude of the cable was $2 \overline{Y} = 0.23D$.

Several points concerning the vortex shedding from the cable-sphere system are notable. The three central spheres ($\overline{z}/D = -20, 0, 20$) locked-on to a submultiple (one half) of the cable vibration frequency. The lock-on region of the cable strumming in Fig. 23 extended from $-24 \leqslant \overline{z}/D \leqslant 29$, or over 53 diameters. This is a significant increase from the comparable bare cable experiments. For example, when $2 \overline{Y} = 0.29D$ for the bare cable the lock-on region extended over 44 diameters, and when $2 \overline{Y} = 0.23D$ the lock-on region extended over 34 diameters. When three spheres ($\overline{z}/D = -28$, 0, +28) were attached to the cable, with $2 \overline{Y}/D = 0.235$, the lock-on region extended over 61 cable diameters. It is clear that the addition of attached bodies along the cable is not likely to deter the resonant cable strumming vibrations even in a shear flow.

Peltzer (16) observed other significant features relating to cable strumming in a shear flow. A maximum separation distance of twenty cable diameters between the spheres was observed that would force the vortex shedding into cells of constant frequency when the cable was stationary. The cellular structure along the cable with spheres attached was forced into a pattern that was appreciably different from the bare cable in the shear flow when the spacing between the spheres was twenty diameters or less.

Towing Channel Experiments. As part of the overall NCEL cable dynamics research program MAR Incorporated was funded to conduct a program of experiments to investigate strumming suppression and the effects of sensor housings (attached masses) on the overall cable response. Two reports on the results obtained recently have been published (2,3). Some of the results obtained are summarized briefly here and are compared with previous findings from the NRL/DTNSRDC/NCEL cable dynamics program. The tests were conducted on a "strumming rig" at the DTNSRDC that was employed in previous NCEL-sponsored strumming experiments (1). The recent MAR Incorporated experiments and the experimental layout are described in detail in Ref. 3.

Some of the results obtained in these experiments are plotted in Fig. 24. The discrete masses in

all cases were aluminum sensor housings attached at various locations along the steel cable of diameter $D = 0.175$-in. and span of $L = 14.5$-ft. It can be seen from the results in Fig. 24 that the cable was deployed under various conditions in the resonant, cross flow strumming regime during the tests. The results plotted in the figure from the previous DTNSRDC experiments were obtained with a bare cable in all cases, and those results are discussed in detail in Ref. 1.

The attached masses did not deter the strumming, but instead the system consisting of a bare cable plus attached masses reached higher cross flow displacement amplitudes than the bare cable alone during the Mar Incorporated tests. This is because the conditions of Mar's cable experiment were at the onset of the resonant strumming regime in Fig. 24 while the attached mass experiments extended well into the resonant region. All of the tests were conducted in the range of cable and attached mass properties where hydrodynamic effects are dominant (1) and even the addition of discrete masses has little influence on the large-displacement cross flow strumming effects. All of the frequency spectra plotted in Ref. 3 give clear evidence of cross flow strumming at a single resonant frequency.

Cable Strumming in the Ocean. Field studies of the strumming behavior of marine cables were conducted over several summers of the Castine Bay, Maine test site by staff members and students of the Ocean Engineering Department at MIT. The most recent experiments are described in this report and in Refs. 8-12. The previous experiments are described in Refs. 1, 5, 6 and 17.

SEACON II was a major undersea construction experiment the chief goal of which was the measurement of the steady-state response of a complex three-dimensional cable structure to ocean currents. The measured array responses were to be employed in a validation of analytical cable design models and computer codes as described by Kretschmer et al (18). A second goal of the SEACON II experiment was to demonstrate and evaluate new developments in ocean engineering which were required to design, implant, operate, and recover fixed undersea cable structures.

The SEACON II structure consisted of a delta-shaped module with three mooring legs. It was implanted in 2900-ft of water in the Santa Monica Basin by the Naval Civil Engineering Laboratory dur-

62
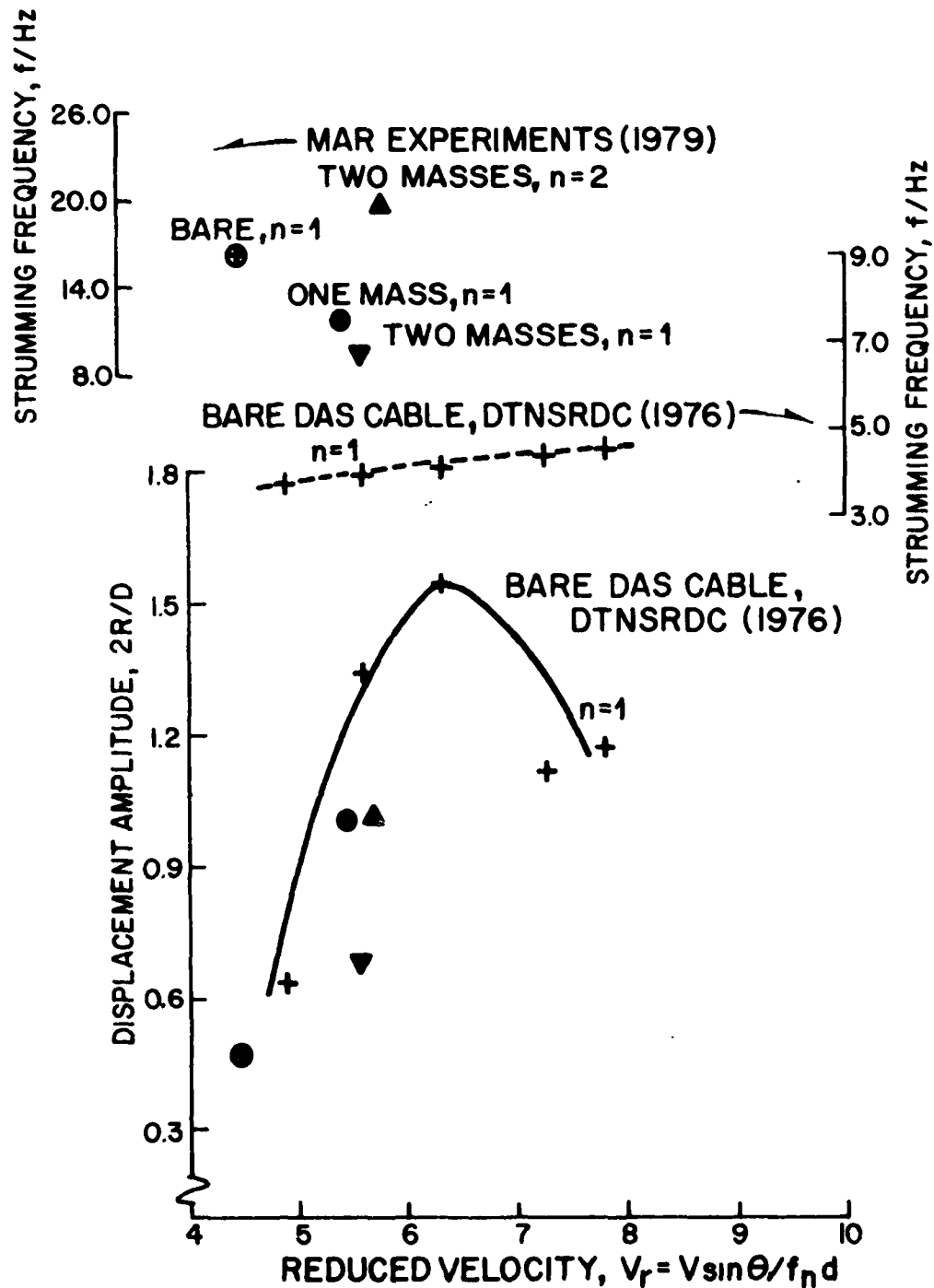
Fig. 24 — Strumming displacement amplitudes for a small diameter cable with attached masses: data from Griffin et al (1) and Kline et al. (2). Here *R* is the *resultant* of the in-line and cross-flow strumming components.

ing 1974 and was retrieved during 1976. The top of the cable structure was positioned 450-ft below the water surface. The mooring legs were 4080-ft long and each arm of the delta was 1000-ft long. An artist's view of the completed structure is shown in Fig. 25. Two mooring legs were attached to explosive anchors embedded in the sea floor and the third leg was attached to a 12500-lb clump anchor. The entire cable structure was instrumented in order to collect current and array position data.

The data were used to validate the NCEL computer code DECELI. This code, previously called DESADE, was developed at NRL by Skop and Mark in 1973. The delta cables experienced uniform currents over their respective lengths and often were subject to cable strumming. These strumming vibrations led to increased steady drag coefficients and static deflections as described in the next section of this report. Details of the SEACON II implantation, design and recovery are given by Kretschmer et al. (18).

Another cable strumming experiment (the Bermude Testspan) was conducted by the U.S. Navy from December 1973 to February 1974. The site of the experiment was near Argus Island, Bermuda. A 840-ft long, 0.63-in. diameter electromechanical cable was suspended horizontally in the water at a depth of 92-ft. The cable had no strumming suppression devices attached, but it had numerous weights, instrumentation devices, and floats distributed over its length. The unfaired cable and instrumentation were similar to the cables which made up the horizontal delta segments of the SEACON II array. Two current meters were suspended near the mid-span point of the cable. Only a limited amount of data were obtained from this experiment.

Kennedy and Vandiver (19) have analyzed the results of this experiment and have reached several conclusions. They found that the strumming response of the cable was typical of a broadband random process and that resonant and nonresonant lock-on were rare. The high modal density, which resulted in responses from the 10th to the 150th mode, and extreme variations in current speed and direction were chiefly responsible for the broadband response of the test span. The peak rms cross flow displacement amplitude experienced by the Bermude Testspan was estimated by Kennedy and Vandiver to be $\bar{Y} = \pm 0.5D$.
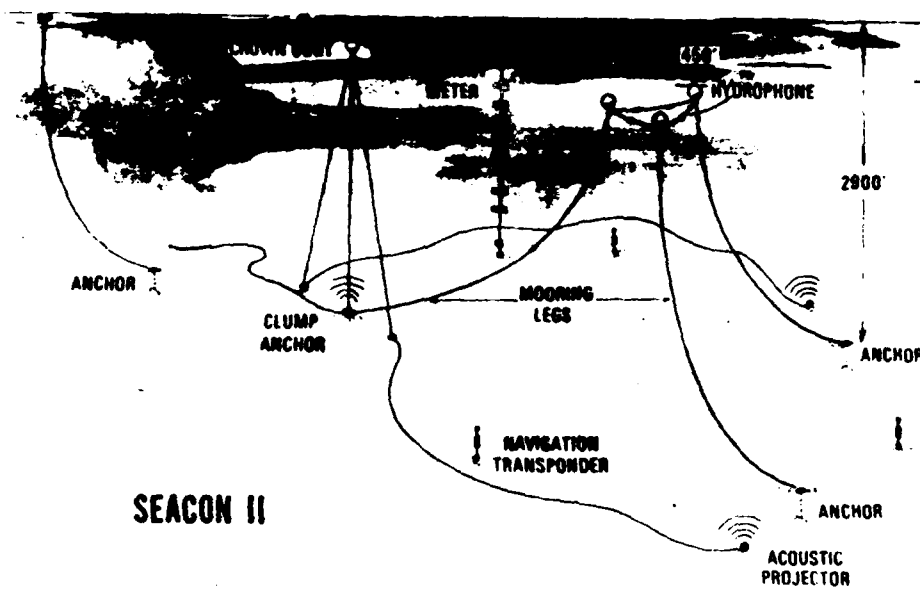
Fig. 25 — A schematic drawing of the SEACON II experimental mooring that was implanted and retrieved by the Naval Civil Engineering Laboratory during the 1970's.

A more extensive discussion of these and some other recent cable strumming field experiments is given in Refs. 1 and 17.

7.3 Hydrodynamic Drag

An important side effect which results from the oscillations of structures and cables due to vortex shedding is the amplification of mean drag force (or the drag coefficient C_D). The drag force amplification measured under a variety of conditions has been summarized in a recent NCEL report (1) and in a more recent and related paper (17). A methodology for employing these measurements in the analysis of marine cable structures was developed by Skop, Griffin and Ramberg (20). This approach has been extended to the case of flexible, cylindrical marine structures by Griffin (21,22). A step-by-step method for approaching this problem is given in Refs. 1, 21 and 22, and is summarized in Appendix C of this report.

The measured mean drag coefficients (C_D) for several strumming cables are plotted against the Reynolds number (Re) in Fig. 26. As a basis for comparison the typical drag coefficients for a stationary circular cylinder and several nominally stationary braided and plaited marine cables also are plotted in the figure. The relatively large scatter in the stationary cable data is due to variations in the low cable tension values at the lowest flow speeds (Reynolds numbers). All of the cable strumming experiments were conducted in one of the towing channels at the DTNSRDC. The dashed line was simply faired through the strumming data. It is clear that the drag coefficients for the strumming cables are increased substantially (by as much as a factor of two) for a variety of Kevlar cables over a wide range of towing speeds or Reynolds numbers between Re $= 3(10^3)$ and $3(10^4)$.

The experimental test program conducted at the Castine field site has provided a more extensive data base for the strumming response of relatively long marine cables and cylindrical pipes under controlled conditions. The drag measurements made at the site with the long flexible pipe are discussed in a separate paper by Vandiver (23). A time history of the cable drag coefficient C_D and the current V
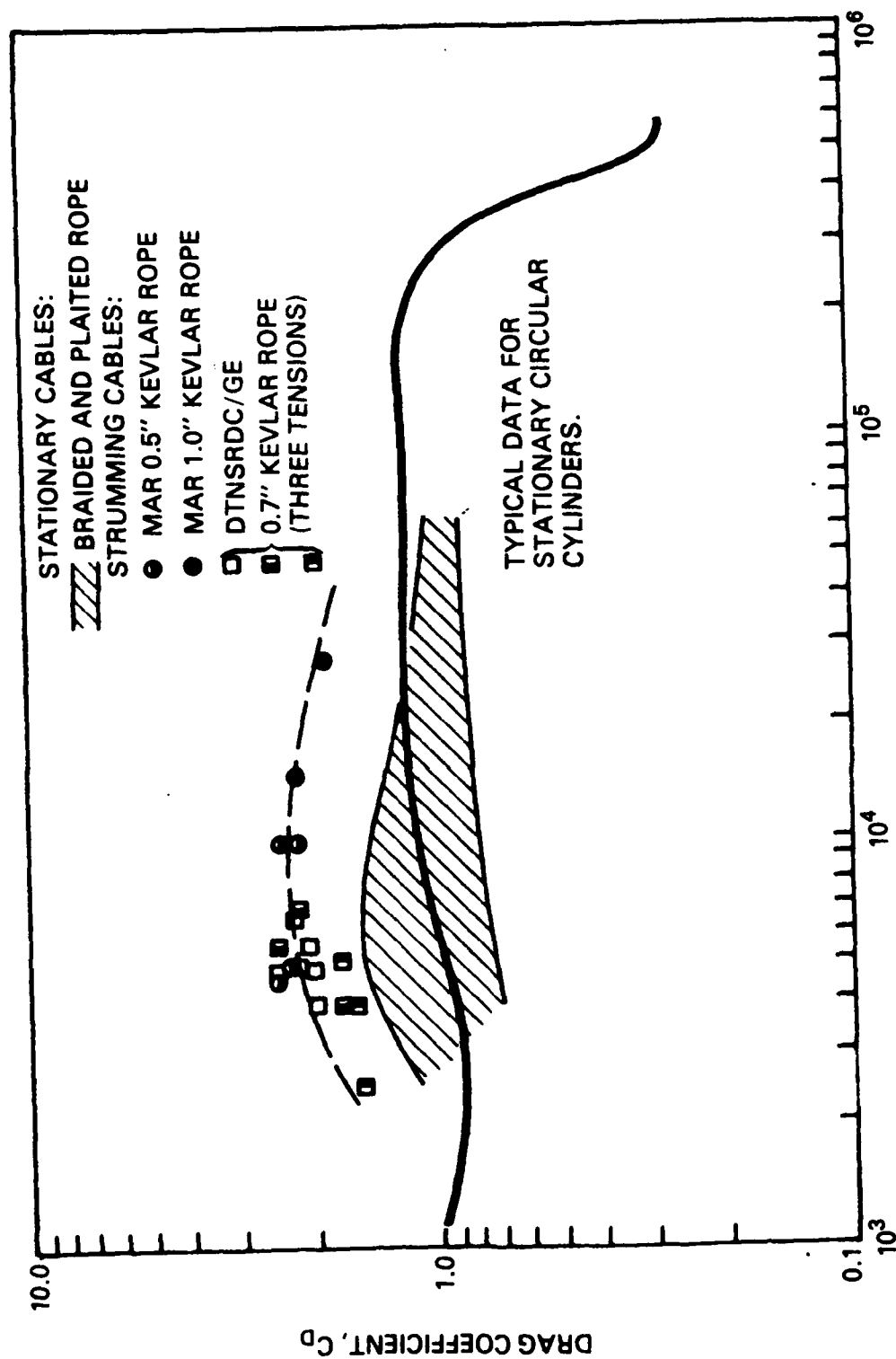
Fig. 26 — The drag coefficient C_D plotted against the Reynolds number Re for several synthetic fiber marine cables. A curve of C_D versus Re for typical stationary cylinders is plotted as a reference. All of the cable strumming experiments were conducted at the David Taylor Naval Ship R&D Center. The original figure was provided by D.J. Meggitt of the Naval Civil Engineering Laboratory.

67

are plotted in Fig. 27. The data are taken from a typical run with the cable only and not attached masses. From the approximately 35 minutes of data recorded with the cable strumming it is clear that the hydrodynamic drag is increased consistently from the level that is typical of a stationary cylinder or cable (C_D = 1 to 1.5). The measurements of C_D are consistently between 2 and 3 for the time interval shown when the current velocity is near 1.2 kt. The strumming response of the cable was in the first six (n = 1 to 6) natural modes.

An example taken from one of the more complex tests (Run 20 of Table 1) is shown in Fig. 28. Six cylindrical masses were attached to the cable: two light ones at $L/8$ and $L/2$; and four heavy ones at $L/3$, $5L/8$, $3L/4$ and $7L/8$. The RMS strumming response data shown for a two and one half hour time period in Fig. 28 were recorded at $3L/4$, where both one of the attached masses and an accelerometer pair were located. Several segments of the drag and strumming displacement amplitude plots are at relatively constant levels. These probably represent time periods of resonance or 'lock-in' between the vortex shedding and the strumming. Several examples taken over a shorter time period (448 seconds) are now discussed.

A segment of data derived from Run 10 of Table 1 is shown in Fig. 29. Two heavy masses were attached to the cable at $L/3$ and $2L/3$. The drag coefficient, the current speed, and the horizontal and vertical rms strumming displacement amplitudes all are plotted in Fig. 29 for a typical 448 second time period during this test run. The measurements were made with the accelerometer pair at $5L/8$ along the cable. Frequency spectra for each of the horizontal and vertical accelerometers are shown in Fig. 30. Three stacked graphs are shown for the two directions and each graph represents a strumming frequency spectrum taken from a two and one-half minute segment of the data file for this test run. The displacement output derived from the vertical accelerometer is predominantly at a frequency near 3 Hz, with a smaller spike near 1 Hz. The spectra derived from the horizontal accelerometer are characterized by peaks at twice those of the vertical accelerometer. This is as expected since the fluctuating drag force in the horizontal direction has a frequency of twice the fluctuating lift force due to vortex shedding. The predicted natural frequency of the n = 5 mode for this test run is 3.1 Hz. It is likely then
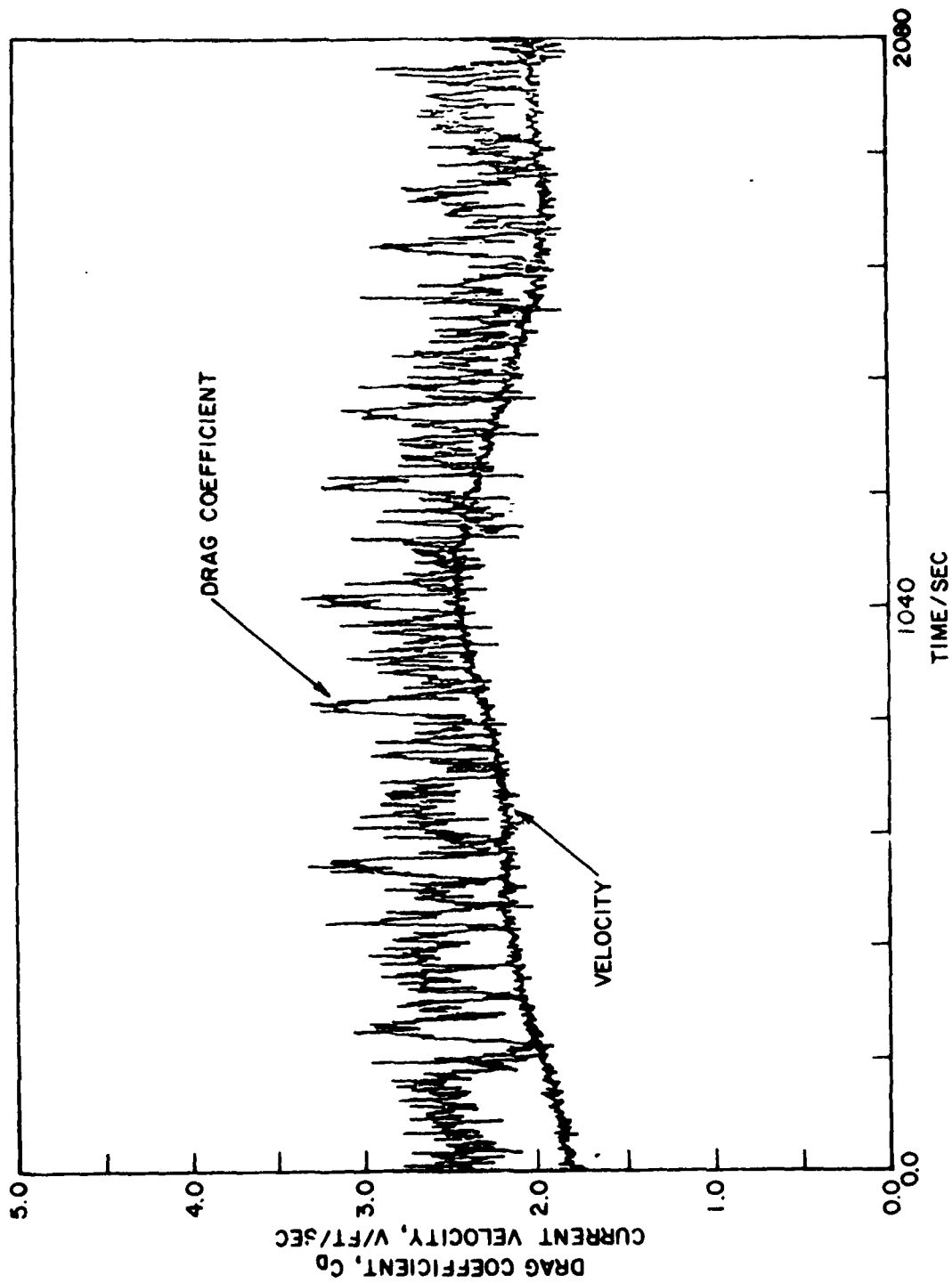
Fig 27 — A time history of the drag coefficient C_D and the current velocity V recorded during the 1981 Castine Bay field test with a bare cable. Cable properties as in Table 2.

69
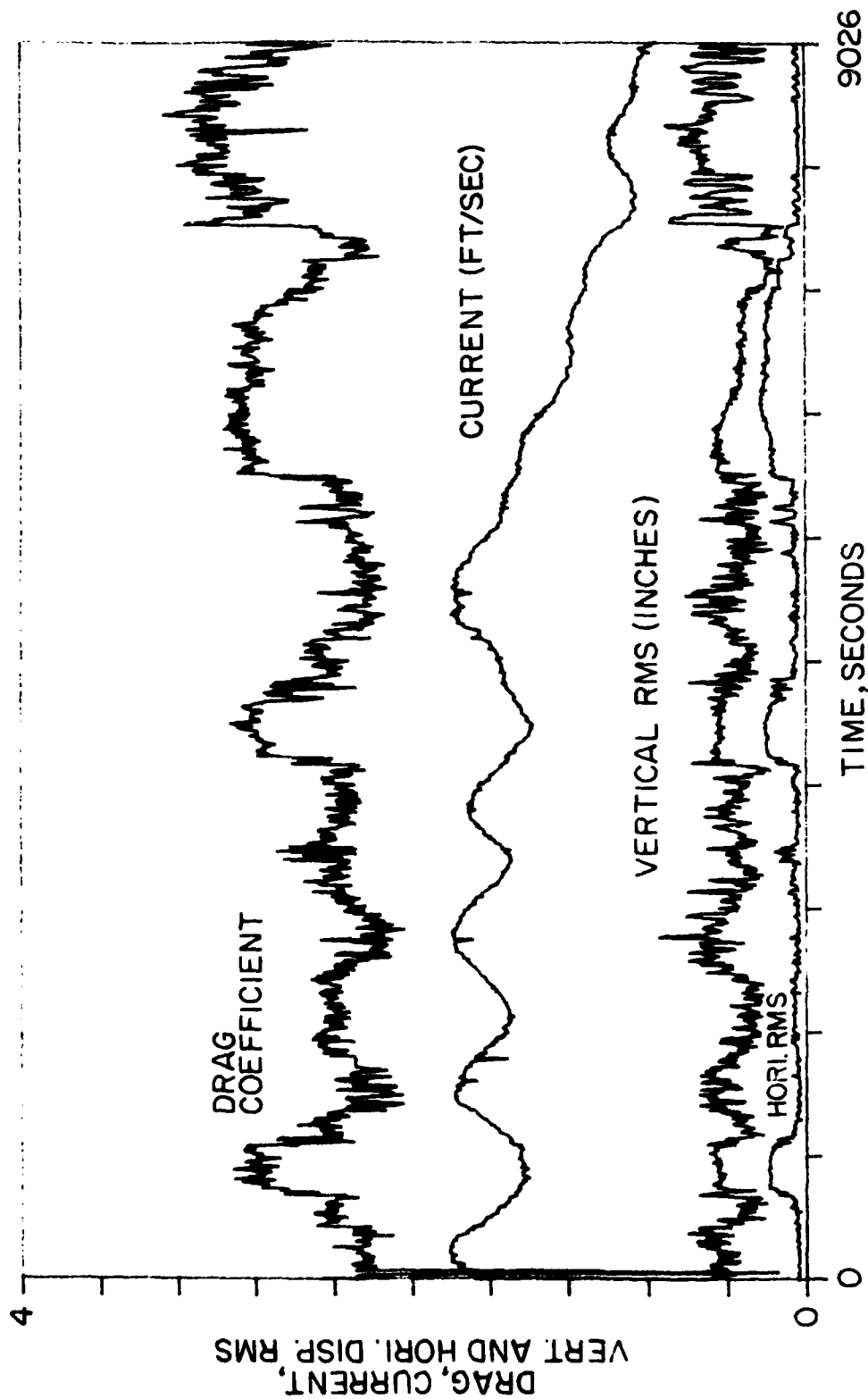
Fig. 28 — A two and one half hour time record of the hydrodynamic drag coefficient, the current, and the vertical and horizontal strumming displacement amplitudes for a cable with six attached masses (Run 20 of Table 1). The rms strumming amplitudes were derived from the accelerometer pair at 3L/4 along the cable.

70

that the strumming responses shown in Figs. 29 and 30 are either at or near this resonant frequency. The response spectra also may contain some energy at the Strouhal frequency of the flow and this may account for the twin peaks in some of the spectra.

The coefficient of the hydrodynamic drag force was amplified considerably, to $C_D =$ 2.2 to 3.1, as shown in Fig. 29. This is a substantial increase from the typical drag coefficient of $C_D \sim 1$ to 1.5 for a stationary cable. The vertical displacement amplitude of the cable strumming varied between $\overline{Y} = \pm 0.2$ and 0.6 in (rms). This relatively small amplitude at the $5L/8$ location is consistent with vibrations in the $n = 5$ cable mode, since a node of the vibration pattern then is to be expected at $3L/5$ nearby. The level of the drag amplification would appear to indicate that a somewhat larger amplitude should be expected at the antinodes of the cable vibration.

Another example taken from one of the more complex tests (Run 14 of Table 1) is shown in Fig. 31. Four heavy cylindrical masses were attached to the cable: at $L/8$, $3L/8$, $5L/8$ and $7L/8$. The cable tension was approximately 600 lb. The strumming response data shown for the 448 sec time period in Fig. 31 were recorded at $5L/8$ where both one of the attached masses and an accelerometer pair were located. The vibration level over the time of the test run was approximately $\overline{Y} = \pm 0.3$ to 0.45 in (rms), indicating that the attached mass did not act as a node of the cable system vibration pattern. The drag coefficient of the force on the system is $C_D =$ 2.4 to 3.2 which represents a substantial amplification from the stationary bare cable value of $C_D \doteq 1.2$. The relative contributions of the cable and the masses to the overall drag have not been determined. The frequency spectra for the vertical and horizontal displacement-time histories in Fig. 32 again clearly show resonant spectral speaks at the vortex shedding frequency (vertical) and twice the vortex shedding frequency (horizontal). The cable strumming vibrations in this example again are most likely to be in the fifth mode ($n = 5$).

A third example is given in Fig. 33. For this case (Run 16 of Table 1) six heavy masses were attached to the cable: at $L/6$, $L/3$, $L/2$, $5L/8$, $3L/4$ and $7L/8$. The cable strumming response measurements were made at $L/6$, again a location of both a mass and a pair of accelerometers. The drag coefficient in this case varied from about $C_D =$ 2.4 to 2.8. Over most of the time history shown the
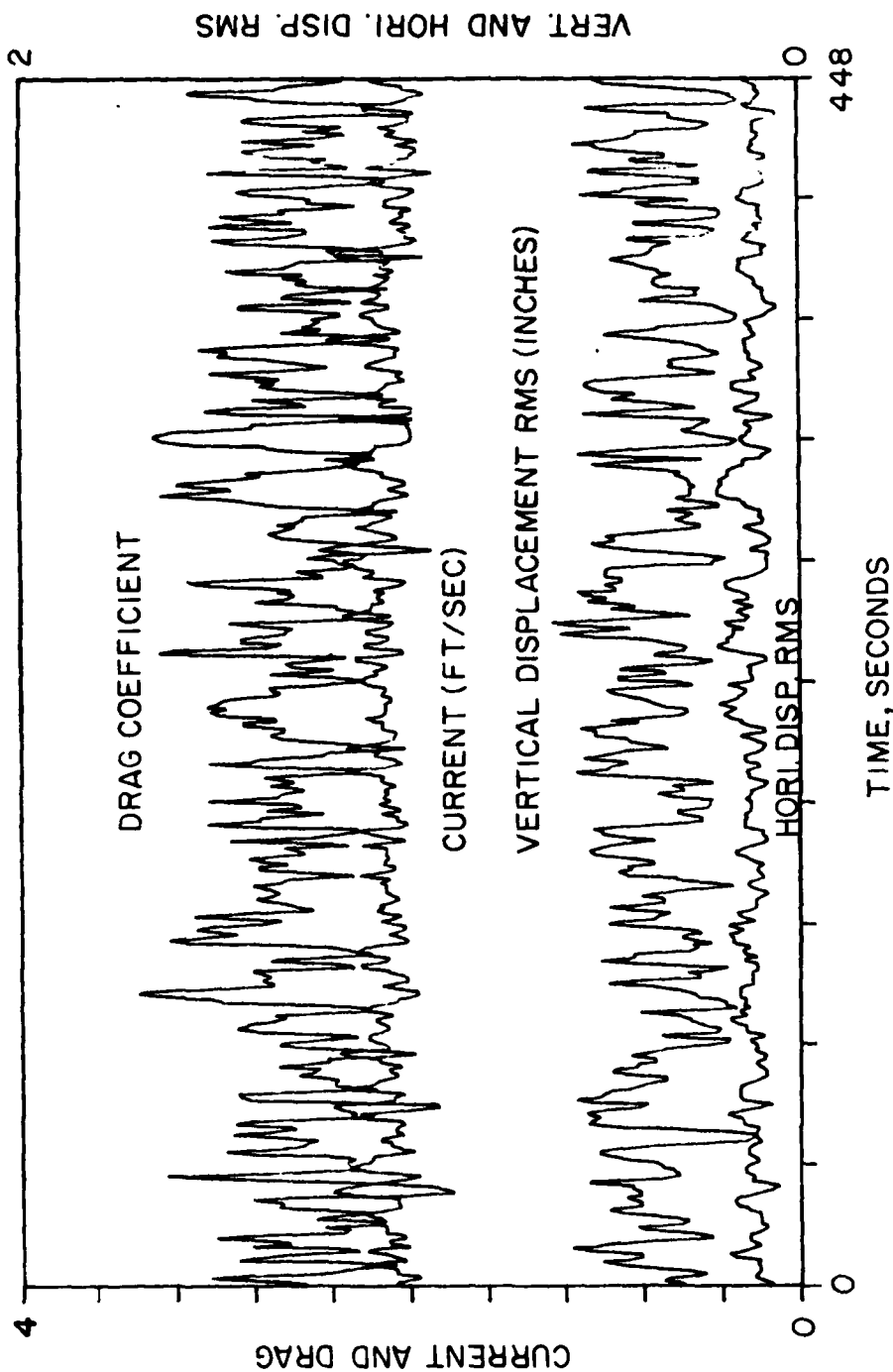
Fig 29 — A time history of the drag coefficient, the current speed, and the vertical and horizontal strumming displacement amplitudes for the cable with two heavy attached cylindrical masses (Run 10 of Table 1). The rms displacement amplitudes were derived from the outputs of the accelerometer pair at 5L/8 along the cable.

72

POWER SPECTRAL DENSITY
(MAXIMUM ENTROPY METHOD)
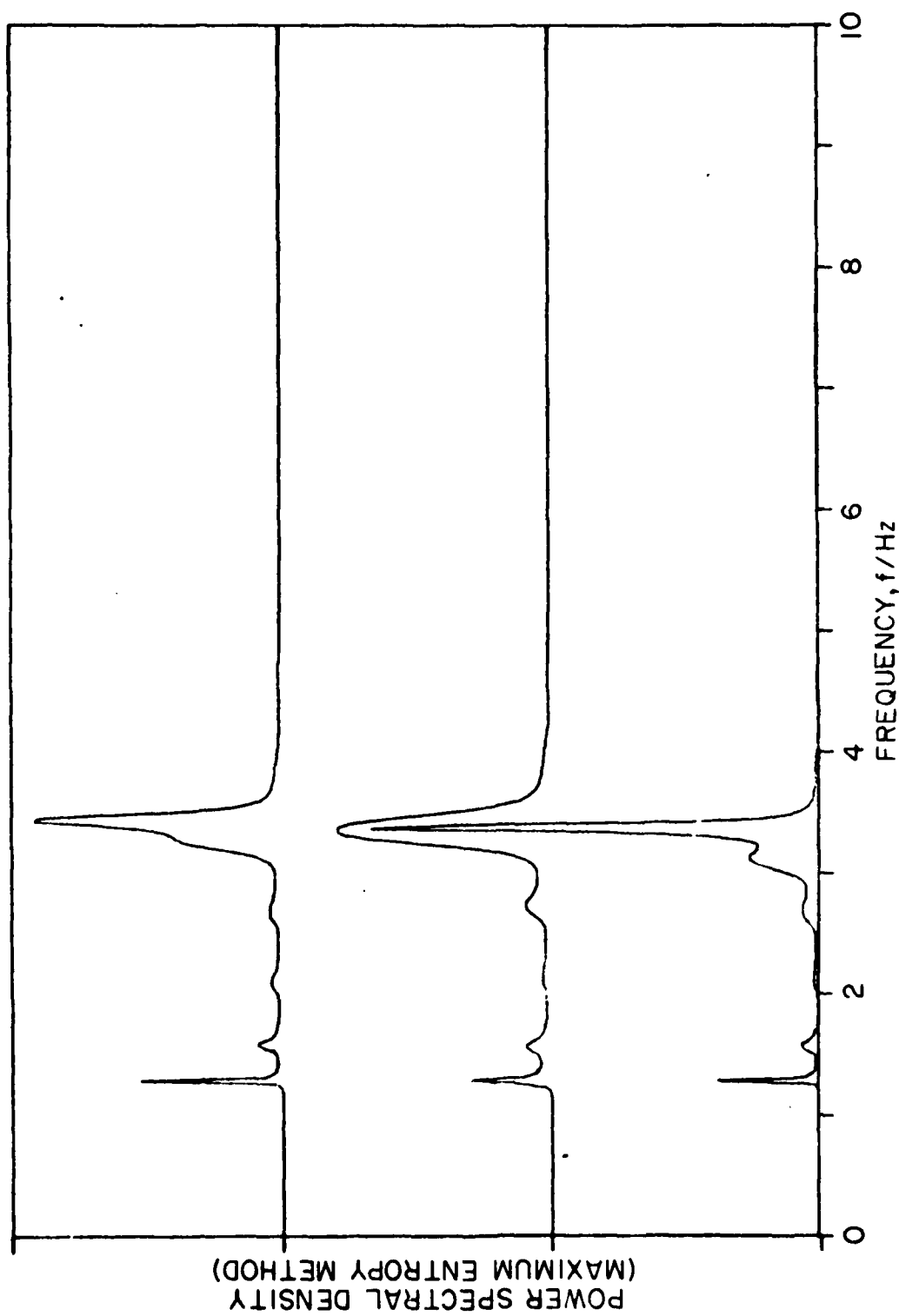
FREQUENCY, f/Hz

Fig. 30(a) — Vertical displacement amplitude.

Fig. 30 — Strumming frequency spectra for the cable with two attached masses (Run 10 of table 1).

73

Fig. 30(b) — Horizontal displacement amplitude.

POWER SPECTRAL DENSITY
(MAXIMUM ENTROPY METHOD)

FREQUENCY, f / Hz

74
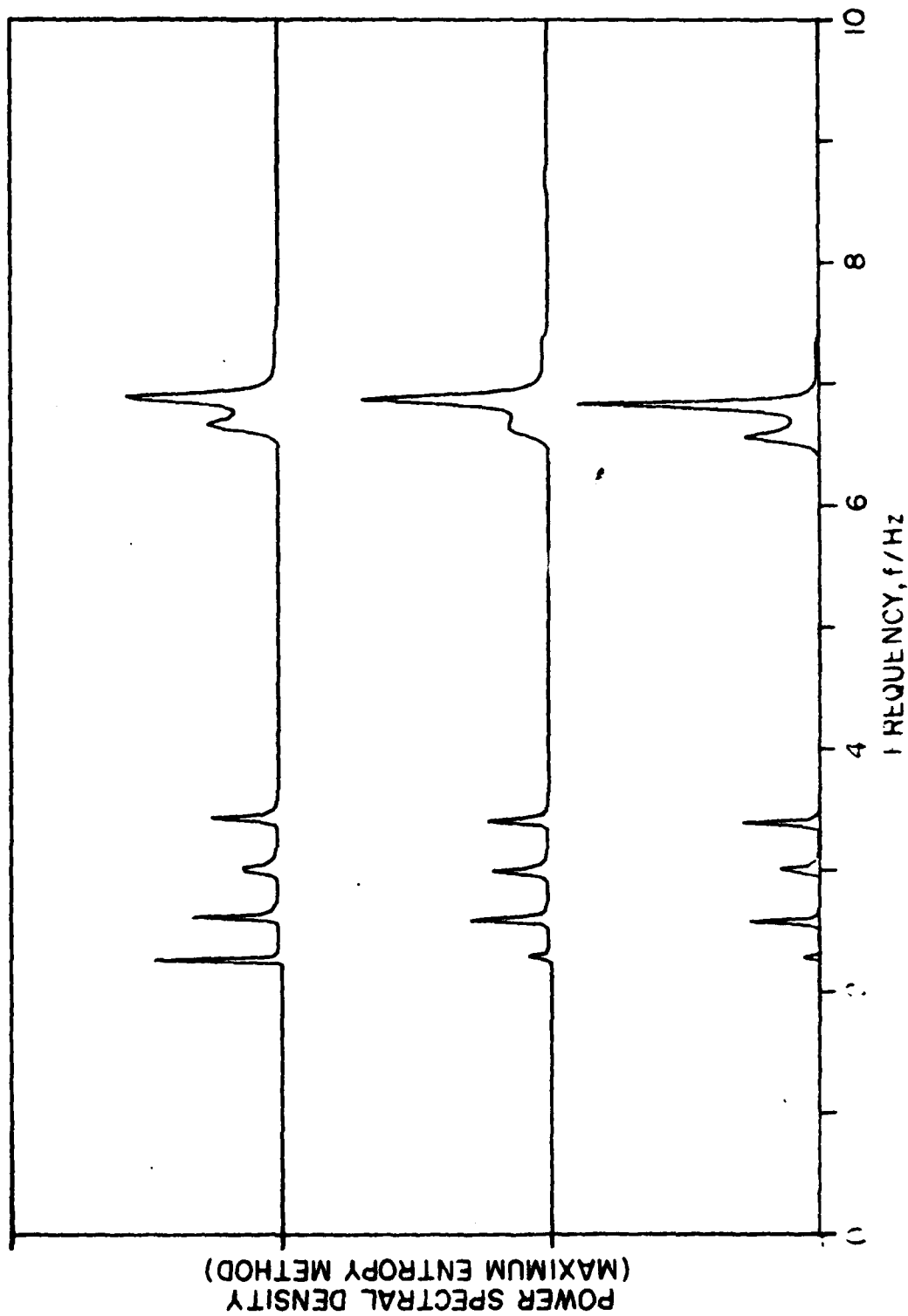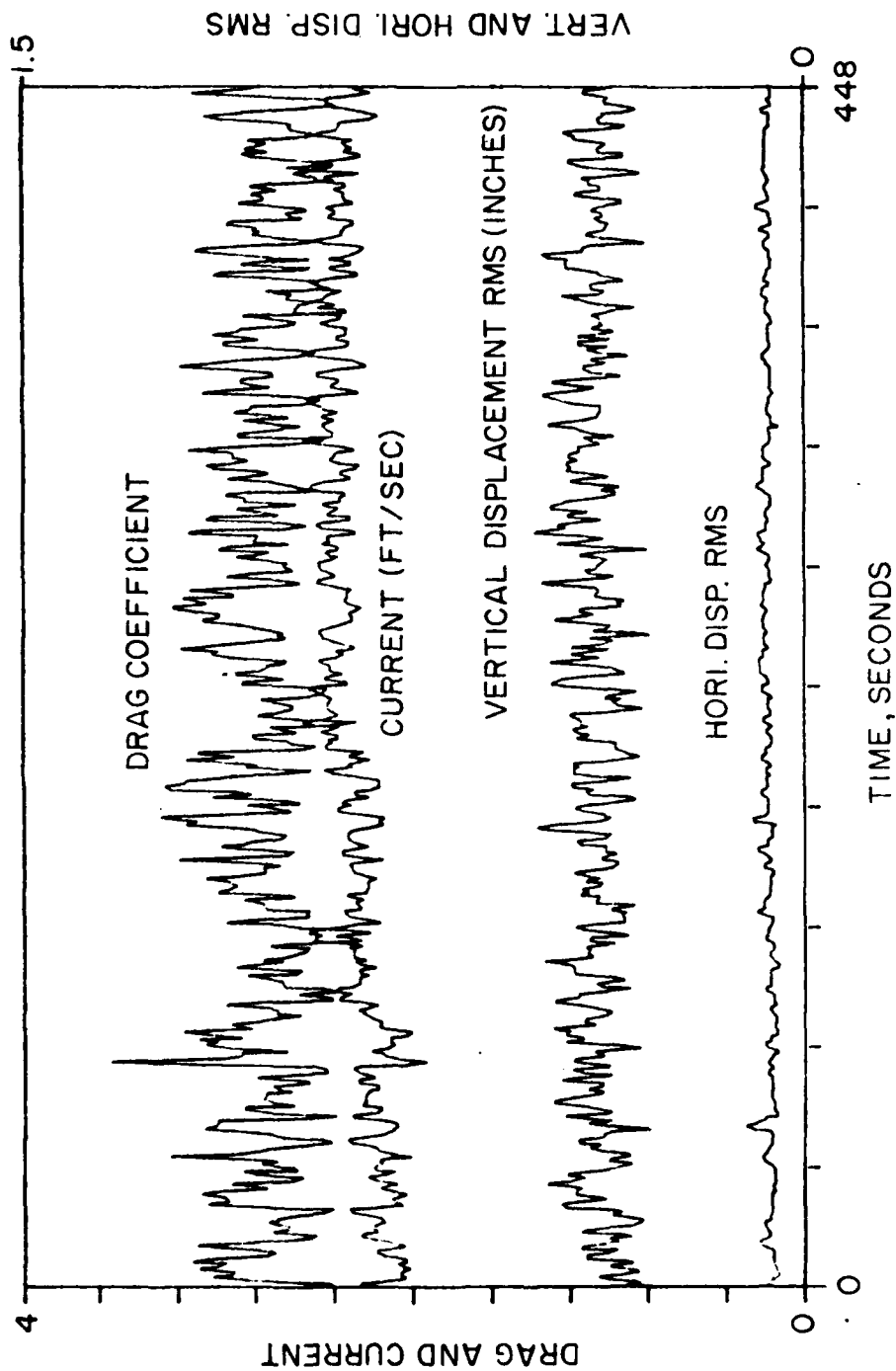
Fig. 31 — A time history of the drag coefficient, the current speed, and the vertical and horizontal strumming displacement amplitude for the cable with four heavy attached cylindrical masses (Run 14 of Table 1). The rms displacement amplitudes were derived from the outputs of the accelerometer pair at 5L/8 along the cable.

75
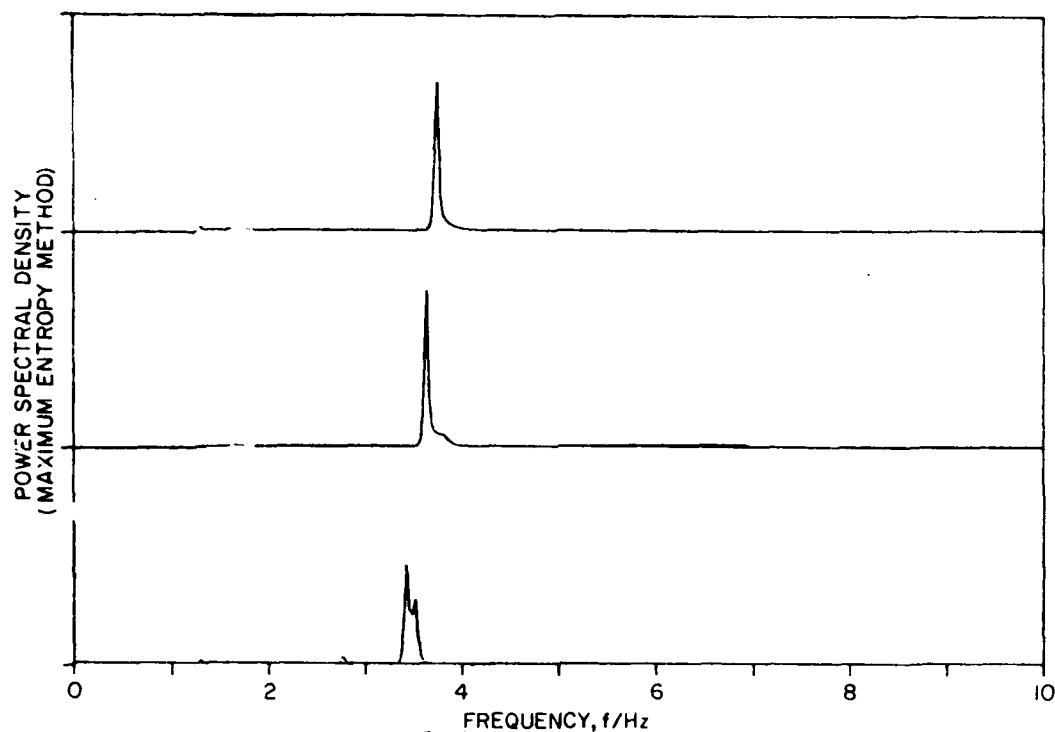
Fig. 32(a) — Vertical displacement amplitude.
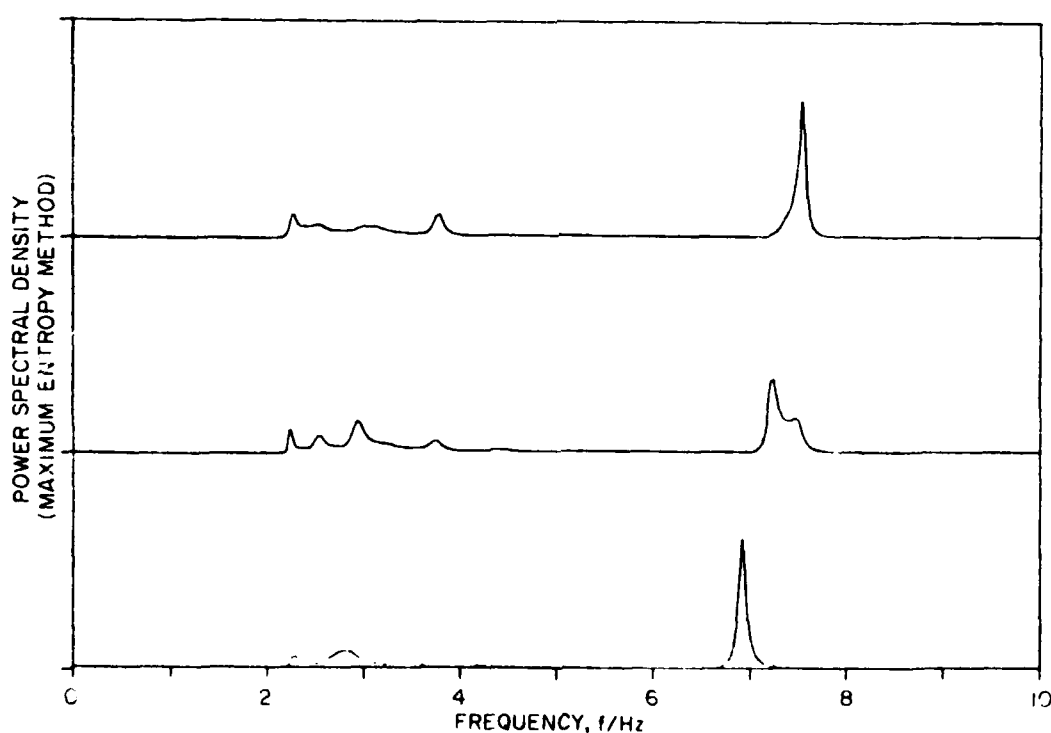
Fig. 32(b) — Horizontal displacement amplitude.

Fig. 32 — Strumming frequency spectra for the cable with four attached masses (Run 14 of Table 1)

76
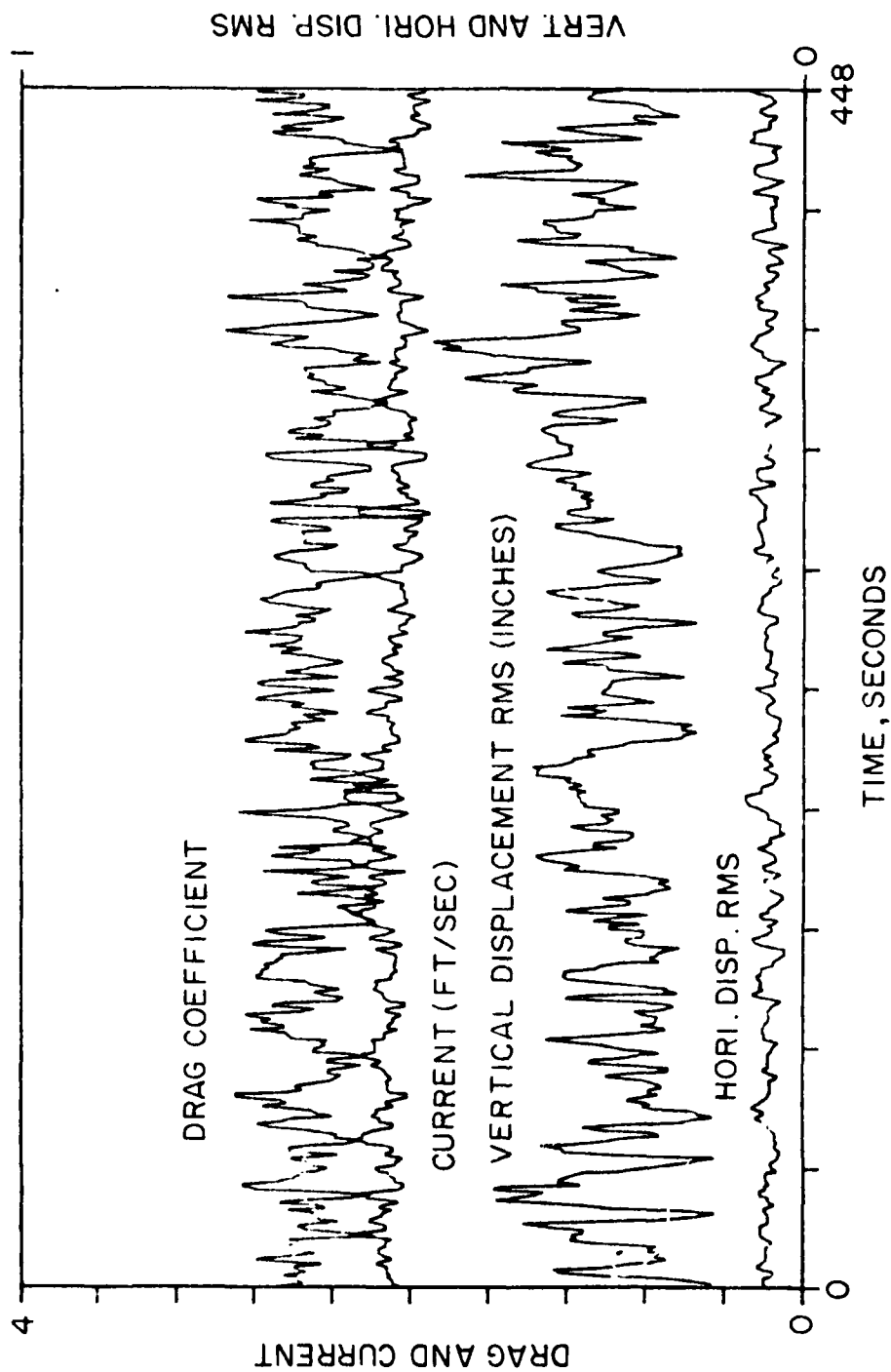
Fig. 33 — A time history of the drag coefficient, the current speed, and the vertical and horizontal strumming displacement amplitudes for the cable with six heavy attached cylindrical masses (Run 16 of Table 1). The rms displacement amplitudes were derived from the outputs of the accelerometer pair at L/6 along the cable

displacement amplitude varied between $\overline{Y} = 0.1$ and 0.4 in (rms). The frequency spectra of the measured vertical and horizontal strumming displacement amplitudes shown in Fig. 34 are non-resonant with several (five to six) distinct frequency spikes. It is likely that the cable response consists of several modes. These are three typical examples of the strumming drag for the cable with attached masses. Similar increases in drag were measured for all of the test runs with masses attached to the cable.

Several test runs were conducted with a bare cable during these tests. A 300 second time history for one such test is shown in Fig. 35. The cable was resonantly strumming at 1.9 Hz in the third mode normal to the current and nonresonantly in the fifth mode in line with the flow at 3.8 Hz. The vertical displacement amplitude is approximately $\overline{Y} = \pm 0.6$ to 0.7 D(rms) over the length of the record (7,8). The average drag force coefficient on the cable is approximately $C_D \simeq 3.2$; this is considerably greater than the drag coefficient $C_D = 1$ to 1.5 that would be expected if the cable were restrained from oscillating under these same flow conditions. The drag coefficint on the strumming cable was predicted with the equation (see Appendix C)

$$C_{D,\text{AVG}} = C_{D0}[1 + 1.043 \, (2 \, \overline{Y}_{\text{RMS}}/D)^{0.65}],$$

which was derived from the original results of Skop, Griffin and Ramberg (20). The strumming drag coefficient predicted using this equation is in the range $C_D = 2.4$ to 2.6 as shown in Fig. 35. This is somewhat below the drag force coefficient measured at the field site, but the predicted values are reasonable. The predicted drag on the oscillating cylindrical pipe was virtually indistinguishable from the measured drag coefficient (8,23).

The NATFREQ code was modified as described in Appendix C in order to account for the drag on the attached masses. This now is done in the two subroutines TTDRG and TWDRG of the code. The overall mean drag coefficients for Runs 10, 14, 16 and 20 in Table 1 were computed in order to assess the effect of the attached masses on the overall hydrodynamic force. The final results are given in Table 6. The attached masses, between two and six in number, do not greatly affect the overall drag on the system. However, the stationary cylinder drag coefficient was reduced to $C_{D0} = 0.8$ to take account of the small aspect ratio ($L/D = 3.4$) of the cylindrical masses. For a cable with a large number of attached masses there is likely to be a proportionately greater effect on the drag. The comparison is
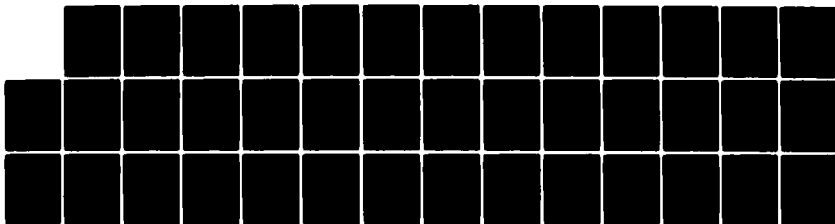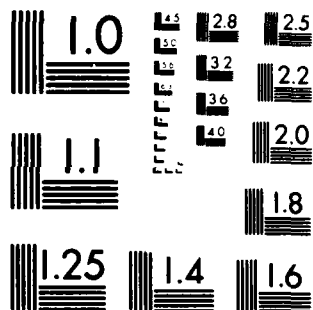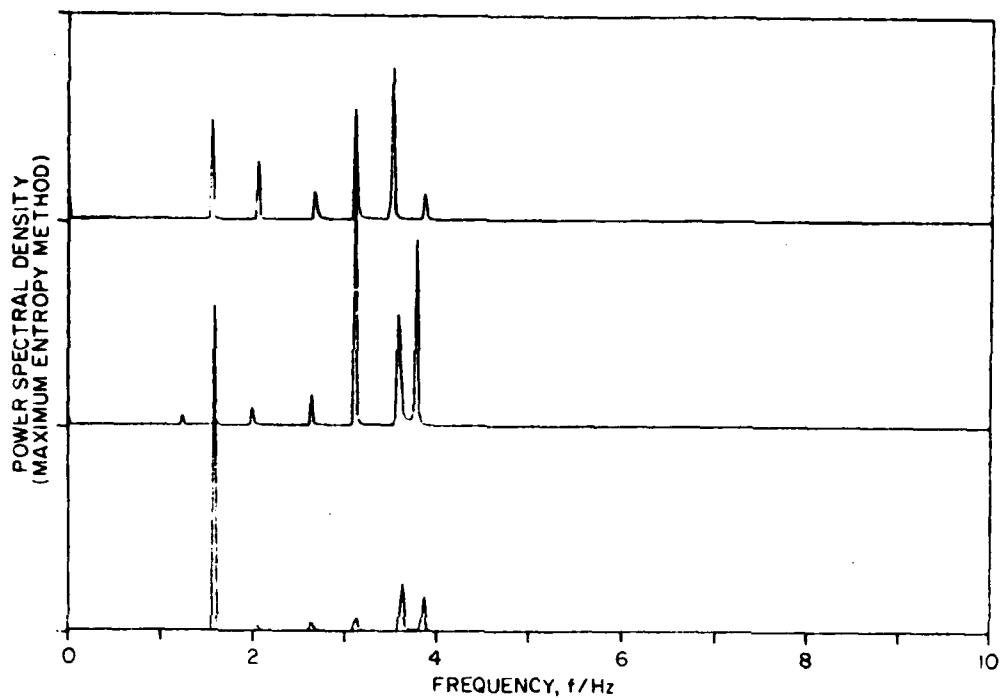
Fig. 34(a) — Vertical displacement amplitude.
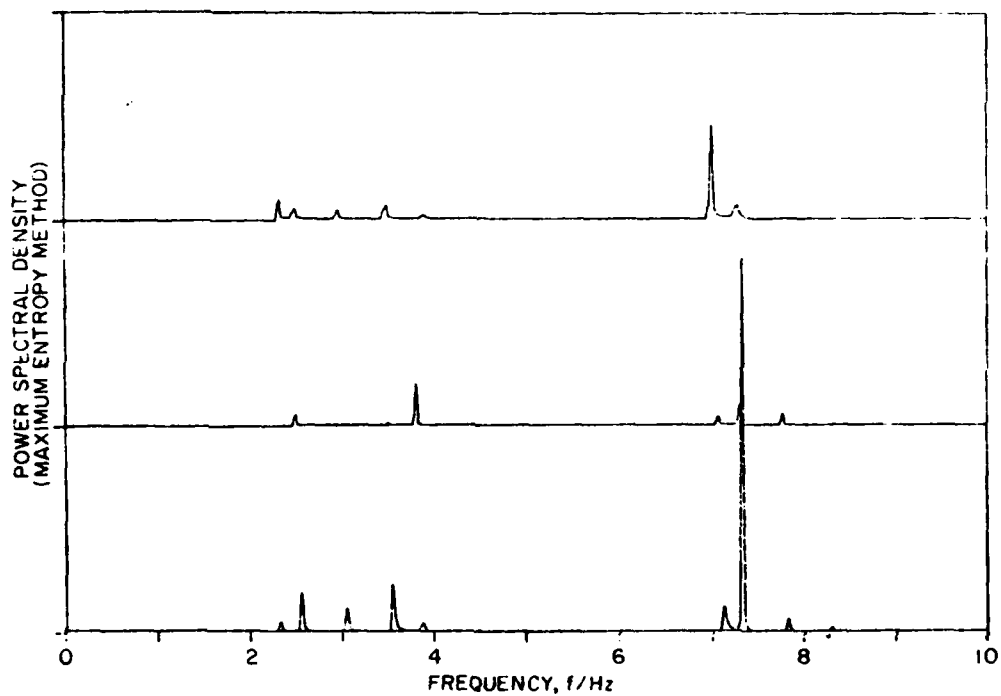
Fig. 34(b) — Horizontal displacement amplitude.

Fig. 34 — Strumming frequency spectra for the cable with six attached masses (Run 16 of Table 1).

79

Fig. 35 — Time histories of the measured and predicted drag coefficients C_D, the rms cable strumming displacement amplitudes, and the current speed for the bare cable (7,8). RMS displacement data were derived from the accelerometer pair located at $x = L/6$.

only qualitative because the predominant modes of response corresponding to the drag-time histories in Figs. 28, 29, 31 and 33 are not known. The average drag coefficients for the mode $n = 4$ are given in the table as examples. These are representative of the cable strumming responses measured during the experiments. The computed drag coefficients are generally within or close to the range measured at the Castine Bay test site. These results provide a reasonable basis for concluding that the NATFREQ computer code can be used with some confidence to provide engineering estimates of the mean hydrodynamic drag forces on marine cables with arrays of discrete masses attached to them.

Table 6
Hydrodynamic Drag Forces
1981 Castine Bay Field Experiments,
Marine Cables with Attached Masses

Test Number	Range[†]	Drag Coefficient, Cable (Avg.)[††]	Drag Coefficient, Cable & Masses (Avg.)[†††]
10	2.2-3.2	3.00	3.11
14	2.4-3.2	2.76	3 01
16	2.1-2.9	2.82	3.13
20	2.1-3.1	2.83	3.15

[†]Measured at the test site.
[††]Computed using NATFREQ; Mode number $n = 4$, $C_{D0} = 1.2$.
[†††]Computed using NATFREQ; Mode number $n = 4$, $C_{D0} = 1.2$.
(cable), $C_{D0} = 0.8$ (attached masses).

The amplification of the drag measured during these field experiments is comparable to the drag increases due to vortex shedding that have been measured in recent laboratory-scale experiments with cables and circular cylinders (23,24). For example, Overvik (24) measured drag coefficients of $C_D = 2.5$ when a model riser segment (a bare circular cylinder) was oscillating in water with $\bar{Y} = \pm 1.1 D$. This is an increase of 230 percent from the comparable measurement when the cylinder was restrained from oscillating. Griffin et al (17) have summarized recent laboratory-scale measurements of the drag on strumming cables. Comparable increases in C_D were commonly obtained in the tests that were reported.

7.4 Validation of NATFREQ

The results obtained in air can be used with the in-water cable strumming results to validate the NATFREQ computer code for use in engineering calculations. The natural frequencies for the cable in water were derived by C.Y. Liu at MIT from spectral analysis of the Castine Bay field test data. In most instances the measured frequencies plotted in figures are averages derived from two or three spectral estimates.

<u>Measurements in Water</u>. Comparable measurements of the cable's natural frequencies to those made in air were also made from data collected while the cable was strumming in water. The natural frequencies were derived from power spectral density plots for each cable-added mass configuration and were computed from 136 seconds of data. Two examples of the spectral density-frequency plots of the vertical acceleration signal are shown in Figs. 36 and 37. The averaged spectra were taken over a 136 second time period, or over 4096 points. The vertical lines represent NATFREQ-predicted frequencies.

The accelerometer pairs located at $L/8$ and $L/2$ were employed in the analysis. It was anticipated that the $L/2$ location would be a node for the even ($n = 2, 4$, etc.) cable modes, so that differences in the spectral density plots from the two locations could be used to discriminate between odd and even cable modes. In some cases this proved to be a reasonable approach. Most of the records that were analyzed were characterized by non-resonant strumming behavior, so that each frequency spectrum typically showed a distribution of peaks from which several participating cable modes could be identified with confidence.

A representative comparison of the computed and measured natural frequencies is given in Table 7 for those test runs which have provided reliable accelerometer, tension, and current data. For the listed cases in which the natural frequencies can be discriminated reliably, there is good agreement between the predicted and measured natural frequencies. Generally the differences between the two sets of frequencies are less than ten percent in all cases, and the horizontal and vertical accelerometers
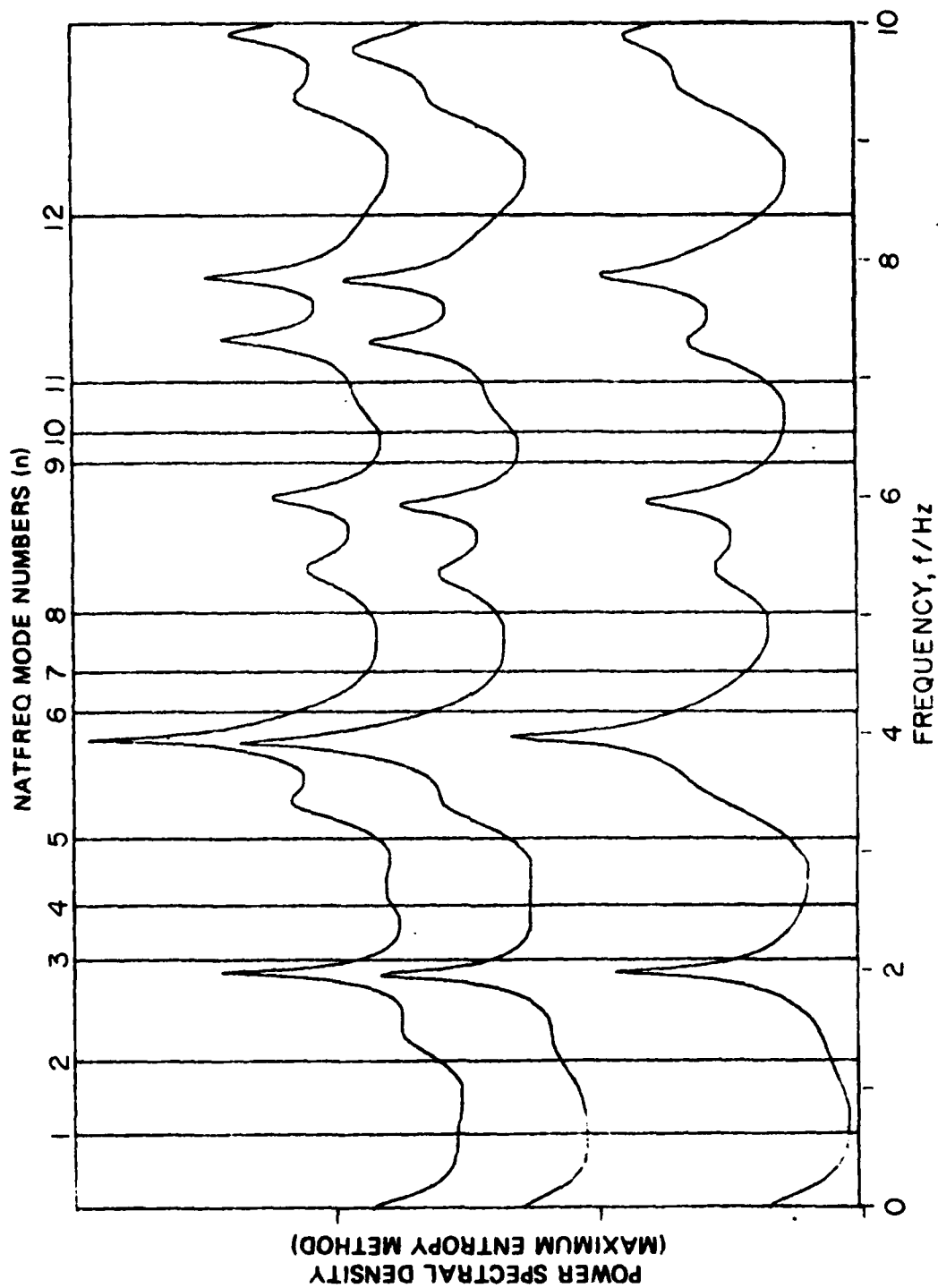
Fig. 36 — Spectral density of the measured natural frequencies in water for the Castine Bay cable with two light attached masses (Run 2 of Table 1). The vertical lines are the NATFREQ-predicted frequencies.

83
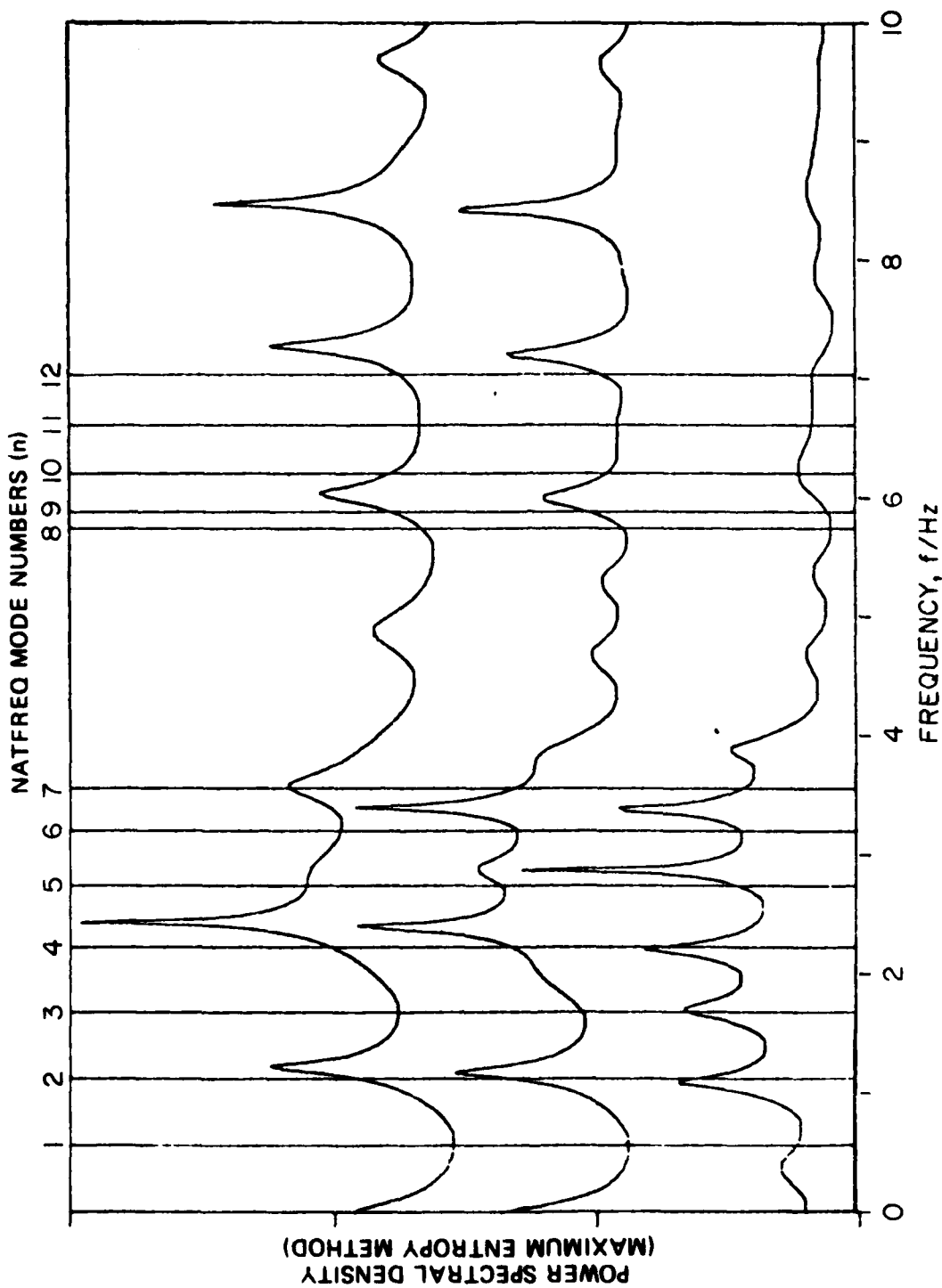
Fig 37 — Spectral density of the measured natural frequencies in water for the Castine Bay cable with seven light attached masses (Run 8 of Table 1). The vertical lines are the NATFREQ-predicted frequencies.

84

Table 7 — Measurements of Natural Frequency (In-Water)
1981 Castine Bay Field Experiment,
Marine Cables with Attached Masses

Test Number[*]	Mode	NATFREQ-Predicted Frequency, Hz	Measured Frequency, Hz	
			Vertical	Horizontal
2	1	0.63	0.72	0.72
	2	1.25	1.40	1.41
	3	2.10	2.20	2.24
	4	2.81	2.70	2.71
	5	3.12	3.30	3.27
	7	4.53	4.82	4.76
4	2	1.21	1.33	1.37
	3	1.80	1.85	1.85
	4	2.37	2.60	2.70
	7	4.64	4.83	4.81
8	1	0.56	0.6	0.6
	2	1.13	1.16	1.16
	3	1.67	1.68	1.69
	4	2.22	2.29	2.37
	5	2.73	2.83	2.87
	7	3.56	3.65	3.67
12	1	0.58	0.76	0.76
	2	1.16	1.26	1.25
	3	1.71	1.72	1.72
	4	2.22	2.20	
	5	2.62	2.67	
16	2	1.10	1.10	1.10
	3	1.62	1.74	1.74
	8	5.30	5.22	

*From Table 1.

at the two measurement locations give almost identical results in virtually all of the modal determinations listed in the table.

The results from two typical test runs are plotted in Figs. 38 and 39. In the first example seven light masses were attached to the cable at $mL/8$, $m = 1$ to 7. The in-water natural frequencies plotted in Fig. 38 confirm the good agreement that is suggested in Table 7, for the cable's natural modes up to $n = 7$. Another example is given in Fig. 39 for the cable with two light masses attached at $L/3$ and $2L/3$. The measured and predicted natural frequencies in water are in agreement up to $n = 7$ and $n = 11$ (not shown in the figure). The latter two frequencies were identified by comparing the spectral plots at $L/8$ and $L/2$, and by noting the presence of peaks in the spectra from the vertical and horizontal accelerometers at $L/2$. On this basis it reasonably can be assumed that the frequencies are odd modes and are equal to $n = 7$ and $n = 11$. It also is clear from Fig. 39 that the measured natural frequencies exhibit the same discontinuous behavior that is predicted when the number of cable segments is equal to the mode number n.

Several in-air natural frequencies also are plotted in Figs. 38 and 39. As had been noted earlier there also is good agreement between the measured and predicted frequencies in these cases. The added mass effect of the water is evident from the computed and measured results. In most cases the predicted natural frequencies are slightly lower than the measured values. An added mass coefficient $C_{am} = 1$ was chosen for both the cable and the cylindrical masses. This value may be slightly high but it is difficult to justify another choice a priori, especially since the measured and predicted frequencies are in such close overall agreement.

It is clear from the results of this comparison that it is possible to predict the natural frequencies of a taut cable with attached masses to better than ten percent. However, at the higher modes the difference in frequency between modes will be considerably less than this value. Then it is difficult or impossible to positively identify which spectral frequency is associated with which predicted mode. Such detailed identification would require more extensive knowledge of the mode shapes of the system. As a practical matter this requires many more measurement locations, with the concomitant expense of additional instrumentation such as accelerometers and a more complex cable construction.
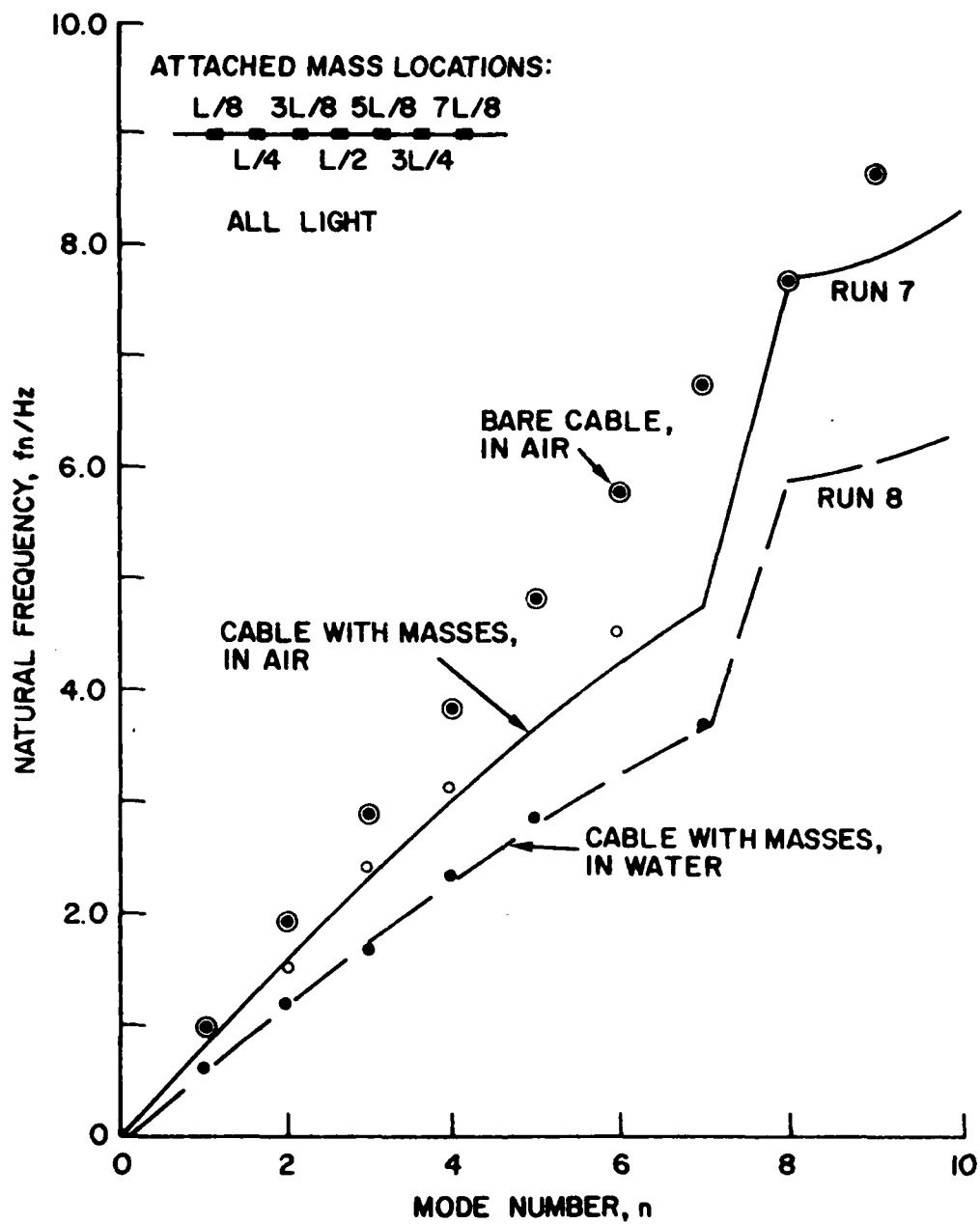
Fig 38 — A comparison between predicted (NATFREQ) and measured natural frequencies for a cable with seven light attached cylindrical masses (Runs 7 and 8 of Table 1). Measured in air, 0, measured in water. ●; remaining legend as in Fig. 14.

87
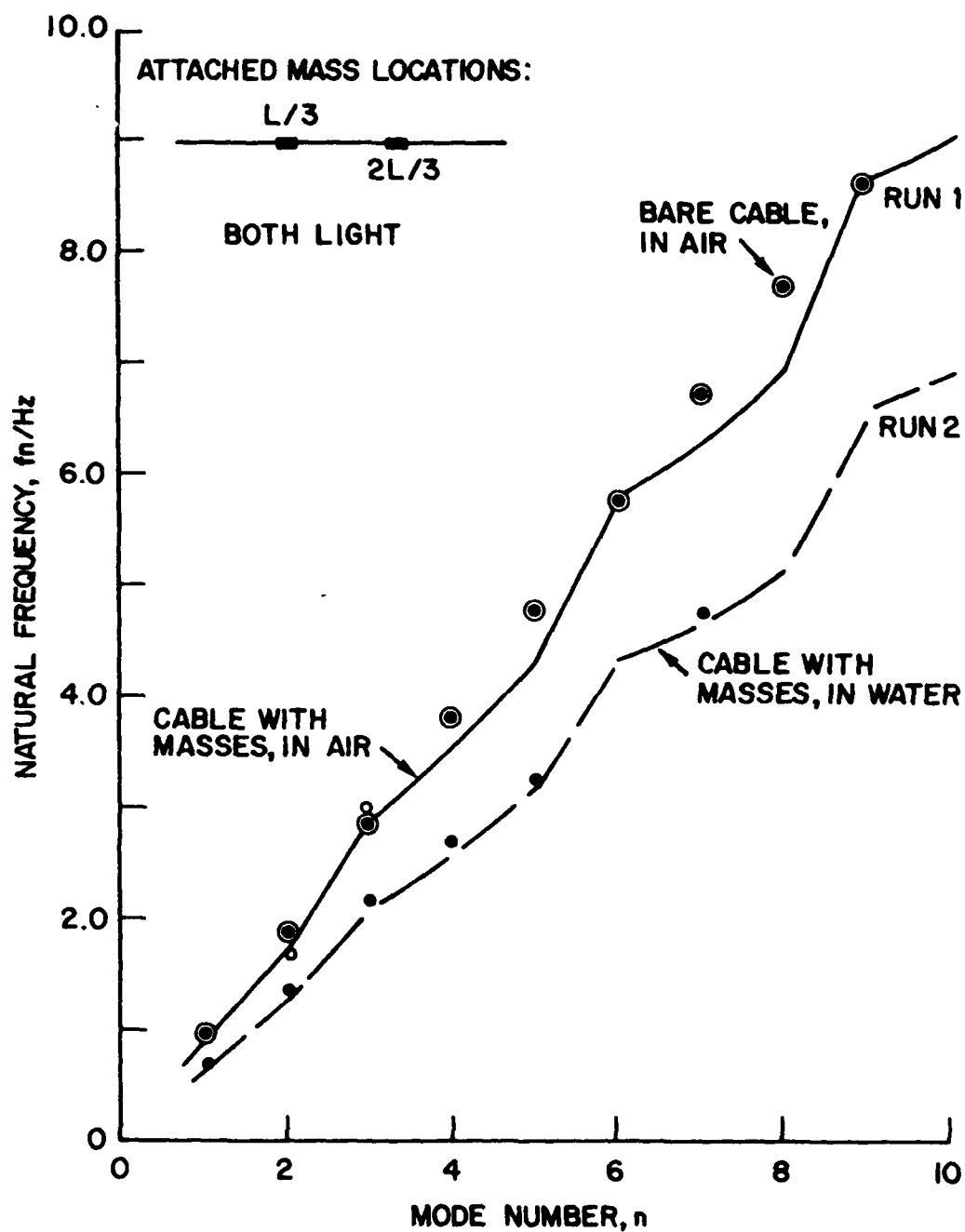
Fig. 39 — A comparison between predicted (NATFREQ) and measured natural frequencies for a cable with two light attached masses (Runs 1 and 2 of Table 1). Measured in air, O: measured in water, ●: remaining legend as in Fig. 11.

8. SUMMARY

8.1 Findings and Conclusions

Both laboratory-scale and field experiments have been conducted to investigate the effects of attached masses on the vortex-excited strumming response of taut marine cables. A comparison has been made in this report between the natural frequencies and mode shapes computed with the NATFREQ computer code and measured during the 1981 Castine Bay field experiment. Also, as background, and for additional comparisons, summaries are given here of the NATFREQ cable analysis algorithm and other recent experiments to study the flow-induced strumming response of cables with arrays of attached masses.

Twenty test runs were conducted during the experimental phase of the program. These consisted of ten pairs of equivalent tests conducted in air and in water. The measured in-air natural frequencies are in good agreement with the NATFREQ predictions for the second and higher (up to $n = 5$) cable modes. The first mode frequency apparently was influenced by the sag of the cable. The measured mode shapes of the cable vibrations in air are in agreement with the computed mode shapes, but only limited mode shape comparisons are possible due to the existing capabilities of the code.

Good agreement also was obtained between the NATFREQ-predicted natural frequencies and the frequencies measured in water. It is clear from the comparison given in this report that it is possible to predict the natural frequencies of a *taut* cable with attached masses to better than ten percent. However, at high cable mode numbers the difference in frequency between modes often is considerably less than this value. Then it is difficult to positively identify which measured cable frequency is associated with which predicted mode.

The results available to-date tend to validate the NATFREQ computer code as a reliable engineering model for predicting the natural frequencies and mode shapes of *taut* marine cables with arrays of discrete masses attached to them.

The static and dynamic analyses of a marine cable system that experiences environmental loading require the calculation of the hydrodynamic drag forces. Strumming of a cable segment due to vortex shedding increases the overall mean drag force and results in a corresponding increase in the cable drag force and coefficient. The calculation of the strumming drag requires as inputs the natural frequencies and mode shapes of the cable. For a cable segment with masses attached to it the NATFREQ code provides this information.

Measurements of the hydrodynamic drag forces during the Castine Bay field experiments consistently produced drag coefficients in the range $C_D = 2$ to 3.2 for the bare cable and the cable with attached masses. This is a substantial amplification of the drag force from the expected level for a stationary cable ($C_D = 1$ to 1.5).

The drag coefficient on the strumming cable was predicted by Vandiver (23) with a strumming drag model that was developed at NRL as part of the overall NCEL cable dynamics research program. The predicted drag on the cable was within about 20 percent of the measured drag. For a complementary experiment at the test site with a flexible circular steel pipe, the predicted drag coefficients were virtually indistinguishable from the measured drag coefficients (23).

The NATFREQ computer code contains a routine for computing the amplified hydrodynamic drag due to strumming. This routine now has been modified to account for the drag on the attached masses (cylindrical and spherical). Previously only the strumming drag on the cable segments between masses was completed.

8.2 Recommendations

Several recommendations have been developed as a result of the comparison between the NATFREQ code predictions and the Castine Bay field tests. These recommendations are:

- Cable sag or slack cable effects often play an important role in the dynamics of marine cables. The NATFREQ code is limited to *taut* cable dynamics. Consideration should be

90

given to the development of a comparable code for the calculation of the natural frequencies and mode shapes of a *slack* cable with attached masses. At least one such code, called SLAK, presently exists in rudimentary form (1).

● Many of the data records from the 1981 Castine field experiment contain lengthy time segments where the cable strumming is nonresonant, i.e. the vibrations and the vortex shedding are not locked-on at a single resonant frequency. Consideration should be given to developing a *simple* but still effective method for taking nonresonant strumming effects into account in determining the cable response and the strumming-induced hydrodynamic drag force and coefficient C_D.

9. REFERENCES

1. O.M. Griffin, S.E. Ramberg, R.A. Skop, D.J. Meggitt and S.S. Sergev, "The Strumming of Marine Cables: State-of-the-Art," NCEL Technical Note No. N-1608 (May 1981).

2. J.E. Kline, A. Brisbane and E.M. Fitzgerald, "A Study of Cable Strumming Suppression," NCEL Contract Report CR81-005 (April 1981).

3. J.E. Kline, E. Fitzgerald, C. Tyler and T. Brzoska, "The Dynamic Response of a Moored Hydrophone Housing Assembly Subjected to a Steady Uniform Flow," MAR Incorporated Technical Report No. 237 (February 1980).

4. S.S. Sergev and W.D. Iwan, "The Natural Frequencies and Mode Shapes of Cables with Attached Masses," NCEL Technical Note No. N-1583 (August 1980); see also Trans. ASME, J. Energy Resources Tech., Vol. 103, 237-242 (1981).

5. J.K. Vandiver and T.W. Pham, "Performance Evaluation of Various Strumming Suppression Devices," MIT Ocean Engineering Department Report 77-2 (March 1977).

6. J.K. Vandiver and C.H. Mazel, "A Field Study of Vortex-Excited Excited Vibrations of Marine Cables," Offshore Technology Conference Paper OTC 2491 (May 1976).

7. J.K. Vandiver and O.M. Griffin, "Measurements of the Vortex-Excited Strumming Vibrations of Marine Cables," Ocean Structural Dynamics Symposium '82 Proceedings, Oregon State University, 325-338 (September 1982).

8. J.C. McGlothlin, "Drag Coefficients of Long Flexible Cylinders Subject to Vortex Induced Vibrations," M.S. Thesis, MIT Ocean Engineering Department (January 1982).

9. W.D. Iwan, "The vortex-induced vibration of nonuniform structural elements," J. Sound and Vib., Vol. 79. 291-302 (November 1981).

10. M.R. Hunt, "Natural Frequencies and Damping Factors for a Cable with Lumped Masses," B.S. Thesis, MIT Ocean Engineering Department (June 1982).

11. E. Moas, "Natural Frequencies and Damping Factors for a Bare Cable and a Pipe," B.S. Thesis, MIT Ocean Engineering Department (June 1982).

12. Jen-Yi Jong and J. Kim Vandiver, "Response Analysis of the Flow-Induced Vibration of Flexible Cylinders Tested at Castine, Maine in July and August of 1981," MIT Ocean Engineering Department Report (15 January 1983).

13. J.K Vandiver, "Natural Frequencies, Mode Shapes, and Damping Ratios for Cylinders Tested at Castine, Maine in the Summer of 1981," MIT Ocean Engineering Department, Unpublished Report (September 1982).

14. S.E. Ramberg and O.M. Griffin, "Free Vibrations of Taut and Slack Marine Cables," Proc. ASCE, J. Structural Div., Vol. 103, No. ST11, 2079-2092 (November 1977).

15. J.K. Vandiver, "A Comparison Between Predicted and Measured Natural Frequencies in Water for the Castine Cable with Attached Masses," MIT Ocean Engineering Department, Unpublished Report (December 15, 1982).

16. R.D. Peltzer, "Vortex Shedding From a Vibrating Cable with Attached Spherical Masses in a Linear Shear Flow," Ph.D. Thesis, Virginia Polytechnic Institute and State University (August 1982); see also NRL Memorandum Report 4940 (October 1982).

17. O.M. Griffin, J.K. Vandiver, R.A. Skop and D.J. Meggitt, "The Strumming Vibrations of Marine Cables," Ocean Science and Engineering, Vol. 7, No. 4, 461-498 (1982).

18. T.R. Kretschmer, G.A. Edgerton and N.D. Albertsen, "Seafloor Construction Experiment, SEACON II; An Instrumented Tri-Moor for Evaluating Undersea Cable Structure Technology," Naval Civil Engineering Laboratory Report R-848 (1976).

19. M. Kennedy and J.K. Vandiver, "A Random Vibration Model for Cable Strumming Prediction," Civil Engineering in the Oceans IV Proceedings, ASCE: New York, 273-292 (1979).

20. R.A. Skop, O.M. Griffin and S.E. Ramberg, "Strumming Predictions for the SEACON II Experimental Mooring," Offshore Technology Conference Preprint OTC 2491 (May 1977).

21. O.M. Griffin, "Steady Hydrodynamic Loads Due to Vortex Shedding from the OTEC Cold Water Pipe," NRL Memorandum Report 4698 (January 1982).

22. O.M. Griffin, "OTEC Cold Water Pipe Design for Problems Caused by Vortex-Excited Oscillations," Ocean Engineering, Vol. 8, 129-209 (1981); see also NRL Memorandum Report 4157 (March 1980).

23. J.K. Vandiver, "Drag Coefficients of Long, Flexible Cylinders," Offshore Technology Conference Paper OTC 4490 (May 1983).

24. T. Overvik, "Hydroelastic Motion of Multiple Risers in a Steady Current," Ph.D. Thesis, Norwegian Institute of Technology (August 1982).

25. M.J. Every, R. King and O.M. Griffin, "Hydrodynamic Loads on Flexible Marine Structures Due to Vortex Shedding," ASME Paper 81-WA/FE-24 (November 1981); also Transactions of the ASME, Journal of Energy Resources Technology, Vol. 104, 330-336 (December 1982).

Appendix A

A LISTING OF THE NATFREQ COMPUTER CODE

```
FTN4,L
      PROGRAM NEWNT
C     PROGRAM NEWNAT(INPUT,OUTPUT,TAPE5=INPUT,TAPE6=OUTPUT)
C     TITLE( 8) IS 80 COLUMNS OF TITLE INFORMATION
C     CDI =0(BLANK) IF NONUNIFORM CABLE WEIGHTS AND DIAMETERS ARE TO BE
C                   SUPPLIED FOR EACH SEGMENT
C          1       IF CABLE WIEGHTS AND DIAMETERS FOR ALL SEGMENTS ARE
C                  SAME AS FIRST SEGMENT
C     CT  =0(BLANK) IF NONUNIFORM CABLE TENSIONS ARE TO BE SUPPLIED FOR
C                   EACH CABLE SEGMENT
C          1       IF CABLE TENSION FOR ALL SEGMENTS IS SAME AS FIRST
C                  SEGMENT
C     NSEG = NO. OF SEGMENTS
C     NPLOT = BLANK -NO PLOT REQUIRED
C             PLOT  -PLOT OF AMPLITUDE
C             SCRL  -EACH MODE, SCRLL  FASHION
C     PLEN = LENGTH OF  DESIRED AMPLITUDE PLOT(IN)
C            DEFAULT = 20.
C     CL(I) = LENGTH OF I-TH CABLE SEGMENT (FT)
C     D(I) = DIAMETER OF I-TH CABLE SEGMENT(IN)
C     CDC(I) = DRAG COEF. OF I-TH CABLE SEGMENT
C     WC(I) = TOTAL WEIGHT OF I-TH CABLE SEGMENT INCLUDING ADDED WATER
C             WEIGHT (LB/FT)
C     TC(I) = TENSION IN I-TH CABLE SEGMENT (LB)
C     AW(I) = TOTAL ADDED WEIGHT AT END OF I-TH CABLE SEGMENT INCLUDING
C             ADDED WATER WEIGHT(LB).   AW(NSEG) IS ARBITRARY.
C     CDA(I) = CD*AREA FOR I-TH ADDED WEIGHT IN FT**2
C     STWT(I) = SPRUNG MASS AT THE END  OF SPRING AT END OF THE I-TH
C               CABLE SEGMENT INCLUDING ADDED WATER WEIGHT (LB)
C     MXMDS = MAX NO OF MODES TO BE FOUND IN SEARCH
C     ACC = ACCURACY PARAMETER IN MODE SEARCH,USE 0.001 NOMINAL
C     OMNAT = NATURAL FREQUENCY OF THE ATTACHED SPRING-MASS COMBINATION
C     OMSTRT = BEGINNING FREQ. FOR MODE SEARCH (RAD/SEC)
C     OMSTOP = ENDING FREQ. FOR MODE SEARCH(RAD/SEC)
C     DELOM = FREQ. SEARCH INCREMENT (RAD/SEC)
C            --CALCULATED INTERNALLY IF DELOM=0
C     UNITS = 1 FREQUENCY SEARCH IN RAD/SEC
C             2 FREQUENCY SEARCH IN HERTZ
C             3 FREQUENCY SEARCH IN FT/SEC
C             4 FREQUENCY SEARCH IN CM/SEC
C             5 FREQUENCY SEARCH IN KNOTS
C     ISUPRS = 0 FULL PRINTOUT OF SEGMENT RESPONSE
C              1 SUPRESS FULL PRINTOUT
C     ZETA = DAMPING RATIO FOR CABLE IN AIR
C     RHOW = WEIGHT DENSITY OF FLUID IN LB/FT**3
C     S(I) = ARC LENGTH TO END OF I-TH SEGMENT
C     CP(I) = COUPLING PARAMETER
C     DU(I) = ARRAY OF DISTINCT CABLE DIAMETERS
C     DS = DIA OF STRUMMING CABLE SEGMENTS
C     STIF(I)=SPRING STIFFNESS AT END OF THE I-TH CABLE SEGMENT(LB/FT)
      COMMON/C1/CL( 21),D( 21),WC( 21),TC( 21),AW( 21),NZX( 21),NSEG,
     1ALP( 21)
      COMMON/C2/A( 21),B( 21),PHAS( 21),PI,BSIZE,AMPL( 21),RAMP  21)
      COMMON/C3/CD( 21)
```
94

```
      COMMON/C4/BMAX, JPLTNO
      COMMON/C6/STIF( 21),STWT( 21)
      COMMON/C7/BN( 21),BNSIZE
      COMMON/C11/CDC( 21),CDA( 21),CP( 21),DS,ZETA,ZETAE,RHOW,RMU,
     1CDAS( 21)
      DIMENSION S( 21),DU( 21)
      INTEGER TITLE(40),UNITS,CDI,CT
      REAL KOMSRT,KOMSTP,KDELOM
      DOUBLE PRECISION OMCD,OMP,X1,X2,B1,B2,BP,BC
C
C******SET FUNCTIONS AND CONSTANTS
      HERTZ(X) = X/(2.*PI)
       JPLTNO=0
      PI = ATAN2(0.,-1.)
      STRHN = 0.21
      ND = 1
C******READ/WRITE INPUT DATA
   10 READ(5,1001)(TITLE(J),J=1,40)
C     IF(EOF(5))9999,11
 1001 FORMAT(40A2)
C  11 CALL DATE(IDAY)
C     CALL TIME(ITIM)
      WRITE(6,1002)(TITLE(K),K=1,40),IDAY,ITIM
 1002 FORMAT(1H1,40A2/6H DATE-,A10,7H  TIME-,A10/1X,80(1H=)//)
      ITIME = 0
      IAPROX = 0
      READ(5,1003)CDI,CT
 1003 FORMAT(2I10)
      READ(5,1004)NSEG,NPLOT,PLEN
 1004 FORMAT(I10,A2,2X,F6.0)
      WRITE(6,1005)ND
 1005 FORMAT(1X,12HDATA SET NO.,I3//17H CABLE PARAMETERS/)
      WRITE(6,1006)
 1006 FORMAT(1X,85HNOTE- ALL WEIGHTS ARE TOTAL EFFECTIVE WEIGHTS AND INC
     1LUDE EFFECTS OF ADDED WATER MASS)
C******READ FIRST CABLE SEGMENT INFO HERE
      READ(5,1016)CL(1),D(1),CDC(1),WC(1),TC(1),AW(1),CDA(1),STIF(1),
     1STWT(1)
 1016 FORMAT(F10.0,2F5.0,6F10.0)
      IF(CDI.EQ.1)WRITE(6,1007)
 1007 FORMAT(7X,51HCABLE WEIGHT AND DIAMETER ARE SAME FOR EACH SEGMENT)
      IF(CT.EQ.1)WRITE(6,1008)
 1008 FORMAT(7X,38HCABLE TENSION IS SAME FOR ALL SEGMENTS)
      WRITE(6,1009)
 1009 FORMAT(//,1X,3HSEG,5X,6HLENGTH,3X,10HARC LENGTH,3X,
     1 4HDIAM,3X,4HDRAG,3X,9HWT/LENGTH,3X,7HTENSION,
     2 3X,8HATTACHED,3X,7HCD*AREA,3X,7HATT SPR,4X,6HSPRUNG,
     3 3X,12H SPRING-MASS/
     4 2X,2HNO,6X,4H(FT),7X,4H(FT),6X,4H(IN),3X,4HCOEF,4X,
     5 7H(LB/FT),5X,4H(LB),5X,8HWT  (LB),3X,7H(FT**2),3X,7H(LB/FT),
     6 3X,8HMASS(LB),3X,11HN FREQ (HZ)/)
C******CHECK HERE FOR NON UNIFORM WEIGHT,DIA AND TENSION
      IF(CDI.EQ.0.AND.CT.EQ.0) GO TO 130
C******CHECK HERE FOR NON UNIFORM WEIGHT AND DIA ONLY
```

95

```
      IF(CDI.EQ.0) GO TO 120
C*****CHECK HERE FOR NONUNIFORM TENSION ONLY
      IF(CT.EQ.0) GO TO 110
C*****UNIFORM WEIGHT,DIA AND TENSION
      DO 101 I = 2,NSEG
      READ(5,1011)CL(I),AW(I),CDA(I),STIF(I),STWT(I)
 1011 FORMAT(F10.0,30X,4E10.0)
      WC(I)=WC(1)
      D(I)=D(1)
      CDC(I) = CDC(1)
      TC(I)=TC(1)
  101 CONTINUE
      GO TO 140
C*****NONUNIFORM TENSION ONLY
  110 DO 111 I = 2,NSEG
      READ(5,1012)CL(I),TC(I),AW(I),CDA(I),STIF(I),STWT(I)
 1012 FORMAT(F10.0,20X,5F10.0)
      WC(I)=WC(1)
      CDC(I)=CDC(1)
      D(I)=D(1)
  111 CONTINUE
      GO TO 140
C*****NON UNIFORM WEIGHT AND DIA ONLY
  120 DO 121 I = 2,NSEG
      READ(5,1013)CL(I),D(I),CDC(I),WC(I),AW(I),CDA(I),STIF(I),STWT(I)
 1013 FORMAT(F10.0,2F5.0,F10.0,10X,4F10.0)
      TC(I)=TC(1)
  121 CONTINUE
      GO TO 140
C*****NON UNIFORM  WEIGHT,DIA AND TENSION
  130 DO 131 I = 2,NSEG
      READ(5,1016)CL(I),D(I),CDC(I),WC(I),TC(I),AW(I),CDA(I),STIF(I),
     1STWT(I)
  131 CONTINUE
C*****WRITE OUT CABLE PARAMETERS
  140 CLT = 0.0
      AWT = 0.0
      TMIN = TC(1)
      WMAX = WC(1)
      SARC = 0.0
      DMAX = 0.0
      AW(NSEG) = 0.0
      DO 141 I = 1,NSEG
      S(I) = 0.0
      SARC = SARC+CL(I)
      S(I) = SARC
      OMNAT = 0.
      IF (STWT(I) .NE.0) OMNAT = SQRT(STIF(I)*32.2/STWT(I))/(2.*PI)
      WRITE(6,1014)I,CL(I),S(I),D(I),CDC(I),WC(I),TC(I),AW(I),CDA(I),
     1 STIF(I),STWT(I),OMNAT
 1014 FORMAT(1X,I3,3X,F8.2,3X,F8.2,4X,F5.2,2X,F5.2,3X,F7.2,5X,F7.2,
     1 3X,F7.2,3X,F7.2,2X,F8.2,4X,F7.2,6X,F8.3)
C*****CALCULATE ALPHA(I),CLT,AWT,TMIN,WMAX
      CLT = CLT + CL(I)
```

```
      AWT = AWT + AW(I)+STWT(I)
      IF (TC(I) .LT. TMIN) TMIN = TC(I)
      IF (WC(I) .GT. WMAX) WMAX = WC(I)
      ALP(I)= SQRT(WC(I)/32.2/TC(I))
      IF (D(I) .GT. DMAX) DMAX = D(I)
      IF (I .EQ. 1) DMIN = DMAX
      IF (D(I) .LT. DMIN) DMIN = D(I)
  141 CONTINUE
C*****FIND NO. OF DISTINCT DIA. AND STORE
      K = 1
      DU(1)=D(1)
      IF(CDI.NE.0) GO TO 160
      DO 150 J = 2,NSEG
      K = K + 1
      DU(K)= D(J)
      IL = J-1
      DO 145 I = 1,IL
      IF(ABS((D(J)-D(I))/D(J)).GT..0005) GO TO 145
      K = K - 1
      GO TO 150
  145 CONTINUE
  150 CONTINUE
  160 NOD = K
      IF (AWT/CLT .GT. WMAX) WMAX = AWT/CLT
      READ(5,1015)MXMDS,OMSTRT,OMSTOP,DELOM,ACC,UNITS,ISUPRS,
     1 ZETA,RHOW
 1015 FORMAT(I10,4F10.0,I5,I5,2F10.0)
      IF(RHOW.EQ.0.) RHOW = 62.4
C*****CHANGE FROM INPUT SEARCH UNITS TO RAD/SEC
      CALL UNIT (OMSTRT,OMSTOP,DELOM,UNITS,DMAX,DMIN)
C*****SET DEFAULT ACCURACY TO 0.005 PERCENT
      IF (ACC .LT. 1.0E-7) ACC = 0.00005
      IF (OMSTRT .EQ. 0.0) OMSTRT = 1.0E-10
C*****CALCULATE DELOM - FREQUENCY SEARCH INCREMENT
      IF(DELOM.NE.0.) GO TO 210
      DELOM = SQRT(TMIN*32.2/WMAX)/CLT/20.0
  210 WRITE(6,1017) NSEG
 1017 FORMAT (/24H TOTAL NO OF SEGMENTS = ,I3/)
      WRITE(6,1030) MXMDS
 1030 FORMAT (1X,29HMAXIMUM NO OF MODES SOUGHT = ,I3//
     1 15X,19H MODE SEARCH LIMITS/11X,6H LOWER,4X,6H UPPER/
     2 11X,6H LIMIT,4X,6H LIMIT,2X,10H INCREMENT)
C*****WRITE SEARCH LIMITS IN RAD/SEC
      WRITE(6,1031) OMSTRT,OMSTOP,DELOM
 1031 FORMAT (8H RAD/SEC,3F10.5)
C*****WRITE SEARCH LIMITS IN HERTZ
      HOMSRT = HERTZ(OMSTRT)
      HOMSTP = HERTZ(OMSTOP)
      HDELOM = HERTZ(DELOM)
      WRITE(6,1032) HOMSRT,HOMSTP,HDELOM
 1032 FORMAT (8H   HERTZ,3F10.5)
C*****WRITE SEARCH LIMITS IN FT/SEC
      FOMSRT = OMSTRT*(DMIN/12.)/(2.*PI*STRHN)
      FOMSTP = OMSTOP*(DMAX/12.)/(2.*PI*STRHN)
```

97

```
      FDELOM = DELOM$(DMAX/12.)/(2.$PI$STRHN)
      WRITE(6,1033) FOMSRT,FOMSTP,FDELOM
 1033 FORMAT (8H  FT/SEC,3F10.5)
C$$$$$WRITE SEARCH LIMITS IN CM/SEC
      COMSRT = OMSTRT$(DMIN/12.)/(2.$PI$STRHN)$30.48
      COMSTP = OMSTOP$(DMAX/12.)/(2.$PI$STRHN)$30.48
      CDELOM = DELOM$(DMAX/12.)/(2.$PI$STRHN)$30.48
      WRITE(6,1034) COMSRT,COMSTP,CDELOM
 1034 FORMAT (8H  CM/SEC,3F10.5)
C$$$$$WRITE SEARCH LIMITS IN KNOTS
      KOMSRT = OMSTRT$(DMIN/12.)/(2.$PI$STRHN)$0.5921
      KOMSTP = OMSTOP$(DMAX/12.)/(2.$PI$STRHN)$0.5921
      KDELOM = DELOM$(DMAX/12.)/(2.$PI$STRHN)$0.5921
      WRITE(6,1035)KOMSRT,KOMSTP,KDELOM
 1035 FORMAT (8H  KNOTS,3F10.5)
C$$$$$WRITE INITIAL CABLE DAMPING COEF. AND FLUID DENSITY
      WRITE(6,1036)ZETA,RHOW
 1036 FORMAT(//,32H FRACTION OF CRITICAL DAMPING = ,F7.4,//,
     1 17H FLUID DENSITY = ,1PE10.4,10H (LB/FT$3),/)
C$$$$$BEGIN SEARCH FOR NATURAL FREQUENCIES
      OMP = -1.0
      NROOT = 1
      ISERCH = 0
      OMCD = OMSTRT
  300 IF (OMCD .GE. (OMSTOP + DELOM/10.)) GO TO 500
      IFOUND = 0
  310 CALL SOLV(OMCD)
      BC = B(NSEG + 1)
      IF(IFOUND.NE.0) GO TO 350
      IF(ISERCH.NE.0) GO TO 320
      BP = BC
      ISERCH = 1
  320 IF(BC$BP)340,340,330
  330 OMP = OMCD
      BP = BC
      OMCD = OMCD+ DELOM
      GO TO 300
  340 B1 = BP
      B2 = BC
      X1 = OMP
      X2 = OMCD
  350 IFOUND = IFOUND +1
      IF (IFOUND .GT. 100) GO TO 600
      IF (DABS(BC/BSIZE) .LE. ACC) GO TO 380
      IF(B1$BC LE.0.) GO TO 360
      B1 = BC
      X1 = OMCD
      GO TO 370
  360 B2 = BC
      X2 = OMCD
  370 OMCD = X1-(X2-X1)$B1/(B2-B1)
      GO TO 310
C$$$$$NATURAL FREQUENCY FOUND
  380 CONTINUE
```

98

```fortran
      OMC = OMCD
C$$$$$CALCULATE NOMINAL AMPLITUDE AND PHASE OF EACH SEGMENT
      CALL AMPH
C$$$$$CALCULATE NO. ZEROXINGS AND IDENTIFY MODE NO.
      CALL ZEROX(OMCD,MNO)
C$$$$$LOOP FOR ALL DISTINCT DIAMETERS
      DO 430 K = 1,NOD
      DS = DU(K)
C$$$$$FORM COUPLING ARRAY
      DO 385 I = 1,NSEG
      CP(I) = 0.
      IF(ABS((D(I)-DS)/DS).LT..0005)CP(I) = 1.
  385 CONTINUE
C$$$$$CALCULATE IM FACTOR AND OTHER INTEGRALS
      CALL IMODE(OMC)
C$$$$$CALCULATE EFFECTIVE DAMPING FACTOR AND MASS
      CALL DAMP
C$$$$$CALCULATE TRUE RESPONSE AMPLITUDE FOR EACH SEGMENT
      CALL RESMP
C$$$$$CALCULATE CD/CDO FOR EACH CABLE SEGMENT
      CALL SGDRG(OMCD)
C$$$$$CALCULATE TOTAL DRAG COEFF OF CABLE ALONE
      CALL TTDRG (CDT)
C$$$$$$CALCULATE DRAG COEFF CORRECTION FOR STRUMMING OF
C$$$$$          CYLINDRICAL ATTACHED MASSES
      CALL TWDRG(DCDW)
C$$$$$CALCULATE TOTAL DRAG DUE TO STRUMMING OF CABLES
C$$$$$            AND ATTACHED MASSES
      CDWCT=CDT+DCDW
C$$$$$$WRITE OUT RESULTS FOR THIS MODE
      HOMC = HERTZ(OMC)
      VELFT = OMC*(DS/12.)/(2.*PI*STRHN)
      VELCM = VELFT * 30.48
      VELKTS = VELFT * 0.5921
      BN(NSEG+1) = BN(NSEG+1)/BNSIZE
      IF (ITIME .EQ. 0) GO TO 2011
      GO TO 2012
 2011 WRITE(6,2010)
 2010 FORMAT (1H1)
      ITIME = 1
      GO TO 2013
 2012 WRITE(6,2001)
 2001 FORMAT(///1H ,8(15H$$ --------- $$)/)
 2013 IF (IAPROX .EQ. 0) GO TO 2014
      WRITE(6,2020)
 2020 FORMAT (61H NO CONVERGENCE THIS MODE---APPROXIMATE RESULTS LISTED$
     1$$$$$$//)
      IAPRJX = 0
 2014 WRITE(6,2015)MNO,OMC,HOMC,VELFT,K,VELCM,VELKTS
 2015 FORMAT (9H MODE NO ,I4,/13H FREQUENCY = ,F10.5,8H RAD/SEC.3H = ,
     1 F10.5,6H HERTZ,3X,27H AVERAGE STROUHAL VELOCITY ,F10.5,
     2 7H FT/SEC/54X,21H BASED ON DIAMETER D(,I3.2H) ,F1C.5.7H CM/SEC/
     380X,F10.5,6H KNOTS)
      WRITE(6,2016)RMU,ZETAE
```

99

```fortran
2016 FORMAT(20H EFFECTIVE MASS PARAMETER = ,1PE10.4,
    1 21H EFFECTIVE DAMPING = ,0PF10.6)
     IF(CDI.EQ.1) GO TO 3201
     GO TO 3301
3201 IF(ISUPRS.EQ.1) GO TO 420
     WRITE(6,2002)
2002 FORMAT(/1X,7HSEGMENT,3X,6HLENGTH,2X,10HARC LENGTH,2X,
    1 9HSEG  RESP,2X,8HWAVE LNG,2X,11HNO INTERNAL,
    2 2X,9HDRAG COEF,2X,8HATTACHED,3X,9HMASS RESP/
    3 3X,2HNO,7X,4H(FT),6X,4H(FT),5X,9HAMPL (IN),5X,4H(FT),
    4 6X,6HZEROES,12X,4X,5HWT NO,5X,9HAMPL (IN)/)
     GO TO 3501
3301 WRITE(6,3305)
3305 FORMAT (108X,8H SEGMENT/1X,7HSEGMENT,3X,6HLENGTH,2X,10HARC LENGTH,
    1 2X, 9HSEG  RESP,2X,8HWAVE LNG,2X,11HNO INTERNAL,2X,9HDRAG COEF,
    2 2X,8HATTACHED,3X,9HMASS RESP,7X,18H STROUHAL VELOCITY/
    3 3X,2HNO,7X,4H(FT),6X,4H(FT),5X,9HAMPL (IN),
    4 5X,4H(FT),6X,6HZEROES,12X,4X,5HWT NO,5X,9HAMPL (IN),
    5 3X,6HFT/SEC,4X,6HCM/SEC,5X,5HKNOTS/)
3501 NSEG1 = NSEG - 1
     NZXT = 0
     BMAX = B(1)
     DO 400 I = 1,NSEG1
     IF(B(I) .GT. BMAX) BMAX = B(I)
     IF(NPLOT.NE.2HPL  .OR.NPLOT.EQ.2HSC  ) GO TO 3580
     IF(NZX(I) .GT. 0) GO TO 3570
     GO TO 3580
C
C    SEE IF CABLE AMPLITUDE EXCEEDS MASS AMPL  - USE GREATER
C    VALUE TO SCALE PLOT
C
3570 SEG = 0.0
     STEP = CL(I) / ((NZX(I) + 1.) * 7.)
3571 SEG = SEG + STEP
     IF(SEG .GT. CL(I)) GO TO 3580
     AMP = RAMP(I) * COS(SEG*ALP(I)*OMC-PHAS(I))
     IF(AMP .GT. BMAX) BMAX = AMP
     GO TO 3571
3580 WVL = 2.*PI/ALP(I)/OMC
     NZXT = NZXT + NZX(I)
     IF(CDI.EQ.1) GO TO 3701
     GO TO 3801
3701 WRITE(6,2003)I,CL(I),S(I),RAMP(I),WVL,NZX(I),CD(I),I,BN(I+1)
2003 FORMAT(2X,I3,2X,F10.1,F10.1,2X,F10.4,F11.1,6X,I3,2X,F12.3,
    1 6X,I3,F13.4)
     GO TO 400
3801 VELFT = OMC*(D(I)/12.)/(2.*PI*STRHN)
     VELCM = VELFT*30.48
     VELKTS = VELFT*0.5921
     WRITE(6,2100)I,CL(I),S(I),RAMP(I),WVL,NZX(I),CD(I),I,BN(I+1),
    1 VELFT,VELCM,VELKTS
2100 FORMAT (2X,I3,2X,F10.1,F10.1,2X,F10.4,F11.1,6X,I3,2X,F12.3,
    1 6X,I3,F13.4,3(1X,F9.3))
 400 CONTINUE
```

100

```
       IF(NSEG.NE.1) NZXT = NZXT + NZX(NSEG)
       WVL = 2. * PI/ALP(NSEG)/OMC
       IF(CDI.EQ.1) GO TO 450
       GO TO 470
  450 WRITE(6,2004)NSEG,CL(NSEG),S(NSEG),RAMP(NSEG),WVL,NZX(NSEG)
      1,CD(NSEG),BN(NSEG+1)
 2004 FORMAT (2X,I3,2X,F10.1,F10.1,2X,F10.4,F11.1,6X,I3,2X,F12.3,3X,
      * 8HBOUNDARY,F11.4)
       GO TO 490
  470 VELFT = OMC*(D(NSEG)/12.)/(2.*PI*STRHN)
       VELCM = VELFT*30.48
       VELKTS = VELFT*0.5921
       WRITE(6,2150) NSEG,CL(NSEG),S(NSEG),RAMP(NSEG),WVL,NZX(NSEG),
      1 CD(NSEG),BN(NSEG+1),VELFT,VELCM,VELKTS
 2150 FORMAT (2X,I3,2X,F10.1,F10.1,2X,F10.4,F11.1,6X,I3,2X,F12.3,3X,
      1 8HBOUNDARY,F11.4,3(1X,F9.3))
  490 WRITE(6,2005)CLT,NZXT,CDT
 2005 FORMAT(/,1X,5HTOTAL/ 5X,F12.1,38X,I4,2X,F12.3,26H (ADDED WTS. NOT
      1INCLUDED))
  495 WRITE(6,4000) CDWCT
 4000 FORMAT(61X,F12.3,22H (ADDED WTS. INCLUDED))
       GO TO 430
  420 WRITE(6,2030)CDT,BN(NSEG+1),IFOUND
 2030 FORMAT (/2X,18H AVERAGE CD/CD0 = ,F10.3,
      1 26H (ADDED WTS  NOT INCLUDED),5X,8H AMPL = ,F12.5,5X,
      * 8H ITER = ,I10)
  430 CONTINUE
C*****RESTART SEARCH FOR NEW MODES
       BP = B2
       OMP = X2
       OMCD = OMP + DELOM
       IF(NPLOT.EQ.2HPL )CALL PLMPL (TITLE,MNO,OMCD,VELKTS,PLEN,S)
       IF(NPLOT.EQ.2HSC )CALL SCRLL (TITLE,MNO,OMCD,NROOT,S)
       NROOT = NROOT + 1
       IF(NROOT.LE.MXMDS) GO TO 300
C     SEARCH COMPLETE READ NEW DATA SET
  500 ND = ND + 1
       ITIME = 0
C     GO TO 10
       GO TO 9999
C*****TERMINATE SEARCH IF NO CONVERGENCE
  600 IAPROX = 1
       GO TO 380
C     CLOSE PLOT IFF PLOT WAS PRODUCED
 9999 IF( JPLTNO.NE. 0) CALL PLOT(1.,1.,999)
       STOP
       END
       SUBROUTINE UNIT (A1,B1,C,UNITS,D1,D2)
       COMMON/C2/A( 21),B( 21),PHAS( 21),PI,BSIZE,AMPL( 21),RAMP( 21)
       DIMENSION OMEGA(3),DIAM(2)
       INTEGER UNITS
C*****SUBROUTINE TO CONVERT FROM INPUT UNITS TO RAD/SEC FOR SEARCHING
C     OMEGA(1) = OMSTRT
C     OMEGA(2) = OMSTOP
```

```
C     OMEGA(3) = DELOM
      RAD(X) = X*2.*PI
      STRHN = 0.21
      OMEGA(1) = A1
      OMEGA(2) = B1
      OMEGA(3) = C
      DIAM(1) = D1
      DIAM(2) = D2
      GO TO (30,40,50,60,70),UNITS
C*****UNITS ARE RAD/SEC
   30 RETURN
C*****UNITS ARE HERTZ
   40 DO 42 J=1,3
   42 OMEGA(J) = RAD(OMEGA(J))
      GO TO 100
C*****UNITS ARE FT/SEC
   50 DO 52 I=1,2
   52 OMEGA(I) = OMEGA(I)*2.*PI*STRHN/(DIAM(I)/12.)
      OMEGA(3) = OMEGA(3)*2.*PI*STRHN/(DIAM(1)/12.)
      GO TO 100
C*****UNITS ARE CM/SEC
   60 DO 62 I=1,2
   62 OMEGA(I) = OMEGA(I)/30.48*2.*PI*STRHN/(DIAM(I)/12.)
      OMEGA(3) = OMEGA(3)/30.48*2.*PI*STRHN/(DIAM(1)/12.)
      GO TO 100
C*****UNITS ARE KNOTS
   70 DO 72 I=1,2
   72 OMEGA(I) = OMEGA(I)/0.5921*2.*PI*STRHN/(DIAM(I)/12.)
      OMEGA(3) = OMEGA(3)/0.5921*2.*PI*STRHN/(DIAM(1)/12.)
  100 A1 = OMEGA(1)
      B1 = OMEGA(2)
      C = OMEGA(3)
      RETURN
      END
      SUBROUTINE SOLV(OMC)
      COMMON/C1/CL( 21),D( 21),WC( 21),TC( 21),AW( 21),NZX( 21),NSEG,
     1ALP( 21)
      COMMON/C2/A( 21),B( 21),PHAS( 21),PI,BSIZE,AMPL( 21),RAMP( 21)
      COMMON/C5/AD,BD
      COMMON/C6/STIF( 21),STWT( 21)
      DOUBLE PRECISION AD( 21),BD( 21),ARG,OMC,OMWT,COEF
      AD(1) = 1.0D0
      A(1) = AD(1)
      BD(1)= 0.
      B(1) = BD(1)
      BSIZE = 0.0
      DO 100 I = 1,NSEG
      ARG = ALP(I)*OMC*CL(I)
      WAVL = 2.*PI/ALP(I)/OMC
      AM = DSQRT(AD(I)**2+BD(I)**2)
      IF ((CL(I).GT.WAVL/4.).AND.(AM.GT.BSIZE)) BSIZE = AM
      BD(I+1) = AD(I)*DSIN(ARG)+BD(I)*DCOS(ARG)
      B(I+1) = BD(I+1)
      IF(I.EQ.NSEG) GO TO 100
```

102

```
      OMWT = 0.0
      IF(STWT(I).GT.0.000001)OMWT=SQRT(STIF(I)*32.2/STWT(I))
      IF(DABS(OMWT/OMC).GT.1.0001 .OR. DABS(OMWT/OMC).LT.0.9999)GO TO 90
      WRITE(6,80)OMC
   80 FORMAT(3X,45HSPRUNG MASS ACTING AS ISOLATOR AT FREQUENCY =,F10.5)
   90 COEF = STIF(I)/OMC/(1.0-(OMWT/OMC)**2)-AW(I)*OMC
      AD(I+1) = ALP(I)*(AD(I)*DCOS(ARG)-BD(I)*DSIN(ARG))*TC(I)/ALP(I+1)/
     1 TC(I+1)+COEF      *BD(I+1)/ALP(I+1)/TC(I+1)/32.2
      A(I+1) = AD(I+1)
      IF ((CL(I) .LE. WAVL/4.) .AND. (DABS(BD(I+1)) .GT. BSIZE))
     1 BSIZE = DABS(BD(I+1))
  100 CONTINUE
      RETURN
      END
      SUBROUTINE AMPH
      COMMON/C1/CL( 21),D( 21),WC( 21),TC( 21),AW( 21),NZX( 21),NSEG,
     1ALP( 21)
      COMMON/C2/A( 21),B( 21),PHAS( 21),PI,BSIZE,AMPL( 21),RAMP( 21)
      DO 100 I = 1,NSEG
      C1 =  SQRT(A(I)**2 + B(I)**2)
      C2 =  ATAN2(A(I),B(I))
      AMPL(I) = C1
      PHAS(I)= C2
  100 CONTINUE
      RETURN
      END
      SUBROUTINE IMODE(OMC)
      COMMON/C1/CL( 21),D( 21),WC( 21),TC( 21),AW( 21),NZX( 21),NSEG,
     1ALP( 21)
      COMMON/C2/A( 21),B( 21),PHAS( 21),PI,BSIZE,AMPL( 21),RAMP( 21)
      COMMON/C10/F2,F4,FG,F3,PIM
      COMMON/C11/CDC( 21),CDA( 21),CP( 21),DS,ZETA,ZETAE,RHOW,RMU,
     1CDAS( 21)
      F4 = 0.
      F2 = 0.
      F3 = 0.
      FG = 0.
      DO 100 I=1,NSEG
      ARG = ALP(I)*OMC*CL(I)-PHAS(I)
      PAR = ALP(I)*OMC*CL(I)/2.+( SIN(2.*ARG) +  SIN(2.*PHAS(I)))/4
      F4 = F4 +(AMPL(I)**4*((COS(ARG)**3*SIN(ARG)+COS(PHAS(I))**3*
     1 SIN(PHAS(I)))/4.+0.75*PAR)/ALP(I)/OMC)*WC(I)+AW(I)*B(I+1)**'
      F2 = F2 + (AMPL(I)**2*PAR/ALP(I)/OMC)*WC(I)+AW(I)*B(I+1)**2
      FG = FG + CP(I)*AMPL(I)**2*PAR/ALP(I)/OMC
      NPI = ALP(I)*OMC*CL(I)/PI
      EXTRAA = ALP(I)*OMC*CL(I)-NPI*PI
      GAMMA = PHAS(I)+3.*PI/2.-PI*AINT((PHAS(I)+3.*PI/2.)/PI)
      TERM1 = SIN(EXTRAA-PHAS(I))*(COS(EXTRAA-PHAS(I))**2+2.)
      TERM2 = SIN(PHAS(I))*(COS(PHAS(I))**2+2.)
      TERM3 = (1 -CP(I))*CDC(I)*D(I)*AMPL(I)**3/36./ALP(I)/OMC
      IF(EXTRAA.GT.GAMMA) GO TO 10
      F3 = F3+TERM3*(4.*NPI+ABS(TERM1+TERM2))
      GO TO 100
   10 F3 = F3+TERM3*(4.*NPI+ABS(2.*SIN(GAMMA-PHAS(I))*
```

103

```fortran
    1 (COS(GAMMA-PHAS(I))**2+2.)+TERM2-TERM1))
100 CONTINUE
      PIM = F4/F2
      RETURN
      END
      SUBROUTINE DAMP
      COMMON/C1/CL( 21),D( 21),WC( 21),TC( 21),AW( 21),NZX( 21),NSEG,
     1ALP( 21)
      COMMON/C2/A( 21),B( 21),PHAS( 21),PI,BSIZE,AMPL( 21),RAMP( 21)
      COMMON/C10/F2,F4,FC,F3,PIM
      COMMON/C11/CDC( 21),CDA( 21),CP( 21),DS,ZETA,ZETAE,RHOW,RMU,
     1CDAS( 21)
C*****CALCULATE EFFECTIVE MASS RATIO PARAMETER
      RMU = 576.*F2/PI/RHOW/DS**2/FC
C*****CALCULATE ADDED DAMPING TERM
      ZADDED = 0.
      NSEG1 = NSEG-1
      DO 20 I = 1,NSEG1
      ZADDED = ZADDED+CDA(I)*ABS(B(I+1)**3)
   20 CONTINUE
      ZADDED = DS*RHOW*(ZADDED+F3)/18./PI/SQRT(F2)/SQRT(F4)
C*****SEARCH FOR ZETAE
      ZETAE = ZETA
   25 VAR = (RMU*ZETAE)**1.8
      PAR = 1.+(9.6*VAR)
      DZETA = 1. + 17.28 *ZADDED*RMU**1.8*ZETAE**0.8/PAR**2
      FZETA = ZETAE -ZETA -ZADDED/PAR
      ZETAEN=ZETAE - FZETA/DZETA
      IF(ABS(ZETAEN-ZETAE).LT..0001) GO TO 30
      ZETAE = ZETAEN
      GO TO 25
   30 ZETAE = ZETAEN
      RETURN
      END
      SUBROUTINE RESMP
      COMMON/C1/CL( 21),D( 21),WC( 21),TC( 21),AW( 21),NZX( 21),NSEG,
     1ALP( 21)
      COMMON/C2/A( 21),B( 21),PHAS( 21),PI,BSIZE,AMPL( 21),RAMP( 21)
      COMMON/C7/BN( 21),BNSIZE
      COMMON/C10/F2,F4,FC,F3,PIM
      COMMON/C11/CDC( 21),CDA( 21),CP( 21),DS,ZETA,ZETAE,RHOW,RMU,
     1CDAS( 21)
      AMAX = 1.29/(1.0+0.43*(RMU*ZETAE))**3.35
      CONS = AMAX*DS/SQRT(PIM)
      DO 100 I=1,NSEG
      RAMP(I) = CONS*AMPL(I)
      BN(I) = ABS(CONS*B(I))
  100 CONTINUE
      BNSIZE = ABS(CONS*BSIZE)
      BN(NSEG+1) = ABS(CONS*B(NSEG+1))
      RETURN
      END
      SUBROUTINE SGDRG(OMC)
      COMMON/C1/CL( 21),D( 21),WC( 21),TC( 21),AW( 21),NZX( 21),NSEG,
```

```fortran
     1ALP( 21)
      COMMON/C2/A( 21),B( 21),PHAS( 21),PI,BSIZE,AMPL( 21),RAMP( 21)
      COMMON/C3/CD( 21)
      COMMON/C11/CDC( 21),CDA( 21),CP( 21),DS,ZETA,ZETAE,RHOW,RMU,
     1CDAS( 21)
      DOUBLE PRECISION OMC
      DO 100 I = 1,NSEG
      R1 = -1. * PHAS(I)
      PAR = ALP(I) * OMC * CL(I)
      R2 = PAR + R1 -  INT(PAR/PI)*PI
      CALL SIMP(R1,R2,20,AREA)
      CD(I) = (1. + 1.82024*(RAMP(I)/D(I))**.65*(INT(PAR/PI)*2.2546+
     1 AREA)/PAR)*CDC(I)
  100 CONTINUE
      RETURN
      END
      SUBROUTINE SIMP(R1,R2,N,AREA)
      F(X)= (ABS( COS(X)))**0.65
      DX = (R2-R1)/2./N
      AREA = 0.
      X = R1
      DO 100 I = 1,N
      AREA = AREA + (DX/3.)*(F(X)+4.*F(X+DX)+F(X+2.*DX))
      X = X + 2.*DX
  100 CONTINUE
      RETURN
      END
      SUBROUTINE ZEROX(OMC,MNO)
      COMMON/C1/CL( 21),D( 21),WC( 21),TC( 21),AW( 21),NZX( 21),NSEG,
     1ALP( 21)
      COMMON/C2/A( 21),B( 21),PHAS( 21),PI,BSIZE,AMPL( 21),RAMP( 21)
      COMMON/C5/AD,BD
      DOUBLE PRECISION AD( 21),BD( 21),OMC,PR,PID,PHASD,PH
      PID = DABS( DATN2(0.D0,-1.D0))
      NZX(1) = IDINT(ALP(1)*OMC*CL(1)/PID)
      MNO = NZX(1)
      NSEG1 = NSEG-1
      IF(NSEG.EQ.2) GO TO 110
      DO 100 I=2,NSEG1
      PH = ALP(I)*OMC*CL(I)/PID/2.D0
      IF (BD(I)*BD(I+1) .GT. 0.D0) GO TO 10
      NZX(I) = 2*IDINT(PH) +1
      GO TO 50
   10 NZX(I) = 2*IDINT(PH+0.5D0)
   50 MNO = MNO + NZX(I)
  100 CONTINUE
  110 PHASD =  DATN2(AD(NSEG),BD(NSEG))
      NL = (1+IDINT(DABS(PHASD)*2.D0/PID))/2
      IF (PHASD .LT. 0.D0) NL = -1*NL
      PR = ALP(NSEG)*OMC*CL(NSEG)-PHASD+1.5D0
      NR = (1+IDINT(DABS(PR)*2.D0/PID))/2
      IF (PR .LT. 0.D0) NR = -1*NR
      NZX(NSEG) = NL+NR
      MNO = MNO+NZX(NSEG)
```

105

```
      RETURN
      END
      SUBROUTINE TTDRG (CDT)
      COMMON/C1/CL( 21),D( 21),WC( 21),TC( 21),AW( 21),NZX( 21),NSEG,
     1ALP( 21)
      COMMON/C2/A( 21),B( 21),PHAS( 21),PI,BSIZE,AMPL( 21),RAMP( 21)
      COMMON/C3/CD( 21)
      PR = 0.
      CLT = 0.
      DO 100 I = 1,NSEG
      PR = PR + CL(I)*CD(I)*(D(I)/12.0)
      CLT = CLT + CL(I)*(D(I)/12.0)
100   CONTINUE
      CDT = PR/CLT
      RETURN
      END
      SUBROUTINE TWDRG(DCDW)
      COMMON/C1/CL( 21),D( 21),WC( 21),TC( 21),AW( 21),NZX( 21),NSEG,
     1ALP( 21)
      COMMON/C2/A( 21),B( 21),PHAS( 21),PI,BSIZE,AMPL( 21),RAMP( 21)
      COMMON/C3/CD( 21)
      COMMON/C7/BN( 21),BNSIZE
      COMMON/C11/CDC( 21),CDA( 21),CP( 21),DS,ZETA,ZETAE,RHOW,RMU,
     1CDAS( 21)
      NWSEG=NSEG-1
      PRD=0.0
      DO 80 I=1,NWSEG
      CDAS(I)=((1.0+1.82024*(BN(I+1)/D(I)))**0.65)*CDA(I)
      PRD=PRD+CDAS(I)
80    CONTINUE
      CLT=0.0
      DO 100 I=1,NSEG
      CLT=CLT+CL(I)*D(I)/12.0
100   CONTINUE
      DCDW=PRD/CLT
      RETURN
      END
      BLOCK DATA
      COMMON/C1/CL( 21),D( 21),WC( 21),TC( 21),AW( 21),NZX( 21),NSEG,
     1ALP( 21)
      COMMON/C2/A( 21),B( 21),PHAS( 21),PI,BSIZE,AMPL( 21),RAMP( 21)
      COMMON/C3/CD( 21)
      COMMON/C4/BMAX, JPLTNO
      COMMON/C6/STIF( 21),STWT( 21)
      COMMON/C7/BN( 21),BNSIZE
      COMMON/C11/CDC( 21),CDA( 21),CP( 21),DS,ZETA,ZETAE,RHOW,RMU,
     1CDAS( 21)
      DOUBLE PRECISION AD( 21),BD( 21),ARG,OMC,OMWT,COEF
      COMMON/C5/AD,BD
      COMMON /C10/F2,F4,FG,F3,PIM
      END
```

106

Appendix B

INPUT DATA FOR NATFREQ

TEST RUNS 1-20 FROM TABLE 1

1981 CASTINE BAY TESTS * MARINE CABLES WITH ATTACHED SENSOR HOUSINGS * RUN 1
```
          1           1
          3SCRL
     25.00 1.25  1 2 7.704E-01     512.0 0.441E+01 3.500E-01
     25.00                               0.441E+01 3.500E-01
     25.00                               0.441E+01 3.500E-01
        12       0 0       50.0             0.001    2    0   .01    0.0644
```


1981 CASTINE BAY TESTS * MARINE CABLES WITH ATTACHED SENSOR HOUSINGS * RUN 2
```
          1           1
          3SCRL
     25.00 1.25  1 2 0.132E+01     450.0 0.759E+01 3.500E-01
     25.00                               0.759E+01 3.500E-01
     25.00                               0.759E+01 3.500E-01
        12       0 0       50.0             0.001    2    0   .01     64.0
```


1981 CASTINE BAY TESTS * MARINE CABLES WITH ATTACHED SENSOR HOUSINGS * RUN 3
```
          1           1
          6SCRL
     12.50 1.25  1 2 7.704E-01     500.0 0.441E+01 3.500E-01
     12.50                               0.441E+01 3.500E-01
     12.50                               0.441E+01 3.500E-01
     12.50                               0.441E+01 3.500E-01
     12.50                               0.441E+01 3.500E-01
     12.50                               0.441E+01 3.500E-01
        12       0 0       50.0             0.001    2    0   .01    0.0644
```


1981 CASTINE BAY TESTS * MARINE CABLES WITH ATTACHED SENSOR HOUSINGS * RUN 4
```
          1           1
          6SCRL
     12.50 1.25  1 2 0.132E+01     520.0 0.759E+01 3.500E-01
     12.50                               0.759E+01 3.500E-01
     12.50                               0.759E+01 3.500E-01
     12.50                               0.759E+01 3.500E-01
     12.50                               0.759E+01 3.500E-01
     12.50                               0.759E+01 3.500E-01
        12       0 0       50.0             0.001    2    0    01     64.0
```

1981 CASTINE BAY TESTS * MARINE CABLES WITH ATTACHED SENSOR HOUSINGS * RUN 5
```
        1         1
        5SCRL
    9.375 1.25  1.2 7.704E-01    532.0 0.441E+01 3.500E-01
   18.750                              0.441E+01 3.500E-01
   18.750                              0.441E+01 3.500E-01
   18.750                              0.441E+01 3.500E-01
    9.375                              0.441E+01 3.500E-01
       12      0.0      50.0            0.001    2    0   .01    0.0644
```

1981 CASTINE BAY TESTS * MARINE CABLES WITH ATTACHED SENSOR HOUSINGS * RUN 6
```
        1         1
        5SCRL
    9.375 1.25  1.2 0.132E+01    475.0 0.759E+01 3.500E-01
   18.750                              0.759E+01 3.500E-01
   18.750                              0.759E+01 3.500E-01
   18.750                              0.759E+01 3.500E-01
    9.375                              0.759E+01 3.500E-01
       12      0.0      50.0            0.001    2    0   .01    64.0
```

1981 CASTINE BAY TESTS * MARINE CABLES WITH ATTACHED SENSOR HOUSINGS * RUN 7
```
        1         1
        8SCRL
    9.375 1.25  1.2 7.704E-01    504.0 0.441E+01 3.500E-01
    9.375                              0.441E+01 3.500E-01
    9.375                              0.441E+01 3.500E-01
    9.375                              0.441E+01 3.500E-01
    9.375                              0.441E+01 3.500E-01
    9.375                              0.441E+01 3.500E-01
    9.375                              0.441E+01 3.500E-01
    9.375                              0.441E+01 3.500E-01
       12      0.0      50.0            0.001    2    0   .01    0 0644
```

1981 CASTINE BAY TESTS * MARINE CABLES WITH ATTACHED SENSOR HOUSING' * RUN 8
```
        1         1
        8SCRL
    9.375 1.25  1.2 0.132E+01    475.0 0.759E+01 3.500E-01
    9.375                              0.759E+01 3.500E-01
    9.375                              0.759E+01 3.500E-01
    9.375                              0.759E+01 3.500E-01
    9.375                              0.759E+01 3.500E-01
    9.375                              0.759E+01 3.500E- :
    9.375                              0.759E+01 3.500E-01
    9.375                              0.759E+01 3.500E-01
       12      0.0      50.0            0.001    2   `   01    64.0
```

1981 CASTINE BAY TESTS * MARINE CABLES WITH ATTACHED SENSOR HOUSINGS * RUN 9
```
          1           1
          3SCRL
      25.00 1.25  1 2 7.704E-01     540.0 0.997E+01 3.500E-01
      25.00                               0.997E+01 3.500E-01
      25.00                               0.997E+01 3.500E-01
         12      0 0      50.0              0.001   2    0   .01    0.0644
```

1981 CASTINE BAY TESTS * MARINE CABLES WITH ATTACHED SENSOR HOUSINGS * RUN 10
```
          1           1
          3SCRL
      25.00 1.25  1 2 0.132E+01     600.0 1.370E+01 3.500E-01
      25.00                               1.370E+01 3.500E-01
      25.00                               1.370E+01 3.500E-01
         12      0.0      50.0              0.001   2    0   .01     64.0
```

1981 CASTINE BAY TESTS * MARINE CABLES WITH ATTACHED SENSOR HOUSINGS * RUN 11
```
          1           1
          6SCRL
      12.50 1 25  1 2 7 704E-01     728.0 0.997E+01 3.500E-01
      12.50                               0.997E+01 3.500E-01
      12.50                               0.997E+01 3.500E-01
      12.50                               0.997E+01 3.500E-01
      12.50                               0.997E+01 3.500E-01
      12.50                               0.997E+01 3.500E-01
         12      0.0      50 0              0.001   2    0   .01    0.0644
```

1981 CASTINE BAY TESTS * MARINE CABLES WITH ATTACHED SENSOR HOUSINGS * RUN 12
```
          1           1
          6SCRL
      12.50 1.25  1 2 0 132E+01     580.0 1.370E+01 3.500E-01
      12.50                               1.370E+01 3.500E-01
      12.50                               1.370E+01 3.500E-01
      12.50                               1.370E+01 3.500E-01
      12.50                               1.370E+01 3.500E-01
      12.50                               1 370E+01 3 500E-01
         12      0 0      50 0              0 001   2    0   .01     64.0
```

110

1981 CASTINE BAY TESTS * MARINE CABLES WITH ATTACHED SENSOR HOUSINGS * RUN 13

```
     1          1
     5SCRL
  9.375 1.25  1.2 7.704E-01      650.0 0.997E+01 3.500E-01
 18.750                                0.997E+01 3.500E-01
 18.750                                0.997E+01 3.500E-01
 18.750                                0.997E+01 3.500E-01
  9.375                                0.997E+01 3.500E-01
    12       0.0        50.0             0.001   2   0   .01    0.0644
```

1981 CASTINE BAY TESTS * MARINE CABLES WITH ATTACHED SENSOR HOUSINGS * RUN 14

```
     1          1
     5SCRL
  9.375 1.25  1.2 0 132E+01      650.0 1.370E+01 3.500E-01
 18.750                                1.370E+01 3.500E-01
 18.750                                1.370E+01 3.500E-01
 18.750                                1.370E+01 3.500E-01
  9.375                                1.370E+01 3.500E-01
    12       0.0        50.0             0.001   2   0   .01     64.0
```

1981 CASTINE BAY TESTS * MARINE CABLES WITH ATTACHED SENSOR HOUSINGS * RUN 15

```
     1          1
     7SCRL
 12.50 1.25  1.2 7.704E-01       732.0 0.997E+01 3.500E-01
 12.50                                 0.997E+01 3.500E-01
 12.50                                 0.997E+01 3.500E-01
  9.375                                0.997E+01 3.500E-01
  9.375                                0.997E+01 3.500E-01
  9.375                                0.997E+01 3.500E-01
  9.375                                0.997E+01 3.500E-01
    12       0.0        50.0             0.001   2   0   .01    '.0644
```

1981 CASTINE BAY TESTS * MARINE CABLES WITH ATTACHED SENSOR HOUSINGS * RUN 16

```
     1          1
     7SCRL
 12.50 1.25  1.2 0.132E+01       556.0 1.370E+01 3.500E-01
 12.50                                 1.370E+01 3.500E-01
 12.50                                 1.370E+01 3.500E-01
  9.375                                1.370E+01 3.500E-01
  9.375                                1 370E+01 3.500E-01
  9.375                                1.370E+01 3.500E-01
  9.375                                1.370E+01 3.500E-01
    12       0.0        50 0             0.001   2   0   .01     64.0
```

1981 CASTINE BAY TESTS * MARINE CABLES WITH ATTACHED SENSOR HOUSINGS * RUN 17

```
     1          1
     6SCRL
12.50 1.25  1.2 7.704E-01      800.0 0.997E+01 3.500E-01
12.50                              0.441E+01 3.500E-01
12.50                              0.997E+01 3.500E-01
12.50                              0.441E+01 3.500E-01
12.50                              0.997E+01 3.500E-01
12.50                              0.997E+01 3.500E-01
     12     0.0      50.0             0.001   2   0   .01    0.0644
```

1981 CASTINE BAY TESTS * MARINE CABLES WITH ATTACHED SENSOR HOUSINGS * RUN 18

```
     1          1
     6SCRL
12.50 1.25  1.2 0.132E+01      765.0 1.370E+01 3.500E-01
12.50                              0.759E+01 3.500E-01
12.50                              1.370E+01 3.500E-01
12.50                              0.759E+01 3.500E-01
12.50                              1.370E+01 3.500E-01
12.50                              1.370E+01 3.500E-01
     12     0.0      50.0             0.001   2   0   .01    64.0
```

1981 CASTINE BAY TESTS * MARINE CABLES WITH ATTACHED SENSOR HOUSINGS * RUN 19

```
     1          1
     7SCRL
12.50 1.25  1.2 7.704E-01      800.0 0.441E+01 3.500E-01
12.50                              0.997E+01 3.500E-01
12.50                              0.441E+01 3.500E-01
9.375                              0.997E+01 3.500E-01
9.375                              0.997E+01 3.500E-01
9.375                              0.997E+01 3.500E-01
9.375                              0.997E+01 3.500E-01
     12     0.0      50.0             0.001   2   0   01    0.0644
```

1981 CASTINE BAY TESTS * MARINE CABLES WITH ATTACHED SENSOR HOUSINGS * RUN 20

```
     1          1
     7SCRL
12.50 1.25  1 2 0 132E+01      800.0 0.759E+01 3.500E-01
12.50                              1.370E+01 3.500E-01
12.50                              0.759E+01 3.500E-01
9.375                              1.370E+01 3.500E-01
9 375                              1.370E+01 3.500E-01
9.375                              1.370E+01 3.500E-01
9.375                              1.370E+01 3.500E-01
     12     0.0      50.0             0.001   2   0   1:    64.0
```

Appendix C

STRUMMING DRAG CALCULATIONS

An important side effect which accompanies the oscillations of structures and cables due to vortex shedding is the amplification of the mean hydrodynamic drag force (or the corresponding drag coefficient C_D). A method for employing these measurements in the analysis of marine cable structures was developed by Skop, Griffin and Ramberg (20).[*] This procedure has been improved and extended to the case of flexible, cylindrical marine structures by Griffin and others (1,21,22,25).

A program of tests which were conducted at the David Taylor Naval Ship R&D Center during the 1940's and for which the results were released a few years ago demonstrate the strong resonance due to vortex shedding that typically takes place when a bare circular cylinder or cable moves in steady motion relative to the surrounding water and undergoes large-amplitude cross flow oscillations; see Ref. 21. This cylinder was also fitted with various vortex suppression devices in order to investigate their effectiveness in suppressing the cross flow oscillations. The drag on the cylinder was measured over a range of towing speeds up to 10 knots and the results are plotted in Fig. C1. A clear resonance occurred near $V = 4$ knots and the drag force (and coefficient C_D) was increased by a factor of 220 percent at a towing speed of 4.25 knots. At this and nearby towing speeds, the cross flow displacement amplitude of the cylinder was ± 1.5 to 2 diameters. When the cylinder was towed at speeds above and below the resonance, the usual

$$\text{Drag} \propto (\text{Flow Speed})^2$$

dependence was obtained. Methods for calculating the increased mean drag forces which accompany the vortex shedding are described in the discussion that follows. Details of the method and extensive comparisons with experimental results are given by Griffin (22), and by Every, King and Griffin (25).

The drag coefficient C_D for a cable or structure which vibrates due to vortex shedding is increased

---

[*]Numbers in parentheses denote references listed at the end of this report.
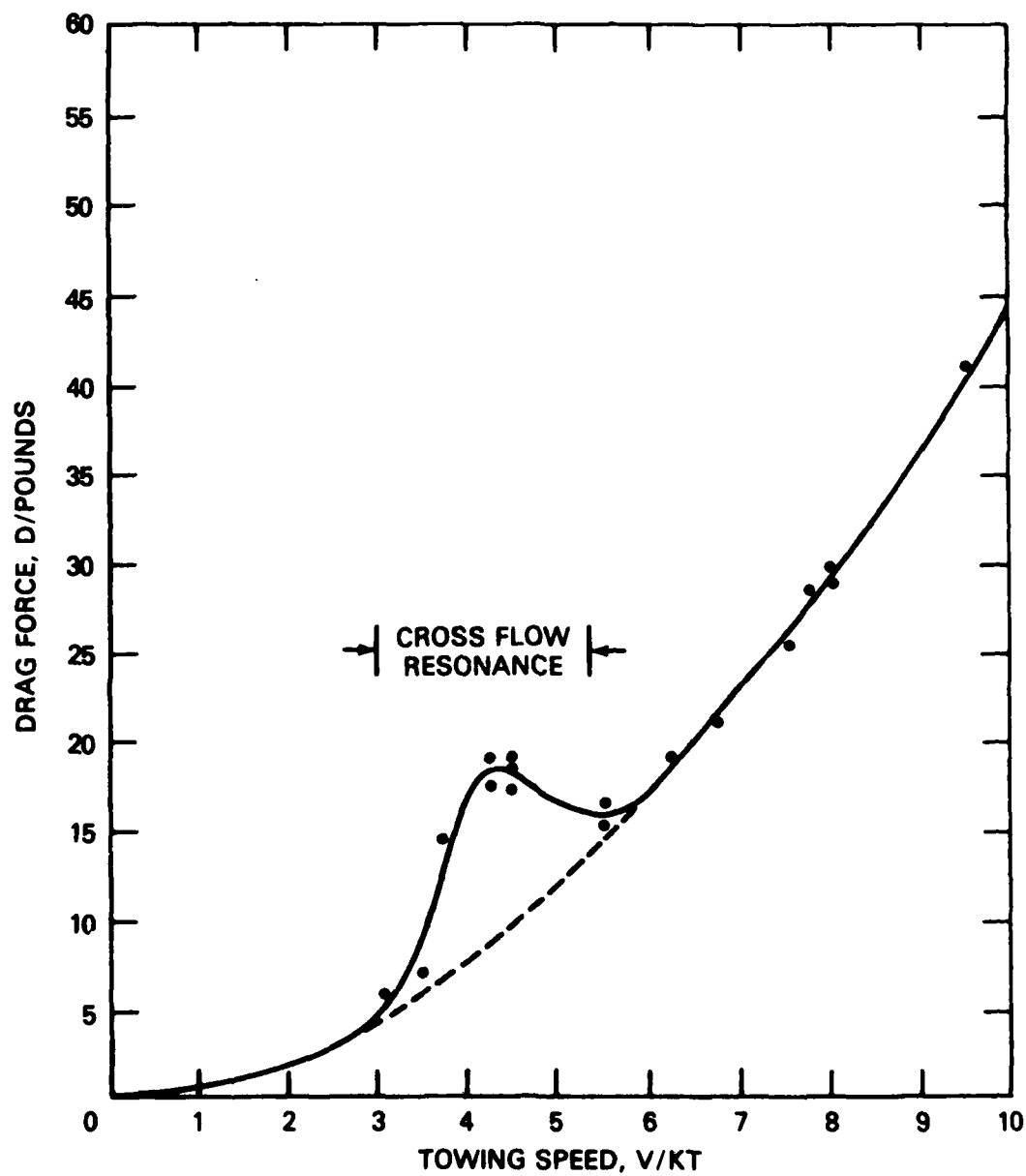
Fig. C1 — Steady drag force measured on a free-ended circular cylinder towed steadily through still water. A clear resonance in the drag due to the vortex-excited oscillations normal to the incident flow is shown between relative flow speeds of $V = 3$ and 6 kts: from Griffin (21).

114

as shown in Figs. 26 and C1 of this report, and Fig. 2.9 of Ref. 1. The ratio of C_D and C_{DO} (the latter is the drag coefficient for a cylinder, cable or other flexible, bluff structure which is restrained from oscillating) is a function of the displacement amplitude and frequency as given by the response parameter (20),

$$w_r = (1 + 2\bar{Y}/D)(V_r St)^{-1}. \tag{C1}$$

Here again $2\bar{Y}$ is the double amplitude of the displacement, V_r is the reduced velocity V/fD and St is the Strouhal number $f_s D/V$. The ratio of the drag coefficients is given by

$$C_D/C_{D0} = 1, \quad w_r < 1 \tag{C2a}$$
$$C_D/C_{DO} = 1 + 1.16(w_r - 1)^{0.65}, \quad w_r \geqslant 1 \tag{C2b}$$

which is a least-squares fit to the data in Fig. 2.9 of Ref. 1. The equation

$$\bar{Y}_{MAX}/D = \frac{1.29\gamma_i}{[1 + 0.43(2\pi St^2 k_s)]^{3.35}} \tag{C3}$$

from Table 4.1 of Ref. 1 can be combined with Eqs. (C2a) and (C2b) to compute the unsteady displacement amplitudes, the drag amplification and the amplified static deflection that is caused by the vortex excited oscillations. The local displacement amplitude along the length of a flexible member such as a cable (in the ith normal mode) is given by

$$\bar{y}(z) = \bar{Y}_i(z) \sin (2\pi f_i t)$$

where

$$\bar{Y}_i(z) = Y_{EFF.MAX} \gamma_i(z). \tag{C4}$$

In this equation

$$\gamma_i = \frac{D\psi_i(z)}{I_i^{1/2}} \tag{C5}$$

where I_i is a modal scaling factor defined in Ref. 1. These equations can be employed to iteratively compute the static deflection of a structure or cable due to the vortex-excited drag amplification as shown in Refs. 1, 20 and 21.

Every, King and Griffin (25) recently have shown by comparison between sample calculations and the experimental data reported by them that this method for calculating the steady drag amplification

115

and deflections is quite accurate and that it can be employed with some confidence to evaluate the hydrodynamic loading, deflections and material stresses on marine structures and cable systems. The and unsteady loads and deflections must be considered in any such evaluation. An example of the comparison reported by Every, King and Griffin is given in Fig. C2.

The average drag coefficient or force (with respect to time) can be derived from Eq. (C2b). The steps required to do this were carried out by McGlothlin (8) who failed to recognize that Eq. (C2b) is based on the *peak* amplitude of vibration for any given mode. When McGlothlin's derivation is corrected to account for the root-mean-square vibration amplitude the correct result is

$$C_{D,\text{AVG}} = C_{DO}[1 + 1.043(2\bar{Y}_{\text{RMS}}/D)^{0.65}]$$

for a sinusoidal mode shape.

The hydrodynamic force due to cable strumming on the system comprised of the cable and attached masses can also be calculated in much the same manner. Then the total drag force is equal to the sum of the drag contributions from the cable strumming and from the attached masses. This can be stated as

$$F_{T,i} = F_{C,i} + F_{W,i}. \tag{C6}$$

Then the two contributions at the ith cable segment are

$$F_{C,i} = \frac{1}{2}\rho\, V^2 L_i D_i C_{DC,i} \tag{C7a}$$

and

$$F_{W,i} = \frac{1}{2}\rho\, V^2 L_{Wi} D_{Wi} C_{DW,i} \tag{C7b}$$

for each of a total of N segments of length L_i and diameter D_i. There are $N-1$ cylindrical attached masses of length L_{Wi} and diameter D_{Wi} situated at the ends of the individual cable segments. Let the total drag force on the segment be defined in terms of the local *cable* diameter D_i and segment length L_i. Then

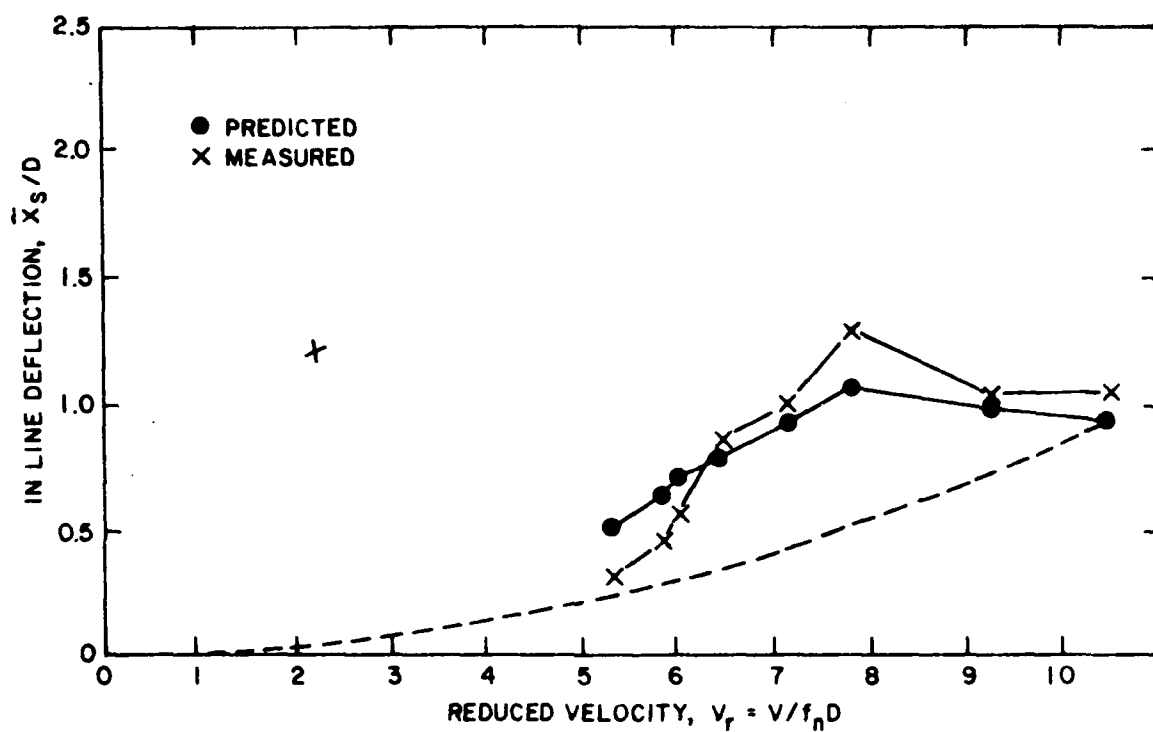$$F_{T,i} = \frac{1}{2}\rho\, V^2 L_i D_i C_{DT,i} \tag{C8}$$

Fig. C2 — The steady tip deflection $\bar{x}_s$ of a cantilever beam, vibrating due to vortex shedding, compared with the measured values for a cylinder of relative density $SG = 3.5$. The prediction using a constant $C_D = 1.2$ (stationary cylinder) is shown by the dashed line; from Every, King and Griffin (25).

and

$$\frac{1}{2} \rho \ V^2 L_i D_i C_{DT, \ i} = \frac{1}{2} \rho \ V^2 L_i D_i C_{DC, \ i} + \frac{1}{2} \rho \ V^2 L_{Wi} D_{Wi} C_{DW,i}. \qquad (C9)$$

When this is simplified and the summation is taken over N cable segments,

$$\sum_{i=1}^{N} L_i D_i C_{DT, \ i} = \sum_{i=1}^{N} L_i D_i C_{DC, \ i} + \sum_{i=1}^{N-1} L_{Wi} \ D_{Wi} \ C_{DW, \ i}. \qquad (C10)$$

The overall average drag coefficient $C_{DT, \ AVG}$ can be defined as

$$\left[\sum_{i=1}^{N} L_i \ D_i \right] C_{DT, \ AVG}. \qquad (C12)$$

Then

$$C_{DT, \ AVG} = \left[\sum_{i=1}^{N} L_i D_i \right]^{-1} \left[\sum_{i=1}^{N} L_i D_i C_{DC, \ i} + \sum_{i=1}^{N-1} L_{Wi} D_{Wi} C_{DW, \ i} \right], \qquad (C13)$$

which is a weighted-average drag coefficient for the entire system based upon the cross-section areas of the cable and the attached masses which are projected into the incident current. For a spherical mass the cross-section area $L_i D_i$ can be replaced by $\pi D_i^2/4$ and the drag coefficient $C_{DW,i}$ by the appropriate drag coefficient for a sphere when an appropriate drag amplification algorithm becomes available. Both drag coefficients $C_{DC, \ i}$ and $C_{DW, \ i}$ are amplified to the strumming. And the cable segment vibration amplitude and the vibration amplitude of the attached mass are computed in the NATFREQ algorithm, so that the drag amplification using Eq. (C2b) can be computed in a straightforward manner. It is assumed that the drag on the attached mass (a cylinder of $L/D = 3.4$) is amplified similarly to the drag on a long cable or cylinder. The summation for the second term on the right hand side is taken over $N - 1$ segments since there are no attached masses at the terminations.

The NATFREQ code was modified to compute the drag on the cable system in this way. This now is done in the two subroutines TTDRG and TWDRG. The drag coefficients computed with the modified version of NATFREQ are compared with selected examples from the field test data in Sec. 7.3 of this report.

118

LMED
8